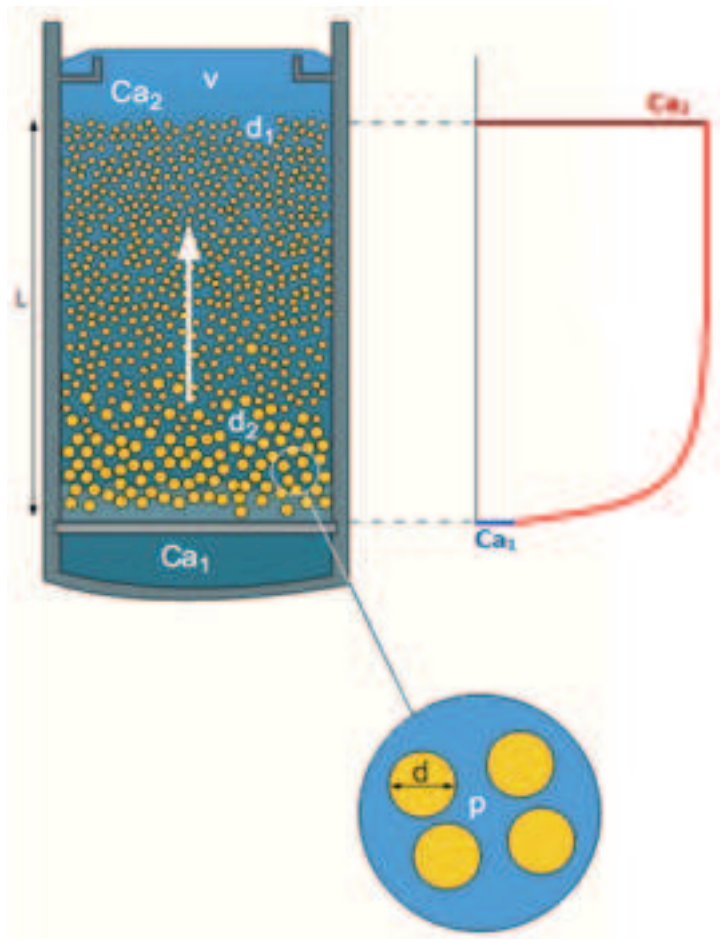# Upflow limestone contactor for soft and de-salinated water

Do Phi Bang

05 September 2012

Upflow limestone contactor for soft and desalinated water

Based on calcite dissolution kinetics and PHREEQC built-in Excel models

Do Phi Bang

for the degree of:
Master of Science in Civil Engineering

Date of submission: 27 August 2012
Date of defense: 05 September 2012

Committee:

Prof.dr.ir. W.G.J. van der Meer	Delft University of Technology
	Sanitary Engineering Section
Ir. P.J. de Moel	Delft University of Technology
	Sanitary Engineering Section
Dr.ir. J.Q.J.C. Verberk	Delft University of Technology
	Sanitary Engineering Section
Dr.ir. P.J. Visser	Delft University of Technology
	Hydraulic Engineering Section
Dr. Lin Yi Pin	National University of Singapore
	Environmental Engineering Section

Sanitary Engineering Section, Department of Water Management
Faculty of Civil Engineering and Geosciences
Delft University of Technology, Delft

Abstract

Desalinated or demineralised water or even soft water is characteristically low in hardness, alkalinity and pH. Thus, these kinds of water need to be re-conditioned (re-mineralized) before distributing for usage as drinking water. The produced water is expected to satisfy the following requirements: safe quality for human health, no quality change during distribution and no demolishing of the distribution infrastructure (no corrosion or excessive scaling). In order to achieve both targets, the water alkalinity, pH and calcium saturation level must be considered as the three main parameters in re-mineralization process. In general, limestone contactors are frequently used for increasing these three parameters before the water can be distributed. This technology should be considered as one of the most popular conditioning techniques used in drinking water treatment field nowadays. Typical examples are limestone contactors of Ashkelon Desalination plant in Israel, Larnaka sea water reversed osmosis (SWRO) plant in Cyprus and Barcelona SWRO plant in Spain.

In fact, the determining factor for remineralized water quality is the kinetics of limestone dissolution. There are several theoretical models (PWP, Chou) as well as practical models (Dreybrodt) to describe the calcite dissolution kinetics. However, the theoretical models tend to idealize the real kinetics in practice while the empirical models are not systematic and constituent to be widely applied. Consequently, this study would mainly focus on developing the two popular theoretical kinetics models (PWP and Chou) to a practical model with theoretical basis that could fully capture the practical calcite dissolution kinetics. On top of that, a layer model concept would be introduced as the base for further developing the downflow and upflow limestone contactor model. Subsequently, simulated results indicate that upflow model is technically more superior to downflow hence providing more economical benefits as well. Vosbeck, Anderlohr's experiments as well as the marble filtration recorded data at Hoenderloo pumping station of Vitens (Netherlands) would be utilized for building and verifying models throughout this research. In the end, an optimal design would be introduced for the remineralizing process at Hoenderloo marble filtration with the aim to increase the filtering capacity, effluent quality and reducing the operational costs at the same time.

In addition to the technical research, a computer based program was built in Excel application with PHREEQC embedded, which includes all of the developed kinetics models for calcite dissolution. The program is developed in order to assist the users as an accurate yet handy tool for quickly predicting or simulating certain calcite dissolution kinetics.

Acknowledgement

Table of contents

List of figures

List of tables

List of abbreviations

CCDP: Calcium carbonate dissolution potential
CCPP: Calcium carbonate precipitation potential (opposite definition of CCDP)
CRF: Correction factor
DOC: Dissolved organic carbon
PCM: PWP-Chou-Morse
PWP: Plummer-Wigley-Parkhurst
SI: Saturation Index
TDS: Total Dissolved Solids
TH: Total hardness
TOC: Total organic carbon
WHO: World Health Organization

Nomenclature

ΔG	:	Gibbs free energy of reaction
a	:	activities of the calcium and carbonate ions in solution
A/V	:	surface over volume ratio
a_1, a_2, a_3:		surface area rate constant for reaction 1, 2 and 3 introduced for PCM model
b	:	increasing factor of n_0
b	:	saturated level decrement
c	:	the concentration in the bulk fluid
Ca	:	current calcium concentration in the solution
Ca_e	:	calcium concentration in the saturated solution
c_s	:	the equilibrium concentration at the surface
D	:	the diffusion coefficient of the dissolved components
dC	:	concentration change
IAP	:	ion activity product = $a_{Ca}a_{CO3}$
k_1, k_2, k_3:		surface area rate constant for reaction 1, 2 and 3
K_2	:	equilibrium constants for $HCO_3^- = H^+ + CO_3^{2-}$
k_4	:	surface area rate factor for the backward reaction
K_c	:	equilibrium constants for $CaCO_3 = Ca^{2+} + CO_3^{2-}$
K_s	:	solubility product
k_t	:	transport rate constant
n, n_0	:	Morse's dissolution rate order
n_0	:	initial dissolution rate order
nCO_2	:	number of moles of carbon dioxide dissolved in the solution
pCO_2	:	initial partial pressure of carbon dioxide
R	:	diffusion rate/gas constant/overall dissolution rate or surface rate
r_1, r_2, r_3:		surface area rates for reaction 1, 2 or 3
r_4	:	surface area rates for the backward reaction
R_b, k_b	:	backward (precipitation) rate
r_{diss}	:	dissolution (forward) rate
R_f, k_f	:	forward (dissolution) rate
r_{prec}	:	precipitation (backward) rate
SI	:	saturation index ($\log(IAP/K_s)$)
T	:	absolute temperature
T	:	Kelvin temperature
t^oC	:	Celsius temperature
$\alpha_1, \alpha_2, \alpha_3$:		correction factor for rate constants a_1, a_2, a_3
β	:	correction factor for b
δ	:	the thickness of the diffusion boundary layer
η	:	correction factor for rate order n
Ω	:	saturation state = $IAP/K_s = \exp(\Delta G/RT)$

1. Introduction

1.1. Background

Nowadays in the modern era, fresh water supply is under a huge demanding pressure. Many countries especially in the Middle East region which have booming economics over the past two decades such as Kuwait, Qatar, UAE, Israel etc. actually have very limited access to natural fresh water as shown in Figure 1.
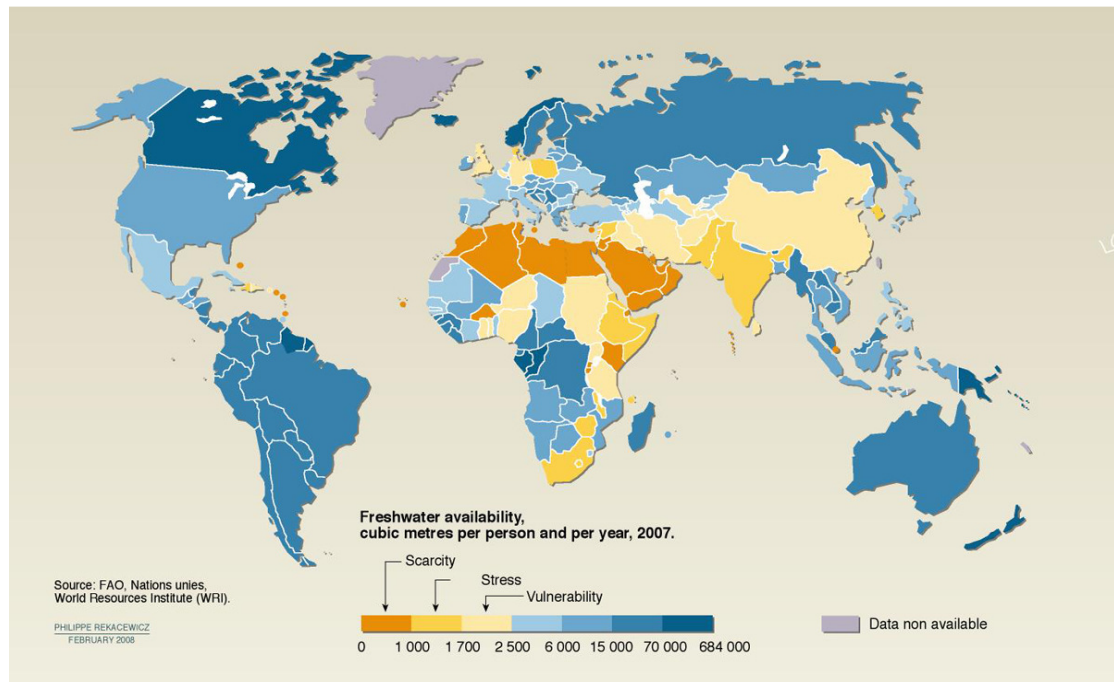
Figure 1: World map of freshwater availability in 2007 (UNEP, 2008)

In order to meet their increasing water demands, ocean water has been extracted for desalinating or demineralising process to be consumable for human. Consequently, demineralised water is becoming more common in the water industry nowadays. In fact, after going through this process, most minerals in water including hardness ions would be significantly reduced to a minimal level which makes desalinated water characteristically similar to the soft water in nature. While the effects of frequent consuming soft water on human health are still a topic in debate, the corrosion effect on the distributional system when soft water circulates is, however, practically evident. Water pipe's corrosion could introduce metals and extraneous matter into the supplying water which is meant to be consumed domestically at the end. Therefore, remineralizing (re-conditioning) desalinated or soft water is an important step before supplying to the consumers.

Currently, there are many different technical methods to re-condition soft water which are widely applied all over the world. Besides chemical dosing and water blending, limestone dissolving is considered as one of the most popular remineralizing techniques in drinking water technology these days. By letting soft water run through a limestone bed with a certain flow rate, calcium and bicarbonate ions are gradually introduced to the water through the dissolution process of the calcite grains in the filter bed. With certain benefits in both economical and technical aspects, limestone contactor is gaining more attentions in the drinking water industry, thus, requires more knowledge and throughout understanding especially in the basic mechanism of dissolving calcite.

1.2. Motivation and objectives

Although a number of studies have been conducted in the field of calcite dissolution, not many have addressed the topic to develop a limestone contactor simulation model which is built on a theoretical basis yet feasible enough to be applied in practice. This shortage is the main driven motivation for this study which is aimed to develop a dissolution model of calcium carbonate which could satisfy both concerned aspects.

The calcite dissolution kinetics plays the key role in the efficiency of limestone contactor in practice. There are several theoretical kinetics models which, however, are not applicable to simulate the practical calcium carbonate dissolution in practice. In contrast, the empirical models are normally too specific or not constituent enough to be widely applied as a systematic model. Therefore, there is a need for establishing kinetics models that could predict the limestone dissolution in practice industry with a better accuracy. The established model could be applied for analyzing different influence factors on the dissolution process which formulate the base for a better design of practical marble filter in terms of produced quality and economic benefits. In addition, the established model must be available and well-presented to be readily applied in practice industry. This could be achievable by combining PHREEQC – an aqueous chemistry application with a more basic computing application as Excel.

1.3. Methodology

Based on the measured data of Vosbeck on dissolution kinetics of different calcite types: pure calcite (Baker) and natural limestone (acidized Juraperle), the theoretical kinetics models such as PWP and Chou could be improved to better capture those measured references. Better set of rate constants or new parameter could be introduced during the improvement process. However, Vosbeck experiments on calcite dissolution only represent the ideal conditions for the kinetics of calcite. Thus, further improvements on the basis of Anderlohr experiments in limestone filtering bed are required. As a result, the developed kinetics model at this state should be sufficient to simulate the real dissolution process in limestone contactors in practice. Using the developed kinetics model as the elementary basis, a steady state multi-layer model would be established in order to closely capture the real kinetics in practice filtering bed with classified layers of different grain size.

In the end, a case study of Hoenderloo limestone marble filter would be then brought into the picture for practical verification. The differences in filtering conditions including initial water quality, grain size, bed thickness, calcite quality between Anderlohr experiments and Hoenderloo case would be taken into account for this verification step. Last but not least, the developed kinetics model would be applied to analyze for the optimal design of Hoenderloo limestone filter as well as to test for the extreme operating condition in terms of water demand for that optimal design. Upflow contactor model would be investigated during the analyzing step to determine how superior it is compared to downflow model in terms of technical and economical benefits.

In order to limit the time consuming by manual calculations, computer-based models are programmed by PHREEQC (built in Excel) to simulate for all of the developed kinetics models in this study. These models will be programmed and organized in familiar interface for targeted users from water treatment practice field.

1.4. Report content

Literature reviews in the second chapter gives a brief introduction of desalinated or soft water as well as its quality regulations, remineralization methods. A brief summary of existing kinetics model for calcite dissolution is also included in Chapter Two. Chapter Three describes in detail the development process for kinetics model for capturing the dissolution nature of pure calcite and natural calcite in ideal batch experiment (Vosbeck) and filtering bed simulation (Anderlohr). Practice verification with Hoenderloo case study and further improvements would be discussed and presented in Chapter Four. Based on the results from Chapter Four, Chapter Five then carries out model applications for optimal design and scenario analysis. Finally, overall conclusions of this research would be presented in Chapter Six.

2. Literature reviews

2.1. Desalinated water and the increasing trend of usage

For the past decades, the world has seen a dramatic increase of desalinated water production, either blended with other water sources or as a main or sole water source (Greenlee L.F., 2009). Nowadays, desalinated water constitutes a considerable percentage of overall fresh water consumption in certain locations for example Bahrain (94%) and United Arab Emirates (98%) (Dawoud, 2005). This trend is expected to spread out worldwide and increase further in a foreseeable future. Desalinated water is currently used mostly for domestic consumption besides a minor fraction is used for irrigation purposes (Beltran F.J., 2006; Greenlee L.F., 2009).

Unconditioned desalinated water quality can vary significantly depending on the different adopted desalination technologies as well as different design and operation of the desalination process (Withers, 2005). However, overall, desalinated water exhibits typical characteristic of soft water: low to neutral pH, poor buffering capacity, low mineral content as well as alkalinity level. With such slightly acidic quality, desalinated water or generally, very soft water should not be supplied for either domestic consumption or irrigation purposes due to a number of reasons (Delion, 2004). The three main concerns for supplying very soft water in the urbanism context could be listed as: the human health concern, the interaction with the distribution system, potential adverse effects on downstream wastewater treatment plants. Consequently, very soft water such as desalinated water must be conditioned or remineralized before distributing for usage.

2.2. Controlling parameters in remineralization process

The four main quality parameters which determine the remineralization process are Total Hardness (TH) (mainly Ca^{2+} and Mg^{2+} concentration), pH, Calcium Carbonate Precipitation Potential (CCPP) and Alk content. The importance of each parameter in conditioning soft-water is discussed as followed:

Total Hardness (TH) - the water hardness plays an important role in the supplied drinking water. It not only contributes vital minerals to human daily dietary but also prevents corrosion in the distribution pipe system by calcifying and forming a protection layer of calcite (or dolomite) on the inner wall of the pipe in case of positive CCPP.

pH – The negative logarithm of the active H^+ concentration generally indicates the acidic or basic nature of the solution. A low pH corresponds to a high acidic liquid which enhances the dissolution index (CCDP) of $CaCO_3$ in the solution and otherwise. Thus, it is important that the water pH after remineralization process must be elevated compared to the low pH level of the initial desalinated water. For a reasonable range of pH values after remineralization (from 6 to 8.5), a lower pH would result in a higher efficiency of chlorine disinfection (Barbeau, 2004; Gyurek L.L., 1997) while a higher pH results in less corrosion of metals (iron, copper, lead, zinc, nickel, cadmium, etc.). Nevertheless, pH value of a solution could easily vary later by downstream potential chemical reactions given a very low solution's buffering capacity. Therefore, information on Alk which mainly determines the solution buffering capacity is essentially complementary to the pH level in order to define the acid-base characteristic of the water.

Calcium Carbonate Precipitation (or Dissolution) Potential – CCPP (or CCDP) indicates the possible amount of calcium carbonate to precipitate (dissolve) in order to achieve the equilibrium state of the solution. Maintaining a higher threshold of CCPP has been associated with a decrease in corrosion rate in concrete, asbestos cement pipes or cement lining in steel pipes as well as the likelihood of red water occurrence due to iron and copper leakage in

4

metallic pipes. However, it is also important to have an upper threshold for CCPP to avoid excessive $CaCO_3$ scales on pipes and pumping stations.

Alkalinity – Alkalinity is generally defined as the ability of a solution to neutralize acids to the equivalence point of carbonate or bicarbonate. In different systems with different contents, there are different compositions contributing to the total alkalinity. For instances, in typical groundwater or seawater, the measured alkalinity is approximate to:

$$\text{Alkalinity} = [HCO_3^-] + 2[CO_3^{-2}] + [B(OH)_4^-] + [OH^-] + 2[PO_4^{-3}] + [HPO_4^{-2}] + [SiO(OH)_3^-] - [H^+]_{sws} - [HSO_4^-] \quad (1)$$

Where alkalinity is in units of meq/L and [ ] stands for concentration in mmol/L.

Alkalinity is usually given in the unit of meq/L (milliequivalent per liter solution). In chemistry, milliequivalent (meq) is the indication of the amount of a substance required to combine with 1 millimole of a monovalent ion. For instances, in carbonic acid (H_2CO_3), half a millimole of CO_3^{2-} is required for a millimole of monovalent H^+ hence, 1 mmol of CO_3^{2-} is equivalent to 2 meq. Similarly, 1 mmol of HCO_3^- equals to 1 meq because it only combines with 1 mmol of monovalent H^+.

In natural environment, carbonate alkalinity tends to make the most of the total alkalinity due to the common occurrence and dissolution of limestone and presence of carbon dioxide in the atmosphere. For the product drinking water of post treatment plant with typical pH of 7.5 to 9.5, the dominant carbonate specie is HCO_3^- (Figure 2). Thus, bicarbonate would be focused on in this study as the main sources for the remineralized water's alkalinity.
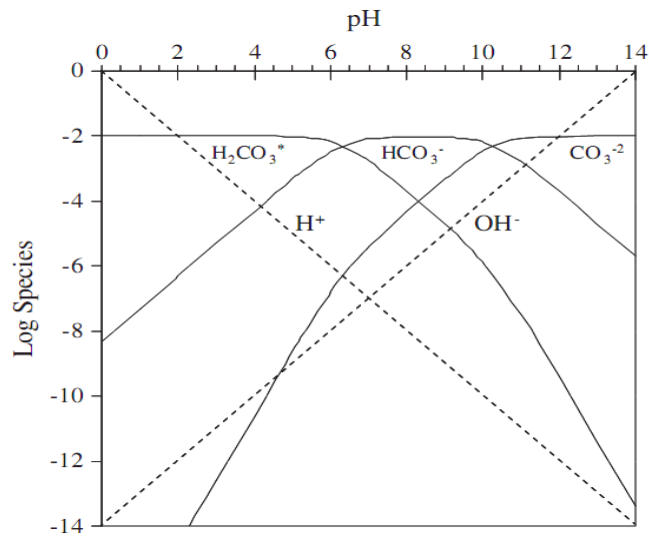
Figure 2: pH log species representation of the carbonate system. CT = 10-2 mol (the concentration of H+ and OH- appears in dashed lines (Birnhack et al., 2011).

High alkalinity is advantageous in desalinated water for a number of reasons:
- Elevating water buffering capacity which provide the water higher capacity in withstanding the changes in pH when strong acid or base are added to the solution
- Increasing Saturation Index (SI) of $CaCO_3$ in case of abundant Ca^{2+} ion in the water, which consequently leads to a decrease in corrosion rate and occurrence of red water events (Imran, 2005; Sontheimer, Kolle, & Snoeyink, 1981).
- Minimizing potential negative effects of blending of desalinated water with other water sources within the distribution system.

Although alkalinity and hardness might have the same unit (mg/L $CaCO_3$) in some studies, they prefer to different measurements:
- Hardness: total calcium (or magnesium) ions in the water
- Alkalinity: total amount of [H^+] or [OH^-] required for obtaining a pH of 4.3 where all of bicarbonates and carbonates have been converted to carbon dioxide.

However, it is important to note that alkalinity and hardness levels need not to be the same especially in natural water, since the bicarbonates can be associated with potassium or sodium, and the calcium or magnesium with chlorides or sulphates. In desalinated water where the content of both hardness and alkalinity is insignificant initially, most remineralization processes would introduce an amount of [Ca^{2+}] which is approximately twice

the amount of [HCO_3^-] appeared in the water simultaneously. Thus, in these processes, the level of (calcium) hardness could be directly linked to the alkalinity introduced.

However, not all guidelines and standards are stringent enough to take into account all of these four parameters for remineralizing water to meet the final user needs in terms of public health, system corrosion and downstream effects on wastewater treatment plant.

2.3. Influenced aspects of drinking water with low mineral content

2.3.1. Human health concern

The latest report from global and regional guidelines such as WHO (2011) and regulation from EU (1998) do not implement a minimum (or even maximum) required level of calcium, magnesium or total hardness level for drinking water (see Annex A.3, A.4). This is due to all the on-going arguments that drinking water does not mean to be a nutrient drink which has to supply all required nutrients and supplements which benefits human health. There are also not enough convincing scientific evidences to show that shortage of calcium and magnesium in daily drinking water would directly lead to dangerous diseases and impacts on human health. These are more likely due to the conditions of daily dietary of each individual in each region.

Nevertheless, maintaining a certain level of TH in drinking water is still a plus to public health. In fact, there are many studies indicate the adverse effects on human health by drinking water with low hardness (calcium and magnesium) content as well as strict regulated levels of these used to be specified in the past (see Annex A.1). The usual recommended minimum concentration of calcium in drinking water required for protection of human health is from 0.5 to 0.6 mmol/L Ca (20 to 24 mg/L) (F. Kozisek, 2003). Besides, based on WHO (2004), the requirement of a positive CCPP value at pH close to 8 (which is normal for remineralized water) makes the total concentration of Ca^{2+} to be within the range of 0.8 to 1.2 mmol/L Ca (32 to 48 mg/L) for the combined effects on protection of human health and distribution system (Birnhack, Voutchkov, & Lahav, 2011). On the other hand, the necessity of introducing magnesium level into drinking water is still under intensive debate because there have been contradictory research result in the relation between low magnesium intake in drinking water and cardiovascular diseases. Despite the ongoing argument, recent publications of the WHO have recommended to maintain minimum magnesium content in drinking water.

2.3.2. Corrosion of distribution system

In some aspects, desalinated water is considered having superior quality compared to the natural water which is likely to be polluted nowadays. Nonetheless, desalinated water as well as naturally soft water is very aggressive and easily leading to corrosion problems in metallic distribution system as shown in many previous studies (see Annex A.2). Corrosion of system pipes is associated with health hazards due to unwanted releases of metal ions such as lead, copper and zinc into the drinking water (Morse & Arvidson, 2002; L. N. Plummer, Wigley, & Parkhurst, 1978a, 1978b). Other studies carried out the relation between pH, alkalinity levels and the dissolved content of corrosion products in distribution system.

A case study in Seattle, US from 1972 to 1981 proved that adjusting pH and alkalinity to suitable ranges could significantly minimize the corrosion problem in the galvanized steel distribution system (AWWA Research Foundation. & DVGW-Technologiezentrum Wasser., 1996). On the other hand, pipe corrosion was also found in different locations (Yanbu and Medina, Al Khobar) in Saudi Arabia from 1979 to 1981 due to the very high content of sodium and chloride content compared to bicarbonate as well as the water is not saturated with calcium carbonate hence no protective layer is formed on the pipe inner walls. In the end, the adopted remedies for all of these cases were to increase the water hardness, pH level as well

as alkalinity content in the water. Moreover, in Effects of Blending on Distribution System Water Quality (Imran, 2005), it has been shown that higher alkalinity would reduce the colour release which also which also represents the release of iron corrosion product into water. However, Imran (2005) also indicated that higher alkalinity would increase the lead release into RO water. Thus, ground water with high alkalinity is beneficial for controlling iron release but detrimental to copper and lead release. The author hence recommends increasing pH level in the water of high alkalinity to a certain range could help controlling copper and lead release although calcium scaling and deposition may occur in the distribution system.

Due to different water sources, distribution system materials around the world, it is not easy to have a global standard on pH and alkalinity level to prevent corrosion. Though no certain health base guideline is proposed for hardness in drinking water, WHO (2011) discussed on the corrosion aspect of supplied drinking water which might greatly affect the final quality for human consumption. However, most corrosion could be overcome or limited under control of the water pH (before supplying). Depending on the material of the piping distribution system, an appropriate pH level range should be selected for the supplying drinking water as shown Table 1.

Table 1: Recommended pH ranges for corrosion control by WHO (2011)

Corrosive material	Controlled pH range
Brass	< 8.3
Copper[1]	8.0 – 8.5
Iron [2]	6.8 – 7.3
Lead[3]	8.0 – 8.5
Zinc[3]	≈ 8.5

(1): Ca less than 24mg/L Ca and pH<6.5 → very aggressive to copper
(2): Besides pH control, alkalinity must be adjusted to at least 0.8 meq/L, super-saturation with CaCO3 of 4 -10 mg/L.
(3): for low alkalinity water

Similarly, the European Directive (EU, 1998) does not specify a requirement for calcium, magnesium, water hardness or bicarbonate levels although the former one (EU, 1980) was more stringent with a minimum level of alkalinity (30 mg/L) as specified in Table 2. Nonetheless, it does not prevent member states from implementing such a requirement into their national legislation. The guided level of pH was suggested to be within 6.5 and 9.5 together with a notice that the supplied drinking water should not be aggressive.

On the other hand, controlling corrosion in concrete or AC (Asbestos Cement) pipe is also important due to the popular application of these pipes in the past which are still operating up to now. For soft or desalinated water with highly negative CCPP or SI calcite, the concrete is susceptible to lime leaching which gradually damages the pipe internally. On the contrary, highly positive CCPP or SI calcite is also not desirable due to the risk of excessive scaling in pipe system. Therefore, an approximate neutral CCPP or SI calcite (≈0) for the supplied water is required in order to avoid those unwanted effects in concrete pipe lines.

2.3.3. Potential adverse effects on wastewater treatment plants

This is a newly recognized issue which is related to the downstream biological wastewater treatment for ammonia and nitrate removal (Mackintosh, 2003). In order to maintain the pH and biological process stability in the wastewater treatment processes such as nitrogen removal, a high alkalinity in wastewater is required (Buhmann & Dreybrodt, 1985; Chou, Garrels, & Wollast, 1989). Therefore, the upstream supplied water should have a certain minimum level of alkalinity which is not too low so that the nitrification process at the treatment plant downstream is stably sustained (Buhmann & Dreybrodt, 1985).

2.3.4. Main concerned quality parameters in remineralized water

At this moment, there is no final conclusion on the negative effects on human health caused by drinking low mineral water. Consequently, there is currently no implemented requirement of minimum calcium and magnesium level in the supplied drinking water even in the global guideline of WHO. Thus, water hardness level is not the key quality index in remineralized water. The main influenced aspect of the supplied drinking water is therefore the sustainability of distribution system and downstream wastewater treatment plant which is also practically evident. Besides, corrosion in distribution system could possibly introduce extraneous substances including metals into the supplied drinking water which could be highly hazardous to the consumers. In order to prevent corrosion in distribution system, it is important to consider all of the system materials including metallic and concrete. In concrete pipes, the supplied water must not be aggressive to cause lime leaching in concrete pipe which requires a calcite SI (or CCPP) close to zero. For most metallic pipes or water equipments, the best way to control severe corrosion is raise the pH range to around 7.3 to 8.5 according to Table 1. In that context, high buffering capacity is also required for maintaining a stable pH level. In order to achieve high buffering capacity solution, high alkalinity level should be introduced. On the other hand, the alkalinity level in supplied water should also be at moderate level in order to maintain a stable operating condition in the downflow wastewater treatment plant.

Therefore, the important parameters in water remineralization are SI (or CCPP), pH and alkalinity in which alkalinity plays the controlling role in maintain the desired water quality supplied to the consumers.

2.4. Requirements of calcite SI (or CCPP), pH and alkalinity content in drinking water

2.4.1. Guidelines and standards for supplied drinking water

Bounded by the EU regulations, the Netherlands has a local standard for Dutch drinking water. In Dutch Waterleidingbesluit which is valid from February 2001 till July 2011, the pH level of drinking water must fall between 7.0 and 9.5; the Saturation Index (SI) of calcium carbonate in drinking water must be above -0.2. Although there is no specific requirement from the latest EU regulation or WHO report, Dutch Waterleidingbesluit specified the alkalinity content must be above 1.0 mmol/L. The EU terms "the supplied drinking water should not be aggressive" had been translated into a minimum value of SI and minimum level of alkalinity (mainly HCO_3^-). Recently, Dutch Drinkwaterbesluit has been published in replacement for the expired Waterleidingbesluit. This new regulation, which is valid from July 2011, actually has no major difference to the former one in terms of pH, SI and bicarbonate levels except for the cancelation of the upper level of total hardness in drinking water. Besides, the SI level (> -0.2) specified in this new regulation is the annual average value.

Overall, the development of drinking water quality requirements in terms of pH, SI, total hardness (calcium and magnesium) and bicarbonate levels could be simplified as shown in Table 2.

Table 2: WHO, EU and Dutch legal standards for aggressiveness parameters in drinking water

	WHO	WHO	EU	EU	Waterleidingbesluit	Drinkwaterbesluit
Published year	1980	2011	1980	1998	2001	2011
pH	-	Varied (Table 1)	≥ 6.5 and ≤ 9.5	≥ 6.5 and ≤ 9.5	≥ 7.0 and ≤ 9.5	≥ 7.0 and ≤ 9.5
SI	-	-	-	-	> - 0.2	> - 0.2 [1]
Alkalinity (meq/L)	≥ 0.5	-	≥ 0.5	-	> 1.0	> 1.0

(1): Annual average

In contradictory to the updated standards and guidelines, the published water quality criteria for post-treatment of soft and corrosive water in the past used to be much more stringent as listed in Table 3. This is due to the fact that the water quality and distribution system materials have varied largely nowadays. Furthermore, global and regional standards of WHO and EU no longer require a minimum level of hardness or alkalinity due to the on-going debates of these content's influence on human health.

Table 3: List of published water quality criteria for post-treatment of soft and corrosive waters (Chou et al., 1989)

Location/Source	Year	Alkalinity meq/L	CCPP (or SI) mmol/L CaCO$_3$	pH
USA	1999	0.8-1.6	0.04-0.1	-
USA	2005	>1.6	SI>0	-
Johannesburg, South Africa	1986	>1.0	0.02-0.05	-
Johannesburg, South Africa	2002	>1.0	0.01-0.02	~8.2
France	2001	1.4-2.4	SI>0	-
Sweden	1999	>1.0	-	7.5-9.5
Israel	2006	>1.6	0.03-1.2	<8.5

According to Birnhack, Voutchkov and Lahav (2011), surveying the relevant literature reveals that the remineralized water quality standards that have been set far ahead in coping with all the possible influenced aspects mentioned in 2.3, only currently exist in Israel since desalinated water is gaining important role with 25% of the total fresh water supply. This Water Quality Standard is the result of a comprehensive work appointed by the Israel Ministry of Health and is now enforced as the official standards for desalinated water.

2.4.2. Research focus range of SI, pH and alkalinity

In order to ensure that there is no extreme calcite dissolution occurring in the distribution system, the SI level after remineralization must be close to zero (for instances, >-0.2 in Dutch standard). A typical pH range of 7.3 to 8.5 would be normally encountered in post treatment plant which is also well within the specified range in most standards. Since the alkalinity requirement varies for different regulations and standards over time, this study will focus on the typical range of required alkalinity in supplied drinking water: 0.5 to 2.0 meq/L.

2.5. Remineralization methods for soft and desalinated water

2.5.1. Direct dosage of NaHCO$_3$

In order to obtain a minimum alkalinity level set by different countries' legislation to make sure the water is not very aggressive to the distribution system, several methods of remineralization have been developed, mostly involve introducing carbon dioxide and dosing a base into water except for the method of direct dosage of sodium bicarbonate (NaHCO$_3$):

$$NaHCO_3 \rightarrow Na^+ + HCO_3^- \tag{2}$$

The main advantages of this method are the simplicity, the relatively low capital cost and required space, the flexibility with regard to product alkalinity concentration. However, this method includes high operational costs due to the high cost of the chemicals and the unavoidable addition of unwanted ions such as Na^+. Furthermore, beneficial ions such as calcium or magnesium are not introduced through this method to raise the water TH and CCPP. In addition, using NaHCO$_3$ will elevate pH since it contains HCO$_3^-$ - the main species of carbonate system. As a result, if lime is subsequently added to increase TH and CCPP level, it is very ineffective because the dissolution potential of lime would significantly decrease with

high pH (even with very low Ca^{2+} content in water). Thus, this approach is rather impractical for remineralizing desalinated water.

Besides, there is also an alternative to introduce Ca^{2+} into the water:

$$CaCl_2 + 2NaHCO_3 \rightarrow Ca^{2+} + 2HCO_3^{2-} + 2Na^+ + 2Cl^- \hspace{3cm} (3)$$
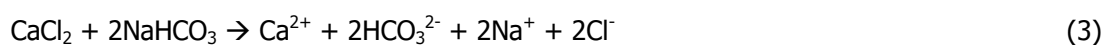
This is also a simple approach but expensive in terms of chemical cost since $CaCl_2$ is often more expensive than lime (Mackintosh, 2003). Besides, this method also introduces unwanted ions such as Na^+ and Cl^- to the solution. Thus, direct dosage of $NaHCO_3$ is not the usual choice for remineralizing water nowadays.

2.5.2.   Dosage of lime and carbon dioxide

One of the most popular methods for remineralization nowadays is the utilization of either quick lime (CaO) or hydrated lime ($Ca(OH)_2$):

$$0.5 \ CaO + 0.5H_2O + CO2 \rightarrow 0.5 \ Ca^{2+} + HCO_3^- \hspace{3cm} (4)$$

$$0.5 \ Ca(OH)_2 + CO_2 \rightarrow 0.5 \ Ca^{2+} + HCO_3^- \hspace{3cm} (5)$$
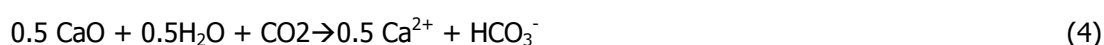
As mentioned in the previous case studies in US and Saudi Arabia (see Annex A.2), for the minimal effect of corrosion, a certain level of calcium, alkalinity is usually required together with a suitable pH range. A high sodium content compared to the bicarbonate and calcium concentrations should be avoided. Thus, lime dosage (either quick lime or hydrated lime) is usually preferred and widely applied (Vitens, 2010).
However, dosage of a base for remineralization would be costly overall on installation and operation for lime. Lime solubility could easily reduce if the permeate is at warm temperature. Besides, dosing either hydrated or quick lime might result in higher turbidity which is not desirable (Dreybrodt, Lauckner, Zaihua, Svensson, & Buhmann, 1996; Svensson & Dreybrodt, 1992; Withers, 2005) and difficulties in maintaining consistent product water pH (Withers, 2005).

2.5.3.   Dosage of caustic soda, soda ash and carbon dioxide

Other alternatives to lime which are also practiced in a few desalination plants are the use of caustic soda and soda ash:

$$NaOH + CO_2 \rightarrow Na^+ + HCO_3^- \hspace{3cm} (6)$$

$$Na_2CO_3 + CO_2 + H_2O \rightarrow 2Na^+ + 2HCO_3^- \hspace{3cm} (7)$$

Although these methods will elevate the pH as well as alkalinity level of the water, the main drawbacks are the lack of TH introduction to the water and extra unwanted ions.

2.5.4.   Blending

An important low-cost method to increase the content of some desired ions in desalinated water is blending with seawater, surface water or groundwater. However, blending is not accurate enough in controlling and limiting different ions at the same time according to a pre-set quality (AWWA). Therefore, blending water is not recommended for domestic use (Imran, 2005). Besides, blending water could have adverse impact on both environmental and economic aspects with the increase of boron, chlorides and sodium ions in water (Dreybrodt et al., 1996). Thus blending technique is not a future promising method for remineralizing.

2.5.5. Limestone contactor

A rather cheaper and simpler method for introducing bicarbonate into water compared to base dosage is limestone contactor which has the same working principle as limestone filtration for neutralization of aggressive water (Moel, Verberk, & Dijk, 2006) :

$$CaCO_3 + CO_2 + H_2O \rightarrow Ca^{2+} + 2HCO_3^- \tag{8}$$

Unlike other methods, calcite dissolution would result in the least unwanted species produced and the highest amount of alkalinity for the same amount of CO_2 and H_2O. According to Birnhack, Voutchkov and Lahav (2011), CO_2 based calcite dissolution is ranked number one in producing highest buffer capacity. Moreover, calcite dissolution has been recognized since 1981 as a flexible and reliable conditioning method. The basic parameters characterizing water stability (calcium, alkalinity and pH) could be adjusted to a safe value (Colombani, 2008). According to Kettunen and Keskitalo (1985), limestone dissolution has been favored as it provides constant alkalinity without overdosing risk.

Limestone contactor is usually more economic wise in terms of capital and chemical expenditures, carbon dioxide usage than the lime-based methods which are widely applied nowadays. Moreover, a much lower turbidity is produced compared to lime-based methods. Nevertheless, high-quality calcite is not always readily available as lime; hence, the lime base technique is still more popular nowadays.

Table 4: Cost of common chemicals for increase of water alkalinity (Mackintosh, 2003)

Chemical	Alkalinity addition (as CaCO$_3$) per mg/l of chemical	Unit chemical costs (US$/ton)	Unit costs in US$/ton per 1 mg/l of added Alkalinity as CaCO$_3$
Calcite	1.00	30-40	30-40
Carbon dioxide	1.14	70-90	61-78
Sulfuric acid	1.02	50-80	49-78
Quicklime	1.78	120-150	67-84
Hydrated lime	1.35	260-280	193-207
Soda ash	0.94	540-580	574-617
Sodium hydroxide	1.25	700-750	560-600
Sodium bicarbonate	0.60	900-950	1500-1583

Overall, limestone contactor is potentially the most popular method in remineralizing desalinated and soft water in future because of many advantages over other methods. This study would thus focus on limestone contactor in achieving the optimal remineralized product water by investigating the kinetics of dissolution rate of calcium carbonate in the contactor.

2.6. Kinetics models and experiments for calcite dissolution

2.6.1. Overview

The dissolution or precipitation of solids in water is dependent on a number of factors. From the mass balance point of view, it could be expressed as followed:

Mass change in solid = Mass change in liquid
Mole change (mol) = Mol change per volume of the same substance (mol/m^3) * volume (m^3)
Hence, $dM = dC * V$ (9)

On the other hand, from the kinetics of solid:
Mass transfer (mol/s) = Area surface rate (mol/m^2/s) * Area (m^2)
Or $dM/dt = R * A$ (10)

Thus,

$$dM = R * A * dt = dC * V$$
$$\Rightarrow \qquad dC = R*(A/V)*dt \tag{11}$$

Where dC   = concentration change   (mol/m^3 or mol/kgw)
       A/V   = surface over volume ration   (m^2/m^3 or m^2/kgw)
       R   = surface rate   (mol/m^2/s)
       dt   = duration   (s)

Note that A value indicates the area of the solid surface that is interacting with the liquid environment and V means the volume of the liquid at the initial state before the dissolution (precipitation) process takes place.

The surface rate R depends on four different mechanisms: diffusion in solid structure, dissolution reaction at the surface, diffusion in the boundary layer and advection in the bulk flow. The slowest transport mechanism among these four would determine the overall surface rate or dissolution rate.
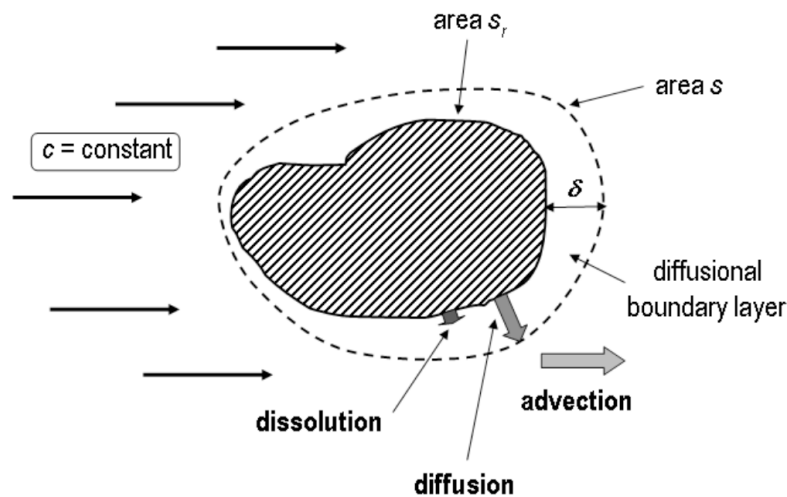
Figure 3: Scheme of the successive mechanisms occurring during the dissolution of a crystal grain in a bulk solution chemistry experiment (Colombani, 2008)

Diffusion in the solid structure:
In this process the solids dissolute in the solid structure itself and the dissolution products (ions) are successively transported by diffusion in the pores of the solid structure to the surface

Dissolution reaction at the surface:
The surface reaction rate is usually the limiting factor of the less soluble solids. The reaction proceeds so slowly that the reaction products would freely diffuse away. The surface determines the rate of dissolution. Adsorption of substances on the surface can accelerate as well as inhibit the reaction.

Dissolution could be seen as a forward reaction in a chemical equilibrium reaction, while precipitation is the backward reaction:

$$CaCO_3 \underset{k_b}{\overset{k_f}{\rightleftharpoons}} Ca^{2+} + CO_3^{2-} \tag{12}$$

The overall rate R_{diss} is given by the sum of the forward R_f and backward R_b reaction rates:

$$R = R_f - R_b = k_f - k_b a_{Ca} a_{CO3} \tag{13}$$

12

In which:

R = overall dissolution rate or surface rate
R_f, k_f = forward (dissolution) rate
R_b, k_b = backward (precipitation) rate
a = activities of the calcium and carbonate ions in solution

At equilibrium, the forward rate balances out the backward rate hence giving zero net rate. Near equilibrium state, k_f could be calculated as:

$$k_f = k_b K_s \tag{14}$$

in which
K_s = solubility product
Hence,

$$R = k_b(K_s - IAP)$$
$$= k_b K_s(1 - IAP/K_s)$$
$$= k_b K_s(1 - \Omega)$$
$$= k_b K_s(1 - \exp(\Delta G/RT)$$
$$\Rightarrow \quad R = k_b K_s(1 - 10^{SI}) \tag{15}$$

In which
IAP = ion activity product = $a_{Ca}a_{CO3}$
Ω = saturation state = $IAP/K_s = \exp(\Delta G/RT)$
ΔG = Gibbs free energy of reaction
R = gas constant
T = absolute temperature
SI = saturation index (log (IAP/K_s))

When   IAP < K_s ➔ SI <0 ➔ dissolution
IAP > K_s ➔ SI >0 ➔ precipitation

The expression of dissolution rate as shown in equation (15) is the original formula for the calcite dissolution (and precipitation) kinetics.

Diffusion in the boundary layer:
The ions formed at the surface have to migrate through the diffusion boundary layer to the bulk flow. In this layer, the concentration rate of change follows Fick's law:

$$R = k_t(c_s - c)$$
$$= (c_s - c)*D/\delta$$
$$= (D/\delta)c_s(1 - c/c_s) \tag{16}$$

In which:

R = diffusion rate
k_t = transport rate constant
D = the diffusion coefficient of the dissolved components
δ = the thickness of the diffusion boundary layer
c_s = the equilibrium concentration at the surface
c = the concentration in the bulk fluid

The diffusion boundary layer is more of a hypothetical layer rather than an observable layer with a certain thickness. The thickness of the layer will be influenced by the hydraulic conditions in the bulk flow.

Advection in the bulk flow:
The transport of the dissolution products in the bulk flow is determined by flow condition. This mechanism is important especially when the flowing rate through the solid surface is extremely low which controls the dissolution process of the solid.

Overall, the dissolution rate of solids such as calcite in the liquid would be mainly determined by the slowest transport mechanism among those four. If the dissolution reaction rate is the determining factor, the dissolution is considered surface controlled. For diffusion rate or advection as the main mechanism, it is classified as transport controlled. It has long been recognized that the calcite dissolution at pH less than approximate 4.0 is controlled by transport mechanism since the H^+ strong attack would lead to very fast reaction at the surface. If the solution pH is above 4.0, it has been widely agreed that calcite dissolution is the controlled mainly by surface reaction. However, mechanism(s) of reaction varies for different studies; thus, many different models of surface rate for calcite dissolution had been introduced with the most common are Morse model, PWP model and Dreybrodt model.
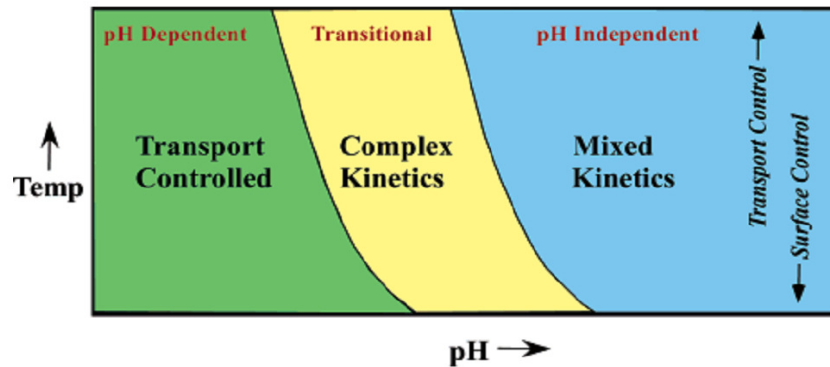
Figure 4: Summary diagram of relationship of transport versus surface-controlled dissolution based on the work of Sjöberg & Rickard (1985)

2.6.2. Carbon dioxide partial pressure influence in limestone contactor

The partial pressure of a gas is defined as the pressure exerted by that gas alone. For a gas dissolved in the liquid, the partial pressure is therefore a measure of thermodynamic activity of that gas's molecules. Hence, the carbon dioxide partial pressure (pCO_2) is proportional to the content of CO_2 dissolved in the solution.
For underground water, there is often an abundant amount of $CaCO_3$ available, thus, the hardness of water is often dependent on the carbon dioxide content in water which will react to dissolve $CaCO_3$ into water according to:

$$CaCO_3 + CO_2 + H_2O \rightarrow Ca^{2+} + 2HCO_3^- \qquad\qquad (17)$$

This is also the main reaction for the limestone contactor process. However, it is important to notice that the carbon dioxide content in water might vary depending on different systems. Generally, there are two types of system in relating to pCO_2: the aerated system and unaerated system.

The aerated system (or open system) is a water system in which the solution freely exchanges CO_2 to the surrounding atmosphere which has a high amount of CO_2 in equilibrium hence CO_2 content in the water is always kept at a constant level for instances surface water with high turbulence (turbulent river flow, water fall) or even underground cave water. For underground cave water, the CO_2 content is also constant and much higher compared to the atmospheric environment, hence, it is also consider an aerated (constant CO_2) system. Thus, while limestone dissolution takes place in an aerated system, CO_2 content is always kept constant in the solution even though CO_2 is consuming for the reaction process.

The unaerated system (or closed system) is, however, a variable CO_2 partial pressure system since CO_2 is not freely exchanged to the surrounding environment or there is not enough CO_2 in and out fluxes to keep the level constant for instances, surface water in stagnant lakes, open sand filter, etc. The limestone contactor is another example of unaerated system. Therefore, CO_2 level would be gradually decreasing during limestone dissolution process in the contactor.

14

2.6.3. Kinetics models of calcite dissolution

PWP (Plummer-Wigley-Parkhurst) model:

There have been many theories in the past tackling the problem of calcite dissolution, however, all failed to take into account the mechanisms at the surface of calcite solid until 1978. In 1978, Plummers and others studied the dissolution kinetics of calcite in stirred CO_2 water systems at CO_2 partial pressure from 0.0003 to 0.97 atm and temperature from 5°C to 60°C by pH-stat and free drift method. They then suggested the PWP model as "a mechanistic model for reactions at the calcite-aqueous solution interface".

The pH-stat method is to determine the dissolution rate far from equilibrium (no precipitation occurs at this range). Three important dependencies of dissolution rate far from equilibrium are identified by this method are: (1) first order dependence on the bulk fluid H^+ activity,(2) linear dependence on the bulk fluid CO_2 partial pressure (pCO_2) and (3) constant forward rate in the region of insignificant H^+ and dissolved CO_2.
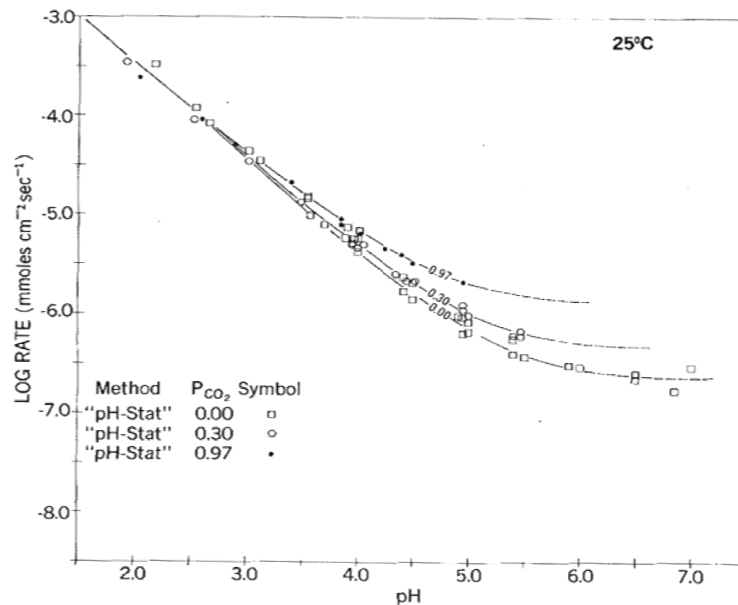
Figure 5: Log rate of calcite dissolution vs bulk fluid pH and pCO₂ (L. N. Plummer et al., 1978a)

The free drift method is used for identifying the reaction rate near equilibrium where both dissolution and precipitation process take places. Similar to the pH-stat method, forward rate dependence on pCO_2 and the constant forward rate in the near absence of H^+ and CO_2 are verified by this method. Furthermore, the backward reaction rate for precipitation of calcite is shown to be linearly proportional to the activity product of Ca^{2+} and HCO_3^- in solution.

PWP model considered the following chemical reaction as the main process for dissolution and precipitation of calcite:

$CaCO_3$	+	$H^+_{(aq)}$	=	$Ca^{2+}_{(aq)} + HCO_3^-_{(aq)}$	(18)
$CaCO_{3\,(s)}$	+	$H_2CO_{3(aq)}$	=	$Ca^{2+}_{(aq)} + 2HCO_3^-_{(aq)}$	(19)
$CaCO_{3\,(s)}$	+	$H_2O_{(aq)}$	=	$Ca^{2+}_{(aq)} + HCO_3^-_{(aq)} + OH^-_{(aq)}$	(20)
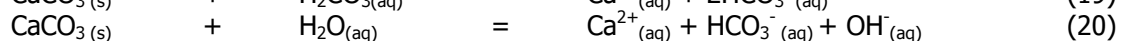
The forward reaction rate of (16), (17) and (18) are determined as following with temperature range of 5 to 60°C:

$$r_{diss} \quad = \quad r_1 + r_2 + r_3 \tag{21}$$

$r_1 = k_1*(H^+)$ with $k_1 = 10^{(0.198 - 444/T)}$

$r_2 = k_2*(H_2CO_3{}^*)$ with $k_2 = 10^{(2.84 - 2177/T)}$

$r_3 = k_3*(H_2O)$ with $k_3 = 10^{(-5.86 - 317/T)}$ for $T \leq 298$ K

                    or $k_3 = 10^{(-1.1 - 1737/T)}$ for $T > 298$ K

in which:

r_1, r_2, r_3	= surface area rates for reaction 1, 2 or 3	mmol/cm^2/s
k_1, k_2, k_3	= surface area rate constant for reaction1, 2 and 3	mmol/cm^2/s
(H^+)	= activity of H^+ = 10^{-pH}	-
$(H_2CO_3{}^*)$	= activity of $H_2CO_3 + CO_2$	-
(H_2O)	= activity of H_2O = 1.0 for low and moderate ion strength	-
T	= temperature	K

The importance of each component (H^+, H_2CO_3 or H_2O) in the surface area rate is greatly dependent on the pH, CO_2 partial pressure pCO_2 and temperature T of the liquid. By equating one term of equation (21) with the other two terms, the boundaries could be plotted as shown in Figure 6 for the case of 25°C. H^+ attack is the dominant forward reaction at pH values lower than those of line 1. Carbonic acid attack is the main mechanism at pCO_2 values above line 2. Similarly, water reaction becomes the most significant mechanism when pCO_2 value is below line 3.
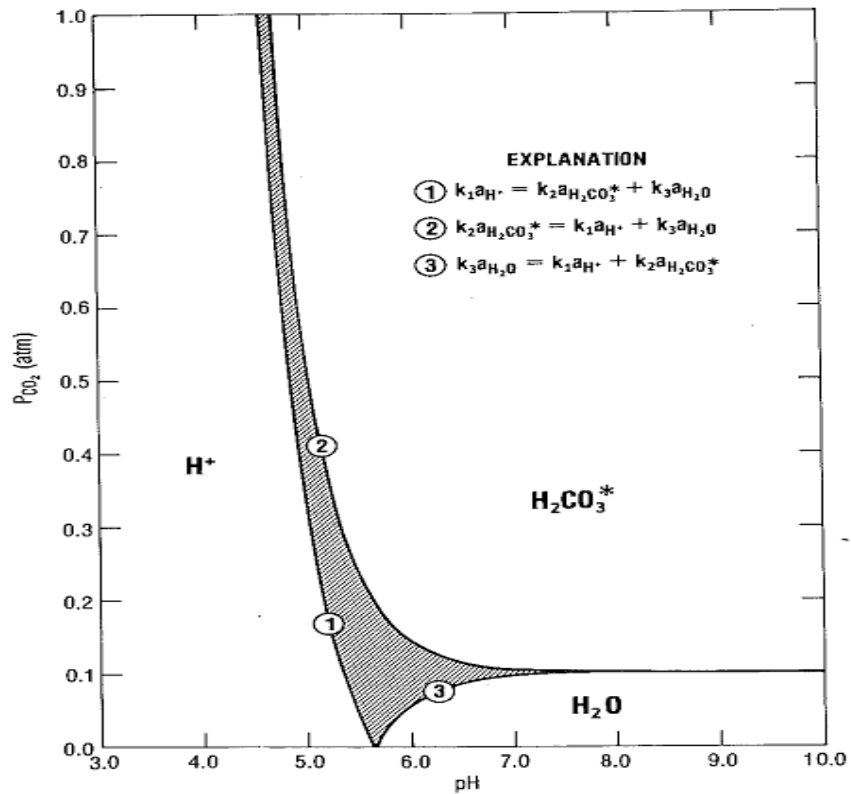
Figure 6: Reaction mechanism contributions to the forward rate of reaction as a function of pH and pCO$_2$ at 25°C (L. N. Plummer et al., 1978a)

The backward (precipitation) reaction of PWP model is adopted as:

$$Ca^{2+} + HCO_3^- \rightarrow CaCO_3 + H^+ \tag{22}$$
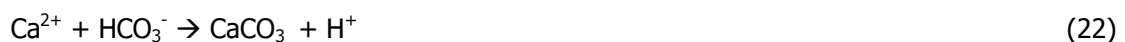
The backward reaction rate was defined as defined as:

$$r_{prec} = r_4 = k_4(Ca^{2+})(HCO_3^-) \tag{23}$$

in which:

16

r_4 = surface area rates for the backward reaction mmol/cm^2/s
k_4 = surface area rate factor for the backward reaction mmol/cm^2/s
(Ca^{2+}) = activity of Ca^{2+} -
(HCO_3^-) = activity of HCO_3^- -

By equating the backward reaction rate r_4 with the sum of the forward reactions of (21), the factor k_4 can be expressed as assuming that the :

$$k_4*(Ca^{2+})(HCO_3^-) = k_1*(H^+)_s + k_2*(H_2CO_3)_s + k_3*(H_2O)_s$$

$\Rightarrow$ $k_4 = [k_1*(H^+)_s + k_2*(H_2CO_3)_s + k_3*(H_2O)_s]/[(Ca^{2+})(HCO_3^-)]$

$\Rightarrow$ $k_4 = \{k_1 + [k_2*(H_2CO_3)_s + k_3*(H_2O)_s]/(H^+)_s\}*[(H^+)_s(CO_3^{2-})_s/(HCO_3^-)_s]/[(Ca^{2+})(CO_3^{2-})]$

where K_2 and K_c are equilibrium constants for $HCO_3^- = H^+ + CO_3^{2-}$ and $CaCO_3 = Ca^{2+} + CO_3^{2-}$ respectively, hence:

$K_2 = (H^+)_s(CO_3^{2-})_s/(HCO_3^-)_s$

$K_c = (Ca^{2+})(CO_3^{2-})$

$\Rightarrow$ $k_4 = \{k_1 + [k_2*(H_2CO_3^*)_s + k_3*(H_2O)_s]/(H^+)_s\}*K_2/K_c$ (24)

Substitute (22) into the total surface rate, the surface rate for unaerated system is achieved:

$\Rightarrow$ $r = r_{diss} - r_{prec} = r_{diss}*[1-(Ca^{2+})(CO_3^{2-})/K_c]= r_{diss}*(1 - \Omega) = r_{diss}*(1-10^{SI})$ (25)

Since $(Ca^{2+})(CO_3^{2-})/K_c = IAP/K_c = \Omega = 10^{SI}$

This equals for the backward reaction:

$\Rightarrow$ $r_{prec} = r_{diss *} \Omega$ (26)

Equation (26) represents the unaerated system cases where pCO_2 could be varied. In aerated system where pCO_2 is a constant, the backward reaction rate is approximately (PHREEQC User guide 1999, p. 43+44):

$r_{prec} = r_{diss *} \Omega^{2/3}$ (27)

$\Rightarrow$ $r = r_{diss} - r_{prec} = r_{diss}*(1 - \Omega^{2/3}) = r_{diss}*(1-10^{(2/3)SI})$ (28)

Chou model:

In 1989, by measuring the dissolution rate of several carbonate minerals in a fluidized bed reactor, filled with mineral particle of 0.35 − 0.40 mm, Chou had come to suggest a change for the PWP model with different backward reaction and specific fitted values of k_1, k_2 and k_3 and k_{-3} for different carbonate minerals (Calcite, Aragonite, Witherite and Magnesite).

The newly adopted dissolution/precipitation reactions by Chou are shown:

$MCO_3 + H^+$ = $M^{2+} + HCO_3^-$ (Forward rate: k_1, backward rate k_{-1}) (29)
$MCO_3 + H_2CO_3$ = $M^{2+} + 2HCO_3^-$ (k_2, k_{-2}) (30)
MCO_3 = $M^{2+} + CO_3^{2-}$ (k_3, k_{-3}) (31)
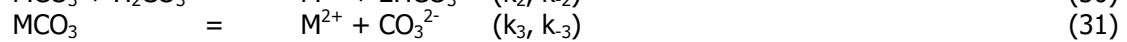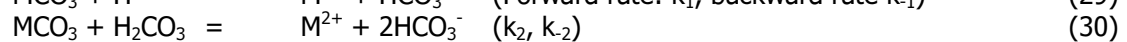
Therefore, the total backward rate is given by the sum of the three backward rates:

$R_b=k_{-1}*(M^{2+})(HCO_3^-) + k_{-2}*(M^{2+})(HCO_3^-)^2 + k_{-3}*(M^{2+})(CO_3^{2-})$ (32)

For each reaction, the equilirium constant implies:

$$K_i = k_i/k_{-i} \tag{33}$$

Hence the backward rate constants could be calculated from the equilibrium constant and the fitted forward rate constants. However, for calcite, by plotting all three components of the total backward rate into one graph, it is obvious to see that the backward rate only becomes significant once the calcite dissolution rate reaching close to the equilibrium level (pH > 7).
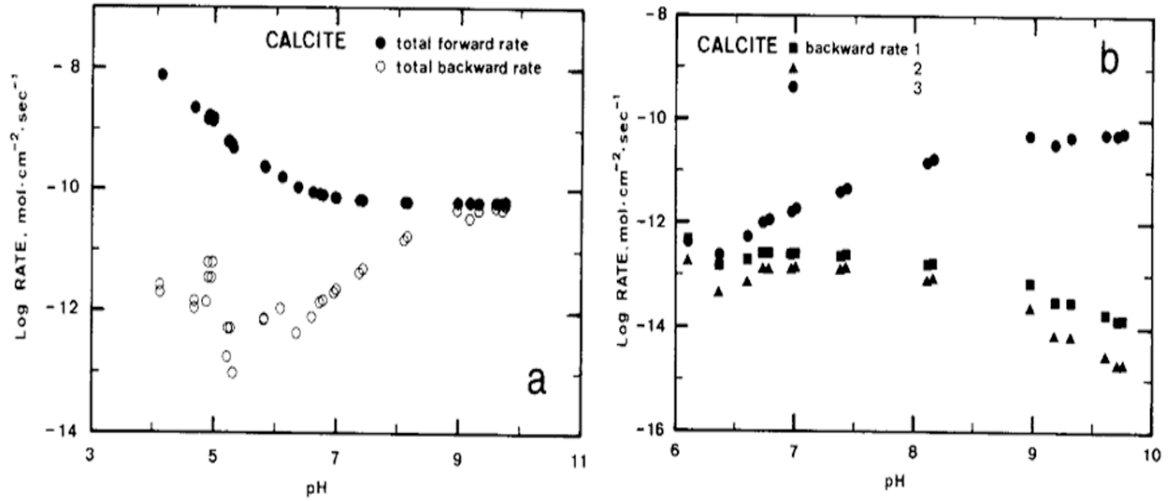
Figure 7: a. The total forward and backward rates of calcite dissolution reactions as a function of pH
      b. The relative contribution of the three backward rates to the total backward rate at pH>6
(Chou et al., 1989)

At this stage, the backward rates of reaction (29) and (30) are just minor compared to (31). Therefore, the backward rate recommended by Chou could be simplified as:

$$r_{-3} = k_{-3}*(Ca^{2+})(CO_3^{2-}) \tag{34}$$

Thus the full net rate equation could be now re-written as:

$$r = k_1*(H^+) + k_2*(H_2CO_3^*) + k_3*(H_2O) - k_{-3}*(Ca^{2+})(CO_3^{2-}) \tag{35}$$

The rate constants determined by Chou for showing best fit with his experiments at 25°C are shown in Table 5.

Table 5: Summary of the values of the kinetics constants (in mmol/cm^{2}s) obtained by Chou for the one-component carbonates at T=25°C

Rate constant	Calcite		Aragonite	Witherite	Magnesite
Formula	CaCO$_3$		CaCO$_3$	BaCO$_3$	MgCO$_3$
Models	Chou	PWP	Chou	Chou	Chou
log k$_1$	-1.05	-1.29	-0.92	-1.12	-5.60
log k$_2$	-4.30	-4.47	-4.40	-4.52	-6.22
log k$_3$	-7.19	-6.92	-7.00	-7.15	-10.35
log k$_{-3}$	2.73	-	2.78	2.69	-2.35

Note that at 25°C, the dissolution constants calculated by PWP model are higher than Chou suggested values for k_1, k_3 while k_2 is lower. The unaerated system dissolution rate of Chou model is similar to PWP except that all rate constants in r_{diss} are now calculated by Chou:

$$r = r_{diss} - r_{prec} = r_{diss}*(1 - \Omega) = r_{diss}*(1-10^{SI}) \tag{36}$$

Chou experiments also showed that magnesite has a surface area rate around 1000 times smaller than other carbonates such as calcite, aragonite and witherite. Thus, the rate of dolomite is between calcite and magnesite (around 10 times smaller than calcite). The assumed mechanism for this is the hindered dissolution of calcite due to the slower dissolution kinetics of magnesite.

Dreybrodt model

Dreybrodt (Buhmann & Dreybrodt, 1985) had suggested three independent processes which mainly controlled the dissolution/precipitation rate:

  i.   The kinetics of dissolution/precipitation at the mineral surface, which is described clearly by the mechanistic rate equation previously suggested by Plummer (PWP equation).
  ii.   The slow reaction $H_2O + CO_2 = H^+ + HCO_3^-$ exerts a significant influences on the rates because stochiometry requires that for each calcium ion released from the solid, one CO_2 molecule must react to form $H^+ + HCO_3^-$. When large mineral surface areas and small volumes of solution this slow reaction can be rate determining.
  iii.   Mass transport of reacting species Ca^{2+}, HCO_3^-, CO_3^{2-}, CO_2 and H_2CO_3 away from and towards the mineral surface by molecular diffusion.

Dreybrodt admitted the PWP equation supplied a sufficient knowledge on the mechanisms at the surface of the limestone with the rate is dependent on the activities of Ca^{2+}, H^+, HCO_3^- and H_2CO_3 and temperature. However, in Plummer experiments, the rate processes were determined under turbulent flow conditions which minimize the rate limiting effects of mass transport on the dissolution process. Moreover, the ratio of volume of the solution to the surface area of the dissolving crystals was so large that CO_2-H_2CO_3 conversion was not rate limiting. Therefore, Plummer suggested equation is only valid for cases where surface reactions are dominant (case (i)). Dreybrodt, however, aimed to set up a model that could take into account all of the three processes above. His experiment (1985) showed that the slow reaction of converting CO_2 play a significant role in calcite dissolution process, where pH is moderate and high, which has not been sufficiently regarded in most studies before his when dealing with calcite dissolution/precipitation. Thus, Dreybrodt assumes the dissolution rate would be driven by the calcite dissolution potential:

$$R = \alpha(c_{eq} - c) \hspace{4cm} (37)$$

Where α = kinetics constant $(cm.s^{-1})$
        c_{eq} = calcium concentration in the solution at equilibrium $(mmol.cm^{-3})$
        c = actual calcium concentration $(mmol.cm^{-3})$

Liu and Dreybrodt (Dreybrodt et al., 1996) also indicated CO_2 conversion tends to be more rate limiting when it happens mainly in the thick diffusion boundary layer (DBL) (above 10^{-3} cm) around the solid surface (mostly laminar flow condition or turbulent layer << DBL) and high pCO_2 (above 0.01 atm).

Besides, Dreybrodt also validated the empirical rate equation type suggested by Palmer (Svensson & Dreybrodt, 1992):

$$c/c_{eq} < x_s : \hspace{1cm} r_1 = k_1(1-c/c_{eq})^{n1} \hspace{3cm} (38)$$
$$c/c_{eq} \geq x_s : \hspace{1cm} r_2 = k_2(1-c/c_{eq})^{n2} \hspace{3cm} (39)$$

where r_1, r_2 = dissolution rate $(mmol/cm^2/s)$
        k_1, k_2 = rate factor $(mmol/cm^2/s)$
        n_1, n_2 = rate order -
        x_s = approaching-saturation (rate limiting) level

With n_1 ranging from 1.5 to 2.2 depending on pCO_2, $n_2 \approx 4.0$, $x_s \approx 0.8$ or can be determined by:

$$x_s = 1 - (k_2/k_1)^{[1/(n1 - n2)]} \tag{40}$$

In Vosbeck's experiment, the measured values on Baker calcite dissolution has been used for fitting Dreybrodt model (equation (38) and (39)) so that specific sets of (k_1, k_2) and (n_1, n_2) for different pCO_2 could be determined as shown in Table 6. One of the curve fitting is shown in Figure 8.

Table 6: Parameters for Dreybrodt model with 7 experiments on Baker calcite (T=10 ^{o}C)

pCO_2	$k_1 \ast 10^7$	n_1	x_s	$k_2 \ast 10^7$	n_2
atm	mmol/cm^2/s	-	-	mmol/cm^2/s	-
0.0003	1.7	1.25	0.46	2.3	2.1
0.001	1.3	1.10	0.55	3.6	2.1
0.005	1.3	0.64	0.90	200	2.5
0.01	0.82	0.56	0.88	6.6	1.5
0.03	0.72	0.73	0.91	39	1.7
0.05	0.73	0.81	0.91	3.2	1.4
0.1	0.99	1.00	0.94	9.3	1.4
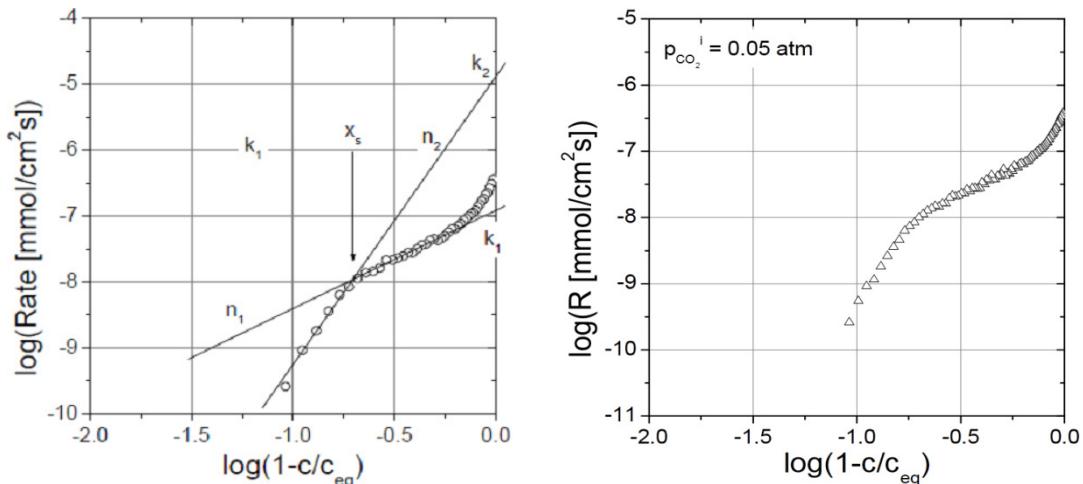
Figure 8: Curve fitting for the Dreybrodt model (left) and measured dissolution rates for pCO_2 = 0.05atm (right) of acidized Juraperle (Vosbeck, 2004)

The table shows hardly any constituent values for the parameters over 7 experiments. Moreover, the ignorance of the high initial dissolution rate in the process fitting might lead to an overestimate of the time consuming for dissolution process in other application. Thus, the Dreybrodt model could not be implied for widely practical application for other water qualities.

Dreybrodt on PWP-Chou model

The results of his experiment in aerated systems showed that the dissolution rates of all natural materials are lower than those of synthetic pure calcite with increasing deviations between the rates when thermodynamic equilibrium is approached. Applying Plummer model to predict the experimental rates, Dreybrodt concluded that Plummer model is in a reasonable agreement for synthetic pure calcite cases (Figure 9) although the difference might increase close to solution's equilibrium. On the other hand, the deviations for natural samples are dramatic. Besides, the rate of natural specimens could be beyond the limit of detection when it is close to equilibrium.
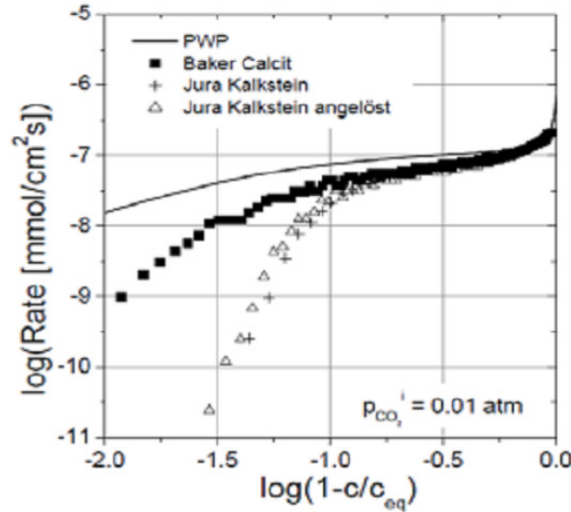
Figure 9: Dissolution rates calculated with the PWP model and measured rates in Vosbeck experiments (pCO$_2$=0.01 atm, T=10 ^{o}C) (Vosbeck, 2004)

2.6.4.   Chosen model to be improved for limestone contactor

PWP and Chou model (unaerated system) are both suitable theoretical models to be improved in this study because limestone contactor is a unaerated system (pCO$_2$ is not constant). Furthermore, the water condition is turbulent hence mass transport is not rate limiting. As a result, the main constrained mechanism is the surface reaction which is well described by PWP-Chou model for unaerated system:

$$R = r_{diss} - r_{prec} = r_{diss}*(1-10^{SI})^n \tag{41}$$

With r_{diss} calculated by PWP or Chou, n is the dissolution rate order which varies for different calcite quality.

However, Plummer (L. N. Plummer, Busenberg, E., 1999) admits that the k$_3$ constant of Chou is better than k$_3$ from the PWP model so he used this newly improved k$_3$ (only available at 25°C) and the backward reaction adopted by Chou could as well be applied in his model. Besides, Plummer claims that PWP model is not suitable for describing the calcite dissolution/precipitation near the equilibrium, but also states there is no other theoretical models have better results.

All in all, PWP model would be accepted in this study as the basic theoretical root with all the proven knowledge background. Since Chou tested model at 25°C for Calcite provides a better set of rate constants (k$_1$, k$_2$, k$_3$ and k$_{-3}$) which is more accurate to be applied in PWP model, the Chou parameters will be extended in this study for different temperatures beside 25°C by applying the PWP rate constant's variation over temperature function for Chou's constant. There are generally two methods to express Chou rate constants over temperature range following PWP relations: by multiplying correction factor and direct shift δ (Van't Hoff relation) for the logarithm curve of the rate constants. The direct shift method is chosen for this study due to its better capture of the original variation of PWP rate constants over temperature (see detail in Annex B.1). Hence the Chou's rate constant could be expressed as a function of temperature as followed (in terms of mmol/cm^{2}s):

$$\log k_1 \quad = -1.29 + 444*(1/298.15 - 1/T) \tag{42}$$

$$\log k_2 \quad = -4.47 + 2177*(1/298.15 - 1/T) \tag{43}$$

$$\log k_3 \quad = -6.92 + 317*(1/298.15 - 1/T) \qquad \text{for } T \leq 298.15 \text{ K} \tag{44}$$

$$\quad = -6.92 + 1737*(1/298.15 - 1/T) \qquad \text{for } T > 298.15 \text{ K} \tag{45}$$

21

This new model is now entitled as PWP-Chou model due to the combination of these two.

The improved variation of rate constants over temperature is shown in Figure 10:
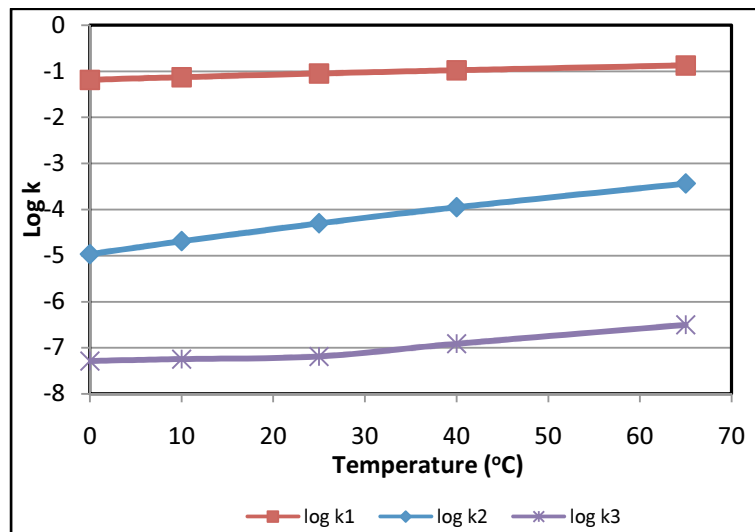
Figure 10: Rate constant variation over temperature (PWP-Chou model)

3. Computer-based model development

3.1. Vosbeck experiment

3.1.1. Introduction

In 2004, Vosbeck introduced her experiment results on measuring the dissolution rates of synthetic calcite and natural limestone under different boundary conditions. Her experiments were focused on determining the influence of initial pCO_2, temperature, dissolved foreign ions and material on the dissolution kinetics of calcium carbonate. Her data sets could significantly contribute in our study on improving the theoretical models (PWP and Chou) to capture the practical dissolution process of different calcite qualities.

In her batch experiments, free-drift method was chosen for measuring dissolution rates in a closed system (unaerated system) condition with certain initial pCO_2. Through the experiments, Vosbeck also validates the Dreybrodt model to be applicable for all measured dissolution rates and suggests different sets of kinetics parameters n_1, n_2, k_1, k_2 and x_s for every set of different boundary conditions including initial pCO_2, different material qualities, foreign ion concentration and temperature. Besides, PWP model was proved to be quite close to the dissolution rates of synthetic calcite (Baker Calcite) but not other types such as Juraperle, acidized Juraperle representing natural limestone which might causes inhibition of dissolution due to foreign ions. The inhibition effects could also happen in experiments with natural water or solution containing foreign ions.

In this study, the focused range for equilibrium alkalinity content is 0.5 - 2.0 meq/L. In order to achieve these three levels, the initial partial pressure of carbon dioxide CO_2 required in an unaerated system such as limestone contactor would be approximately from 0.0047 to 0.02 atm correspondingly. As a result, there are only three sets of Vosbeck data falling in this range: pCO_2 = 0.005; 0.01 or 0.03 atm. The recorded data from Vosbeck experiments with Baker calcite and acidized Juraperle for these sets of initial pCO_2 is shown in Annex B.6.

3.1.2. Best fitting curve on Vosbeck's measured data

The Vosbeck's measured data for each experiment is believed to be sufficiently simulated by the empirical Dreybrodt model. However, the best Dreybrodt fit curve still underestimates the dissolution rate near equilibrium. Besides, the kinetics empirical parameter sets with mean and standard deviation values are generally vague to be applied in practice.
The best fitted curve (red curve) for Vosbeck data is shown in Figure 11 which is plotted from a high order polynomial equation. High order polynomial fitted curves would be used in our study in order to compare with the results generated by the improved models in this study.
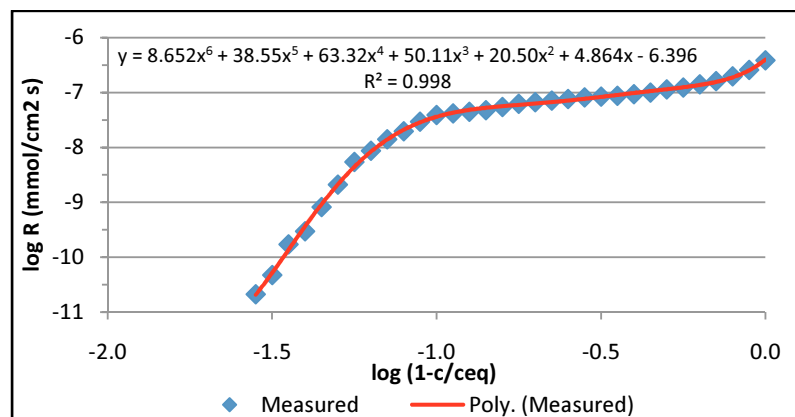
Figure 11: Measured dissolution rates and the high polynomial fitted curve (pCO₂ = 0.01 atm, acidized Jura Limestone)

Since the Vosbeck graphs are provided in dissolution rate over calcium content in logarithm scale which is highly sensitive to any small changes in the rate and the content values. Thus, it is extremely hard to have any models that generate the exact same rate curves. Consequently, comparing with other practical graphs such as pH, SI, Ca and alkalinity content over time scale is a better approach to find out the best simulated models. PHREEQC would be useful to generate those practical graphs giving an assumption of (A/V) ratio since dC = R*(A/V)*dt. Therefore, an accurate input for PHREEQC of the measured Vosbeck data must be available which is no other than the best fit polynomial curves introduced above.

Assuming A/V = 90,000 cm^2/L and input the polynomial fitting data of dissolution rates against Ca content into PHREEQC, PHREEQC would be able to generate important practical graphs of pH, SI, Ca and alkalinity which were not directly provided by Vosbeck.

3.2. PHREEEQC models for calcite dissolution

3.2.1. Aerated system model- PHREEQC default model

In PHREEQC, the default embedded model for calcite dissolution in PHREEQC.dat database is the PWP model from Plummer and others (L. N. Plummer et al., 1978a). However, the model's equation appears in the code is the same as equation (28). This actually originates from the original PWP equation for surface reaction rate:

$$r = k_1*(H^+) + k_2*(H_2CO_3) + k_3*(H_2O) - k_4*(Ca^{2+})(HCO_3^-)$$ (46)

The dissolution rate (or forward rate) r_{diss} contains the first three terms of equation (44). On the other hand, the precipitation rate (or backward rate) r_{prec} contains the last term. In pure water-calcite system, bicarbonate concentration is approximately equal to twice the calcium concentration hence; the backward rate could be approximated as:

$$r_{prec} = k_4*(Ca^{2+})(HCO_3^-) \approx 2k_4*(Ca^{2+})^2$$ (47)

At equilibrium, (Ca^{2+}) is the activity at saturation $(Ca^{2+})_s$. Also r = 0 at equilibrium, so:

$\Rightarrow$ $r_{diss} = r_{prec}$
$\Rightarrow$ $r_{diss} = 2k_4*(Ca^{2+})_s^2$
$\Rightarrow$ $2k_4 = r_{diss} / (Ca^{2+})_s^2$ (48)

By substitute (38) into (36), the following equation is achieved:

$$r = r_{diss}\left\{1 - \left[\frac{(Ca^{2+})}{(Ca^{2+})_s}\right]^2\right\}$$ (49)

In pure CO_2 and calcite system at a constant CO_2 partial pressure (aerated system), the ion activity product (IAP) and equilibrium constant for Calcite is:

$$IAP_{calcite} = \frac{(Ca^{2+})(HCO_3^-)^2}{pCO_2} \approx \frac{4(Ca^{2+})^3}{pCO_2}$$ (50)

$$K_{calcite} \approx \frac{4(Ca^{2+})_s^3}{pCO_2}$$ (51)

Consequently, the calcite dissolution/precipitation rate of PWP model could be approximated as following in an aerated system (open system):

$$r \approx r_{diss}\left\{1 - \left[\frac{IAP}{K_{calcite}}\right]^{2/3}\right\} = r_{diss}\{1 - \Omega^{2/3}\} = r_{diss}\{1 - 10^{SI*(2/3)}\}$$ (52)

24

This is the default equation for calcite kinetics in PHREEQC which consist of the forward reaction rate and the calcite SI in the solution. It is much simpler compared to the full equation with k_4 term which depends on the solution compositions. It is also important to notice that the default calcite dissolution model is only for aerated (open) systems where the ion activity of bicarbonate is twice calcium activity. Besides, the full PWP model with equation (46) is not readily available in the PHREEQC.dat database; hence, extra code needs to be introduced in PHREEQC input file. The extra inputted code lines are shown in Annex B.7.

However, in Annex B.7, it has been shown that different results are generated by applying equation (46) and (52) in PHREEQC simulation for the same problem. This could be due to the assumption that the bicarbonate activity must be twice the calcium activity of the PHREEQC default model. In fact, the bicarbonate activity is not approximately twice the calcium activity by checking PHREEQC output file of the default model simulation at any state which might be due to the calculation sequences of PHREEQC. Consequently, the assumption is invalid and the PHREEQC default model is not very accurate for aerated system. Thus, the full PWP model is recommended in case of aerated system.

3.2.2. Unaerated (closed) system model

As mentioned, the default embedded model for calcite dissolution/precipitation in PHREEQC.dat database is only for the aerated (open) system with the surface rate equation in terms of SI and forward rate as shown in equation (52). Thus, new code needs to be introduced in the input file for the problem of unaerated systems such as the limestone contactor process. The full PWP model could be a solution to these systems. Furthermore, a more simplified model's equation similar to the default model equation, which only depends on the forward reaction rate and the calcite SI, could also be developed from the original full PWP model equation:

$$r = k_1*(H^+) + k_2*(H_2CO_3) + k_3*(H_2O) - k_4*(Ca^{2+})(HCO_3^-) \tag{53}$$

Where $r_{diss} = k_1*(H^+) + k_2*(H_2CO_3) + k_3*(H_2O)$
$\qquad r_{prec} = k_4*(Ca^{2+})(HCO_3^-)$

At equilibrium: $r = 0$ or $r_{diss} = r_{prec}$

$\Rightarrow \quad k_4*(Ca^{2+})_s(HCO_3^-)_s = k'_1*(H^+)_s + k_2*(H_2CO_3)_s + k_3*(H_2O)_s$
$\Rightarrow \quad k_4 = [k'_1*(H^+)_s + k_2*(H_2CO_3)_s + k_3*(H_2O)_s]/[(Ca^{2+})_s(HCO_3^-)_s]$
$\Rightarrow \quad k_4 = \{k'_1 + [k_2*(H_2CO_3)_s + k_3*(H_2O)_s]/(H^+)_s\}*[(H^+)_s(CO_3^{2-})_s/(HCO_3^-)_s]/[(Ca^{2+})_s(HCO_3^-)_s]$

$\Rightarrow \quad k_4 = \{k_1 + [k_2*(H_2CO_3^*)_s + k_3*(H_2O)_s]/(H^+)_s\}*K_2/K_c \tag{54}$

With K_2 and K_c are equilibrium constants for $HCO_3^- = H^+ + CO_3^{2-}$ and $CaCO_3 = Ca^{2+} + CO_3^{2-}$ respectively, the subscript (s) denotes the activity at the adsorption layer (between crystal surface and boundary layer), assumed that the H^+ concentration in the bulk flow is approximate the concentration at the boundary layer (hence $k'_1 = k_1$).

Therefore, the full equation for PWP model as (51) could be re-written with only three dependent rate constants: k_1, k_2 and k_3.

For the simplified model, substitute (52) into (51), the following equation is achieved:

$$r = r_{diss} - \{k_1*(H^+) + (H^+)*[k_2*(H_2CO_3) + k_3*(H_2O)]/(H^+)_s\} *K_2*(Ca^{2+})(HCO_3^-)/(K_c*(H^+))$$

with: $\quad K_2 = (H^+)(CO_3^{2-})/(HCO_3^-)$

$\qquad K_c = (Ca^{2+})_{eq}(CO_3^{2-})_{eq}$

$$IAP/K_c = (Ca^{2+})(CO_3^{2-})/K_c = \Omega = 10^{SI}$$

Assume the activities at the bulk fluid is equal to at the adsorption surface or $(H^+) = (H^+)_s$

$\Rightarrow \quad r = [k_1*(H^+) + k_2*(H_2CO_3) + k_3*(H_2O)]*(1 - \Omega) = r_{diss}*(1-10^{SI})$ (55)

Equation (55) would be introduced in the new code into the input file for the problem of unaerated system as shown in Annex B.7.

Now applying both full model and simplified model for the same case of calcite dissolution with the following initial conditions: demineralised water with insignificant of mineral and bicarbonate content, initial pCO_2 of 0.01 atm and A/V ratio of 90,000 cm^2/L. Both simulations' results are plotted in Annex B.7 for the ease of comparison. From those figures, it is clear to see that the simulation results by the full PWP model as well as the simplified model are approximately the same. Therefore, for unaerated systems where the solution pCO_2 is not constant, the simplified model could be used to replace for the full PWP model. Thus, simplified PWP model would be the base for further improvement in this study.

3.2.3. Improved PWP-Chou model for Baker calcite dissolution

By plotting the results of the existing PWP model for different cases of initial pCO_2 and comparing with the best fitted measured data of Vosbeck as shown in the following figure in term of pH over time, it is obvious that the PWP model's simulated result is still far from the measured data. As a result, the existing PWP model needs to be further improved. The logarithm scale graph of Calcium content against the dissolution rate clearly shows an enormous difference between the theoretical model and practical experiment, which is partially due to the high sensitivity of the log scale applied for the axes. Hence, the main comparison would be focused on other parameters (SI, pH, Ca).
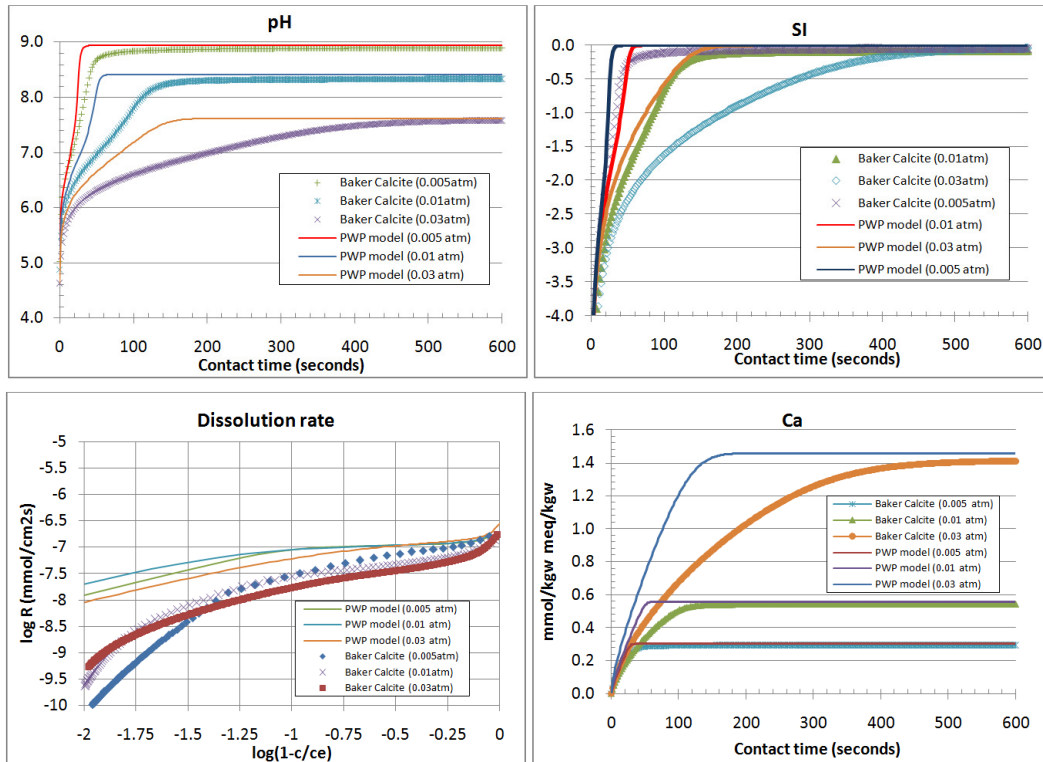
Figure 12: PWP model vs. Vosbeck experiment on Baker Calcite dissolution

For the PWP-Chou model, a similar derivation could be made to achieve the simplified version which only depends on calcite SI as shown as equation (56). The full expression for k_{-3} could be derived from the condition at equilibrium point:

$$k_{-3}*(Ca^{2+})(CO_3^{2-}) = k_1*(H^+)_s + k_2*(H_2CO_3^*)_s + k_3*(H_2O)_s$$
$$\Rightarrow \quad k_{-3} = [k_1*(H^+)_s + k_2*(H_2CO_3^*)_s + k_3*(H_2O)_s]/[(Ca^{2+})(CO_3^{2-})]$$
$$\Rightarrow \quad k_{-3} = [k_1*(H^+)_s + k_2*(H_2CO_3^*)_s + k_3*(H_2O)_s]/K_c = r_{diss}/K_c \quad (56)$$

Assume the H^+ activity at the bulk fluid is equal to at the adsorption layer, boundary layer. Similar to the PWP model, the full PWP-Chou model's equation could now be re-written with only 3 dependent rate constants k_1, k_2 and k_3.

On the other hand, the simplified equation could be achieved by substituting (56) into (35):

$$\Rightarrow \quad r = r_{diss} - (r_{diss}/K_c)(Ca^{2+})(CO_3^{2-}) = r_{diss}*[1- (Ca^{2+})(CO_3^{2-})/K_c]$$
$$\Rightarrow \quad r = r_{diss}*(1- IAP/K_c) = r_{diss}*(1 - \Omega) \quad (57)$$

Now applying the PWP-Chou model to the sampling case study of calcite dissolution for unaerated system (demineralised water, initial pCO_2 = 0.01 atm and A/V = 90,000 cm^2/L), the simulation results of these models are shown in relative with the PWP model results in the following graphs (Figure 13). Overall, it is clear to notice that the PWP-Chou model takes more time to reach equilibrium level in the same calcite dissolution simulation which is closer to what happens in practice compared to the PWP model. As a result, the PWP-Chou model could be seen as an improvement from the original PWP model with more practical results as shown in the following figure in terms of pH over time. However, it is still underestimate the time for the desalinated water to reach equilibrium stage with Baker calcite dissolution, hence, further improvement is required.
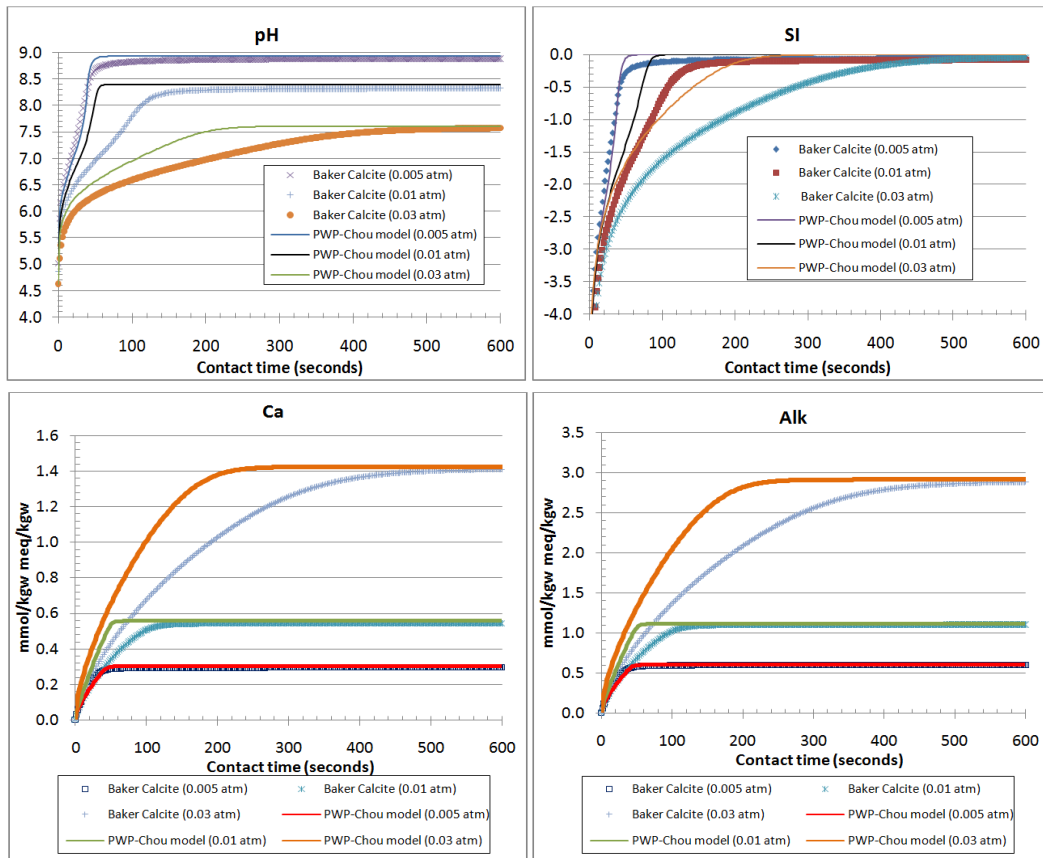
Figure 13: PWP-Chou model vs. Vosbeck experiments on Baker Calcite dissolution

3.2.4. PCM model for synthetic pure calcite (Baker calcite)

Since the improved PWP-Chou model does not capture the measured data from Vosbeck, it is possible to improve the current rate constant k_1, k_2 and k_3. Thus, a new set of rate constants a_1, a_2 and a_3 are now introduced into the PWP-Chou model:

$$r = [a_1*(H^+) + a_2*(H_2CO_3) + a_3*(H_2O)]*(1 - 10^{SI}) = r_{diss}*(1-10^{SI}) \qquad (58)$$

However, trial and error efforts showed that with only three controlling factors, the best simulated equilibrium level is always higher than the measured data; hence, the best simulated model for pure calcite could not be achieved. Therefore, another controlling parameter needs to be introduced. According to Morse suggested model (Morse & Arvidson, 2002), the dissolution rate r_{diss} is proportional to the coefficient $(1-10^{SI})^n$ where n could significantly affect the rate r when SI is approaching zero. It is important to notice that higher n would lead to lower rate coefficient $(1-10^{SI})^n$ hence lower dissolution rate especially significant near equilibrium (SI =0). Besides, the rate lowering effect will extend to a further range from equilibrium for higher n as shown in Figure 14. Thus, higher n decreases the level of the plateaux part of the dissolution kinetics which means the system requires much more time in order to reach the equilibrium point.
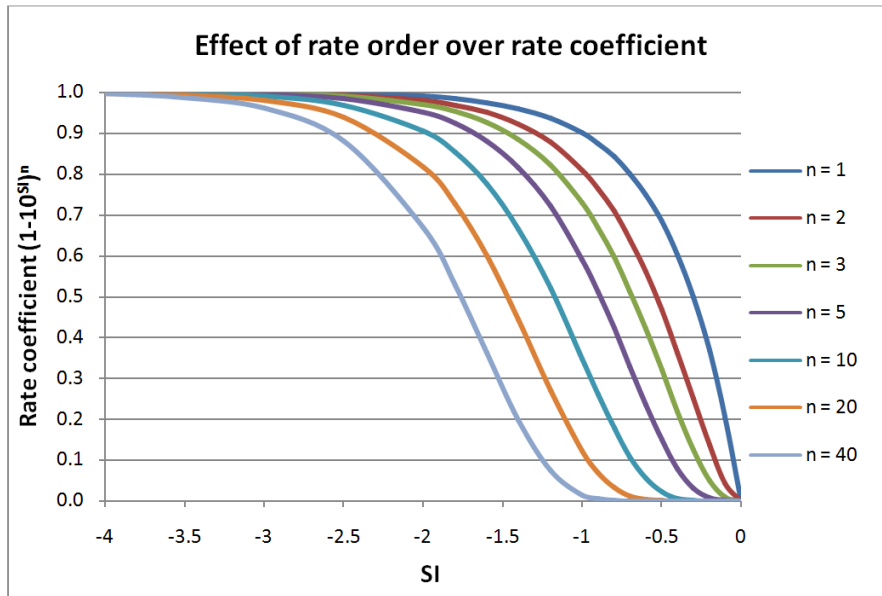
Figure 14: Effect of rate order (n) on rate coefficient over a certain SI range

The new model is entitled as PCM (PWP-Chou-Morse) model is suggested as below:

$$r = [a_1*(H^+) + a_2*(H_2CO_3) + a_3*(H_2O)]*(1 - 10^{SI})^n = r_{diss}*(1-10^{SI})^n \qquad (59)$$

By trials and errors with different values of a_1, a_2, a_3 and n in comparing with Vosbeck's data on Baker calcite, the best set of controlling parameters have been achieved for $pCO_2 = 0.01$ atm at temperature of 10^oC.

Table 7: PCM model's rate constants and order for Baker calcite at $pCO_2 = 0.01$ (t = 10^oC)

Calcite type	Baker
Temperature (ºC)	10
pCO$_2$	0.01
a_1	$4.83*10^{-2}$
a_2	$2.26*10^{-5}$
a_3	$4.25*10^{-8}$
n	3.00

With the above values of controlling parameters, the simulated results of the PCM model capture accurately the Vosbeck measured data's best fit line (Figure 16).

For other initial pCO_2 cases (0.005atm and 0.03atm) at 10^oC, the four specified controlling parameters (a_1, a_2, a_3, n) need correction factors (α_1, α_2, α_3, η) in order to achieve the best fit to the practical data as shown in the following Table 8 and Figure 15. Notice that α_1, α_2 and α_3 would remain constant for other temperatures; only the governing data of a_1, a_2 and a_3 at pCO_2 would be changed and re-calculated on the base of PWP temperature relation. Assuming the main influence of temperature on calcite dissolution lying on the three basic rate constants, additional parameter such as n only plays insignificant role hence only relies on the initial CO_2 content (mmol/L) in water.

Table 8: Correction factor for rate constant and rate order for different pCO_2

pCO_2 (atm)	0.005	0.01	0.03
α_1	2.15	1.00	0.77
α_2	1.09	1.00	0.24
α_3	1.33	1.00	0.85
η	1.03	1.00	0.57
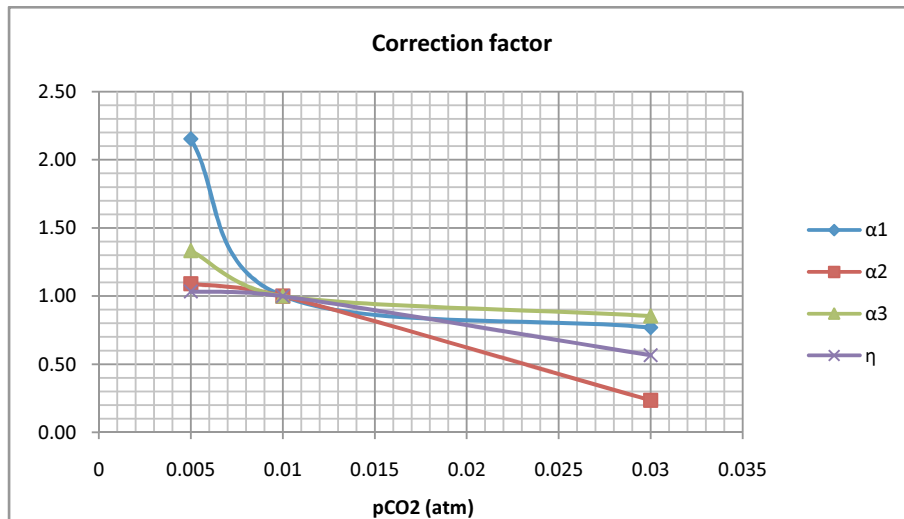
Figure 15: Correction factors of rate constants and rate order for different pCO_2

With the correction factors on those controlling parameters, the simulated results of PCM are generated and plotted on the same graph with the Vosbeck measured data (Figure 16). Overall, all the graphs of practical data (pH, SI, Ca and Alkalinity) clearly indicate that the PCM model for Baker calcite fully captures the practical process. Overall, the PCM model with additional correction factor graphs could be applied for simulating the dissolution process of pure synthetic calcite such as Baker calcite.
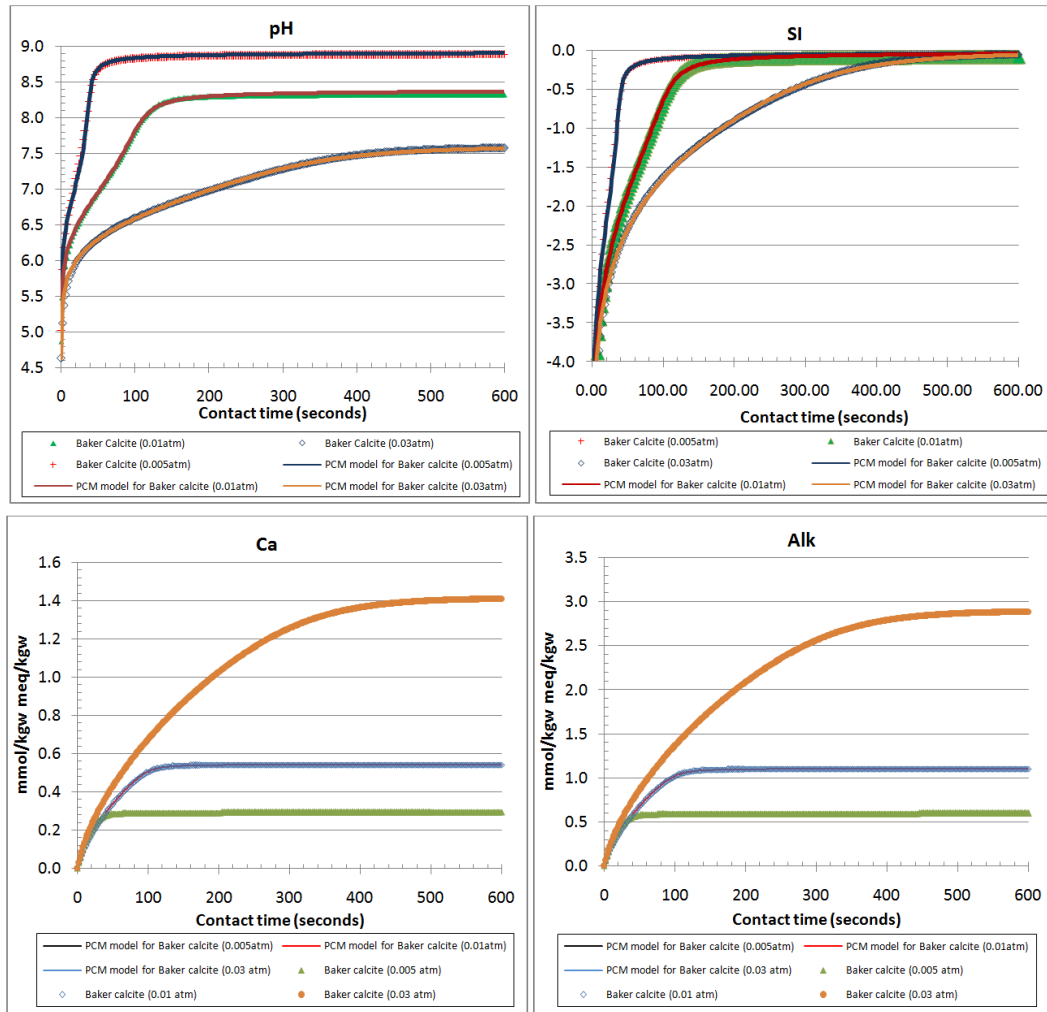
Figure 16: PCM model for pure calcite vs. Vosbeck experiments on Baker Calcite dissolution

The PCM model for pure calcite (Baker calcite) is not only limited to the temperature of Vosbeck experiment (10°C) but also available for a wider range by adopting the PWP temperature dependence relation for the newly introduced rate constants as shown in following equations. Notice that rate order n only influences the dissolution kinetics near equilibrium, hence, is validly assumed to be solely dependent on the initial CO_2 content.

$$\log a_1 = [-1.24 + 444*(1/298.15 - 1/T)] + \log \alpha_1 \tag{60}$$

$$\log a_2 = [-4.26 + 2177*(1/298.15 - 1/T)] + \log \alpha_2 \tag{61}$$

$$\log a_3 = [-7.32 + 317*(1/298.15 - 1/T)] + \log \alpha_3 \quad \text{for } T \leq 273.15 + 25 = 298.15^{\circ}K \tag{62}$$

$$= [-7.32 + 1737*(1/298.15 - 1/T)] + \log \alpha_3 \quad \text{for } T > 298.15^{\circ}K \tag{63}$$

$$n = \eta*3 \tag{64}$$

3.2.5. PCM model for natural calcite (Acidized Juraperle)

The PCM model for pure calcite would be chosen as the base for further improvement to achieve a more practical model for natural calcite (Acidized Juraperle). The same method would be applied by further adjusting 4 parameters a_1, a_2, a_3 and n to find the best fit. First, finding the best fit for the Vosbeck measured data of initial pCO_2 = 0.01atm would be focused on. By adjusting those 4 parameters, the best fit could be found is shown in Figure 17. It is obvious that the PCM model for pure calcite could only simulate correctly the

30

dissolution process of Juraperle in the first 80 seconds. After 80 seconds, the simulated model overestimates the dissolution rate compared to the recorded data. Thus, a further improvement is required.
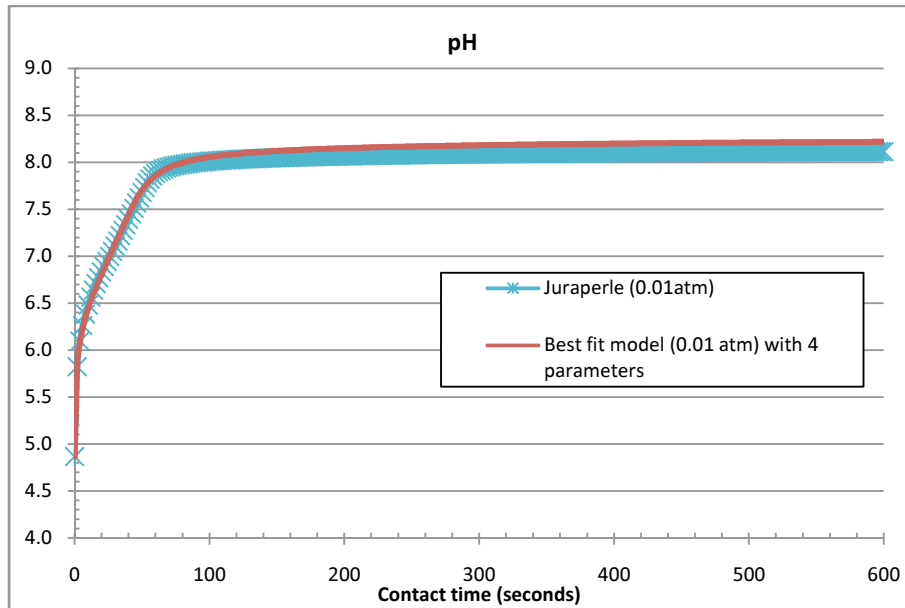
Figure 17: PCM model for pure calcite vs. Vosbeck experiments on Baker Calcite dissolution (pH level)

There are several different approaches have been carried out to obtain the optimized fits for all three cases of different initial pCO_2 including adopting Lasaga model, assuming a pseudo equilibrium SI_e. Unfortunately, these approaches do not provide the best solution as expected which is discussed in detail in the Annex B.7 hence these could be considered as failed attempts.

After trying all those attempts, it is important to notice that our model generates sometimes lower or higher gradient when approaching equilibrium compared to the measured data. This could be fixed by introducing a function for the proportional order n since higher n would lead to lower equilibrium level and otherwise. Hence, n could affect the dissolution rate significantly if $(1-10^{SI})$ is far below 1 meaning SI is close enough to zero or the solution is reaching saturated level. Therefore, a discrete function of n should be introduced to make the dissolution rate of the PCM model lower or higher to capture the measured data.

The discrete equation system for n is:

n	$= n_0$	for	$Ca \leq 0.89 Ca_e$	(65)
	$= n_0*(1+b)$	for	$Ca > 0.89 Ca_e$	(66)
	$= n_0*(1+2b)$	for	$Ca > 0.91 Ca_e$	(67)
	$= n_0*(1+3b)$	for	$Ca > 0.92 Ca_e$	(68)

Where Ca_e : calcium concentration in the saturated solution
       Ca : current calcium concentration in the solution
       n_0 : initial dissolution rate order
       b : increasing factor of n_0

With this function of n, the new PCM model could be entitled as the PCM model for Juraperle calcite. This model consists of 5 parameters (a_1, a_2, a_3, n_o, b) instead of 4. Now applying this for the focal case of Juraperle (0.01 atm), the best fit curves could be found with the following set of 5 controlling parameters:

Table 9: Correction factor for rate constant and rate order for different pCO_2

Calcite type	Juraperle
Temperature (°C)	10
pCO_2	0.01
a_1	$7.06*10^{-2}$
a_2	$4.73*10^{-5}$
a_3	$1.02*10^{-7}$
n	7.5
b	0.13

With the above values of controlling parameters, the simulated results of the PCM model for Juraperle capture accurately the Vosbeck measured data's best fit line. For other pCO_2 (0.005atm and 0.03atm) (at t = 10°C), the 5 controlling parameters (a1, a2, a3, n, b) need correction factors (α1, α2, α3, η, β) in order to achieve the best fit to the practical data:

Table 10: Correction factor for rate constant and rate order for different pCO_2

pCO_2 (atm)	0.005	0.01	0.03
$α_1$	1.05	1.00	0.84
$α_2$	1.22	1.00	0.39
$α_3$	1.06	1.00	0.47
η	4.53	1.00	0.47
β	-0.77	1.00	0.77
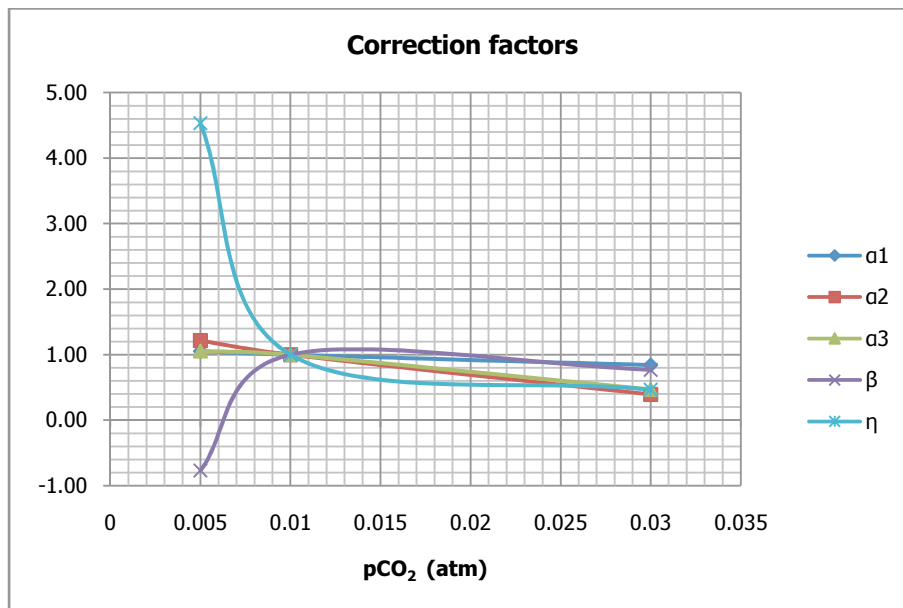
Figure 18: Correction factors of rate constants and rate order for different pCO_2

With the correction factors on those controlling parameters, the simulated results of PCM are generated and plotted on the same graph with the Vosbeck measured data in terms of pH, SI, Ca and Alkalinity content over time as well as calcium concentration against dissolution rate in log scale. The pH graphs clearly indicate that the PCM model for Baker calcite fully captures the practical process. The log scale graph of rate over calcium content does not show the fully match lines of the recorded and the generated data because the log scale graph is very sensitively subjective to any minor numerical differences. Furthermore, the sharp generated angles on the graph represent the external pulse introduced by the discrete function of n. However, the log scale graph of rates versus Ca content is normally not important in practice comparing with other graph such as pH, SI, Ca and Alkalinity content over time. Therefore,

the newly introduced model of PCM could adequately capture the dissolution of Juraperle calcite within the focused range of initial pCO_2 (0.005 – 0.03 atm).

Similar to the PCM model for pure calcite, the version for natural calcite is also available for a wider range of temperature by the temperature relations shown in the below equations.

$$\log a_1 = [-1.07 + 444*(1/298.15 - 1/T)] + \log \alpha_1 \tag{69}$$

$$\log a_2 = [-3.94 + 2177*(1/298.15 - 1/T)] + \log \alpha_2 \tag{70}$$

$$\log a_3 = [-6.94 + 317*(1/298.15 - 1/T)] + \log \alpha_3 \qquad for \qquad T \leq 298.15^o K \tag{71}$$

$$\qquad\quad = [-6.94 + 1737*(1/298.15 - 1/T)] + \log \alpha_3 \qquad for \qquad T > 298.15^o K \tag{72}$$

$$n \qquad = n_0 = \eta*7.5 \qquad\qquad\qquad for \qquad Ca \leq 0.89 \, Ca_e \tag{73}$$

$$\qquad\quad = n_0*(1+b) \;\; = \eta*7.5*(1+\beta*0.13) \qquad for \qquad Ca > 0.89 \, Ca_e \tag{74}$$

$$\qquad\quad = n_0*(1+2b) = \eta*7.5*(1+2\beta*0.13) \qquad for \qquad Ca > 0.91 \, Ca_e \tag{75}$$

$$\qquad\quad = n_0*(1+3b) = \eta*7.5*(1+3\beta*0.13) \qquad for \qquad Ca > 0.92 \, Ca_e \tag{76}$$
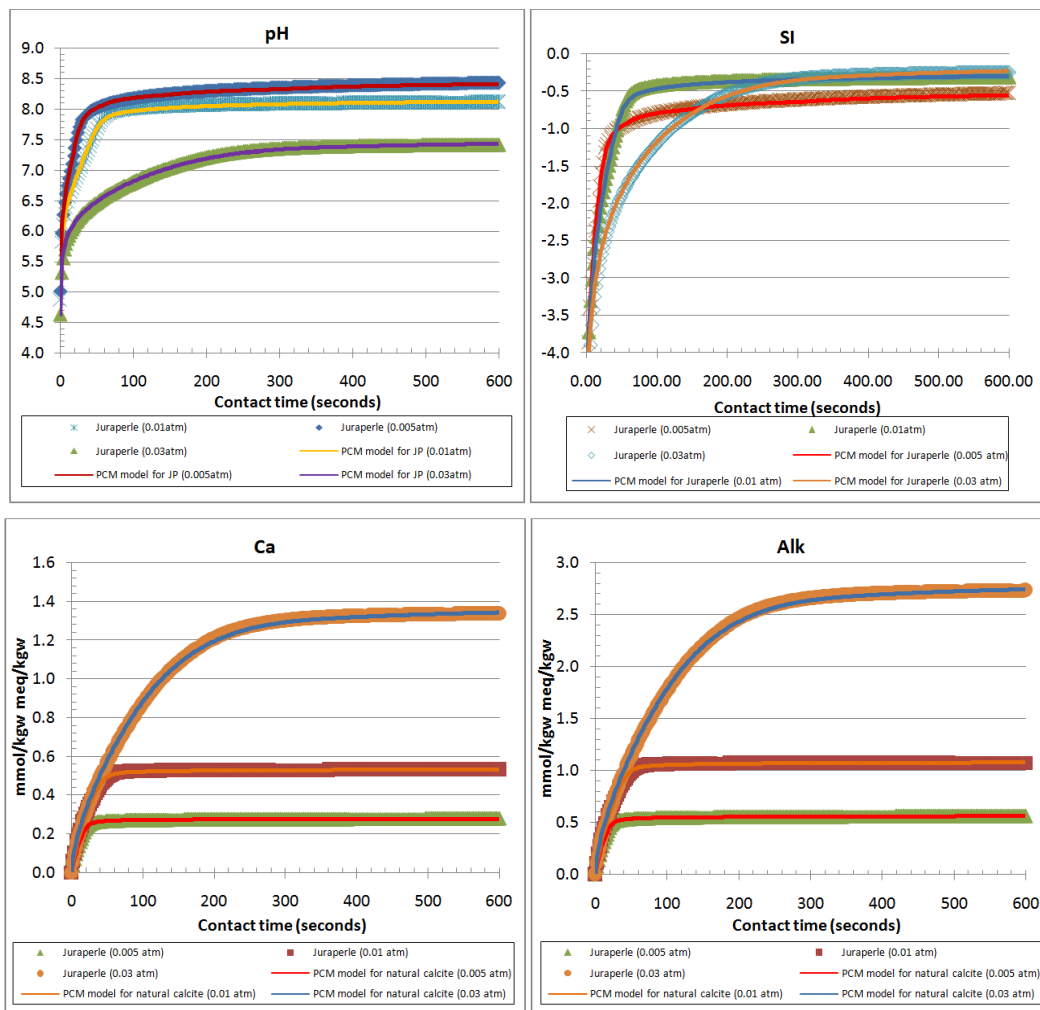
Figure 19: PCM model for natural calcite vs. Vosbeck experiments on Acidized Juraperle dissolution

3.3. Anderlohr experiment

3.3.1. Introduction

The dissolution of natural limestone in a limestone contactor has been studied by Anderlohr (Anderlohr, 1975). He used two tubes in series with length of 2m each containing commercial available crushed and sieved calcite and measurement points are located every 0.2 m along these tubes. Demineralised water is allowed to flow downward through the contactor bed. The experiment outline and relevant information are shown in Figure 20 and Table 11 respectively.

Anderlohr conducted six tests with different initial CO_2 contents or flow rates in the system. The saturation calcium contents in each case are determined by the Heyer test which allows the enormous amount of calcite grains to contact with demineralised water for 24 hours. The dissolution rate was determined by the measured EC (Electrical Conductivity) and partly by measuring calcium and alkalinity. The calcium content at each sample points could then be obtained by these three input parameters.
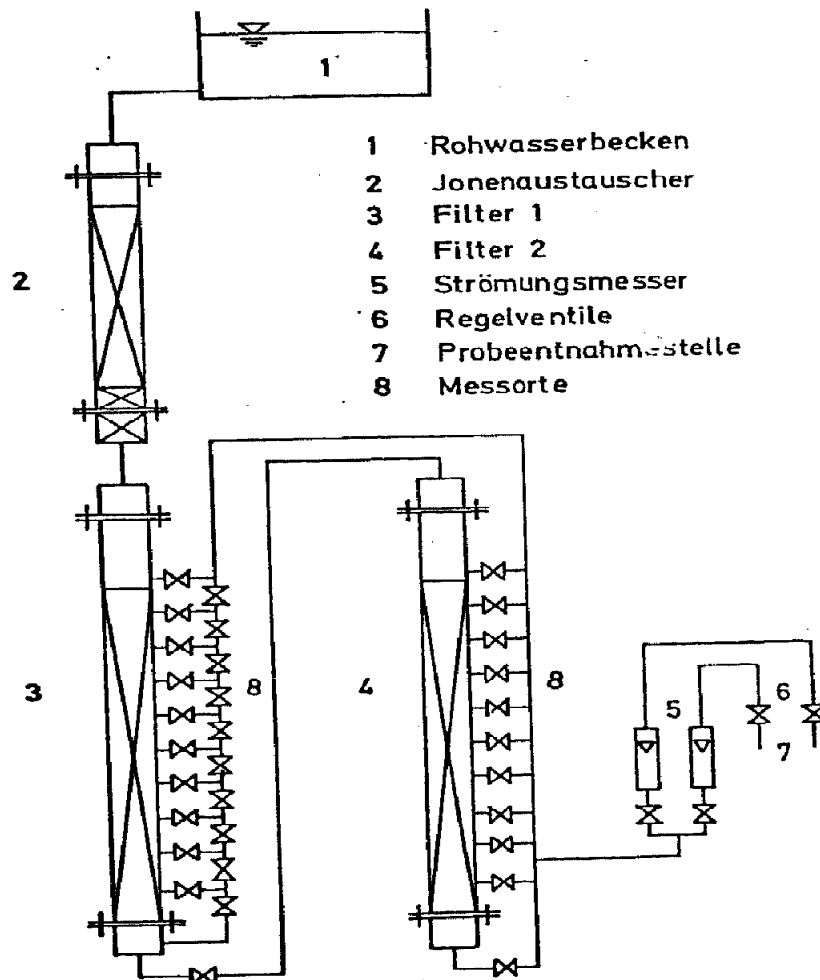
Figure 20: Draft outline of Anderlohr experiment (Anderlohr, 1975)

Table 11: Anderlohr experiment detail information

Tube	Number of tubes	2
	Connecting type	In-Series
	Tubes' inner diameter (mm)	52
	Each tube length (m)	2
	Measurement point's interval (m)	0.2
Filling calcite	Calcite filled length per tube (m)	1.67
	Calcite type	Natural calcite
	Grain diameter (mm)	0.9-1.0
	Filter bed porosity	0.46
Test water	Type	De-mineralized
	Temperature (^{0}C)	20
	CO_2 content (mmol/L)	0.15 -1.3
Water flow	Direction	Downflow
	Filtration rates (m/h)	5, 10, 15

Since this study only focus on the typical range of alkalinity: 0.5 to 2.0 meq/L or 0.25 to 1.0 mmol/L calcium at equilibrium for remineralized water, only test 2, 3 and 5 of Anderlohr would be focused on. The results of each test are shown in the following figures (Figure 21).

Versuch Nr.: 2   Datum: 6.2.75

$v_F = 10$ m/h ; $CO_{2A} = 0,25$ mmol/l ; $Ca_S = 0,295$ mmol/l

Mess-stelle	m - Wert (mmol/l)	Ca^{2+} (mmol/l)	$\varkappa$ (μS/cm)	m -2Ca	$\dfrac{Ca_S - Ca}{Ca_S - Ca_A}$
3	0,55	0,295	51,5	-0,04	o
7			51,5		o "
10			51,5		o "
12	0,55	0,295	51,0	-0,04	o
14			51,0		o "
15			50,8		0,03 "
16	0,53	0,275	50,2	-0,02	0,07
17	0,51	0,265	48,0	-0,02	0,10
18	0,38	0,205	37,2	-0,03	0,305

Versuch Nr.: 3   Datum: 4.2.75

$v_F = 10$ m/h ; $CO_{2A} = 0,50$ mmol/l ; $Ca_S = 0,50$ mmol/l

Mess-stelle	m - Wert (mmol/l)	Ca^{2+} (mmol/l)	$\varkappa$ (μS/cm)	m -2Ca	$\dfrac{Ca_S - Ca}{Ca_S - Ca_A}$
2	1,01	0,50	90,2	-0,01	o
5			90,2		o "
7			90,2		o "
9	1,01	0,50	90,2	-0,01	o
11			90,2		o "
13	1,01	0,50	90,2	-0,01	o
14	0,99	0,495	89,2	-0,02	0,01
15	0,97	0,490	87,3	-0,01	0,039
16	0,93	0,470	83,8	-0,01	0,078
17	0,80	0,415	73,0	-0,03	0,205 "
18			49,0		0,529 "

Versuch Nr.: 5   Datum: 29.1.75

$v_F = 10$ m/h ; $CO_{2A} = 1,18$ mmol/l ; $Ca_S = 1,09$ mmol/l

Mess-stelle	m - Wert (mmol/l)	Ca^{2+} (mmol/l)	$\varkappa$ (μS/cm)	m -2Ca	$\dfrac{Ca_S - Ca}{Ca_S - Ca_A}$
2			182		0,02 "
4	2,06	1,06	180	-0,05	0,028
6			179		0,032 "
8	2,05	1,05	179	-0,02	0,032 "
10			179		0,032 "
12	1,99	1,03	176	-0,01	0,050
14			163		0,124 "
16			133		0,293 "
18			68		0,656 "

Figure 21: Anderlohr's test 2, 3 and 5 measurements (Anderlohr, 1975)

3.3.2. PHREEQC re-simulation of Anderlohr tests

With the help of PHREEQC, the calcium data can be used to calculate the CCDP (Calcium Carbonate Dissolution Potential), pH, SI, CO_2 and EC in each Anderlohr test. Assume the natural calcite used in Anderlohr experiment has the same calcite quality as Vosbeck acidized Juraperle. Since the Anderlohr saturation calcium contents are just practical values, the end point $CCDP_e$ of Anderlohr tests could be assumed to be approximate the CCDP at a certain time in Vosbeck batch experiment for acidized Juraperle. The time at which CCDP of Vosbeck would be extracted, could be reasonably narrowed down by the upper and lower boundary (see Annex C.1). The average CCDP value of these two boundaries is selected for PHREEQC re-simulation of Anderlohr tests. The PHREEQC re-simulated results of the Anderlohr based on the measured data of calcium are shown in Figure 22.
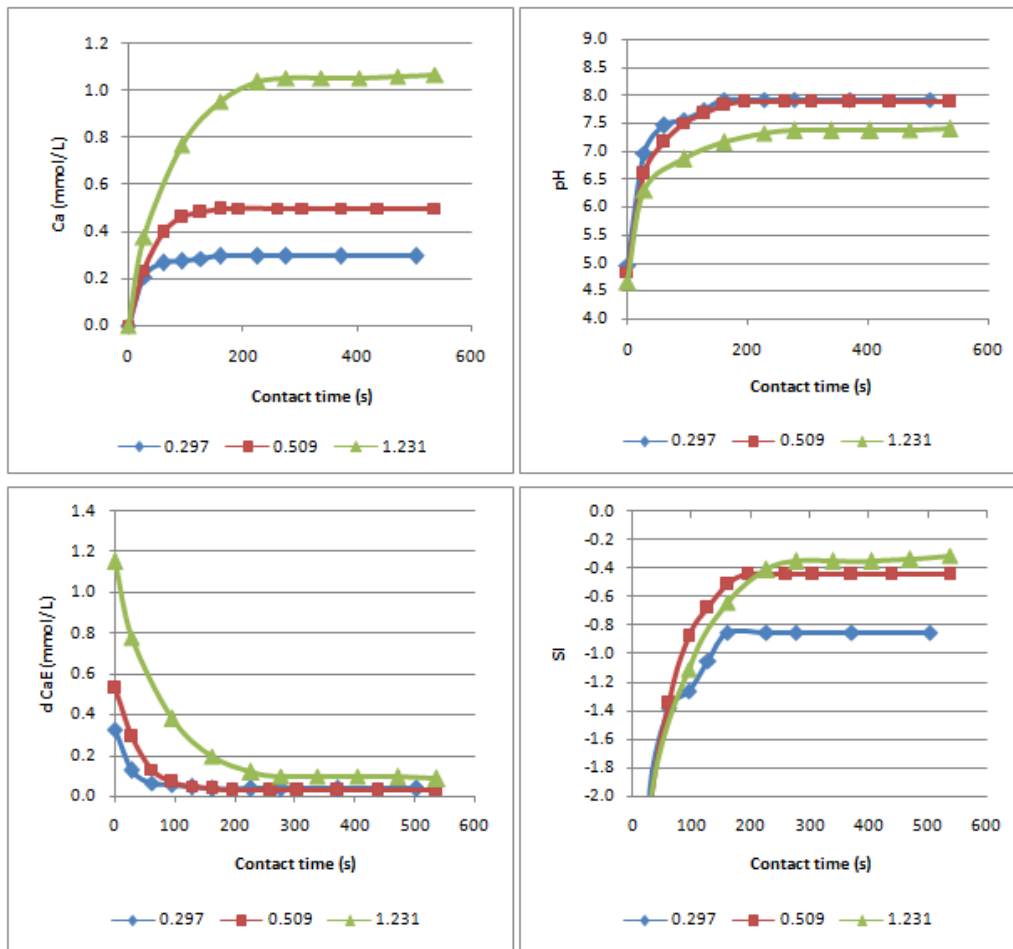
Figure 22: PHREEQC re-simulated results of the Anderlohr tests based on the measured data of calcium

3.3.3. Corrected PCM model for contactor bed

By applying the developed PCM model for natural calcite to simulate Anderlohr tests with two specific grain diameters (0.9 mm and 1.0 mm), the PCM model always generate higher dissolution rates compared to the Anderlohr test results as shown in Figure 23, 24, 25. PCM model results for two diameters are approximately the same even though the smaller grain size seems to have a marginal higher dissolution rates. For Anderlorh tests, SI (and pH) is not accurate enough to be compared since SI is proportional to the logarithm (to base 10) of $[CO_3^{2-}]$ ions, which in turns depend significantly on the initial CO_2 content in the solution. By trial simulation by PHREEQC, it is clear that the initial CO_2 content provided by Anderlohr

which was not measured accurately enough in Anderlohr tests. Besides, the log scale is highly sensitive for even a tiny variant of CO_2 content.
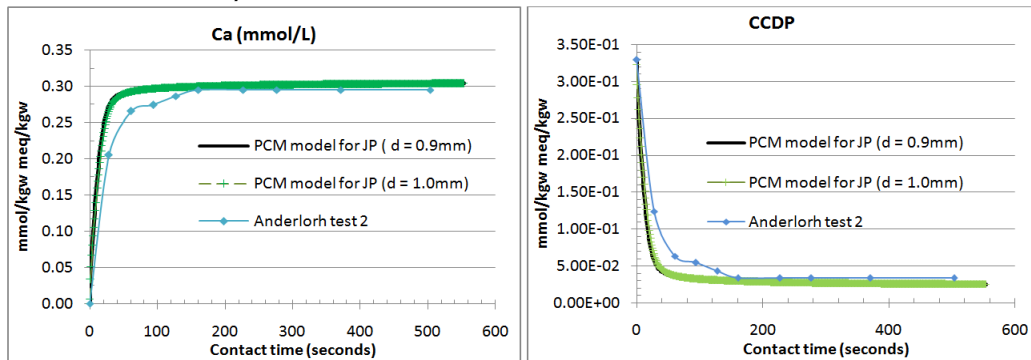
Figure 23: Ca content and solution CCDP of re-simulated Anderlohr test 2 and PCM model simulation
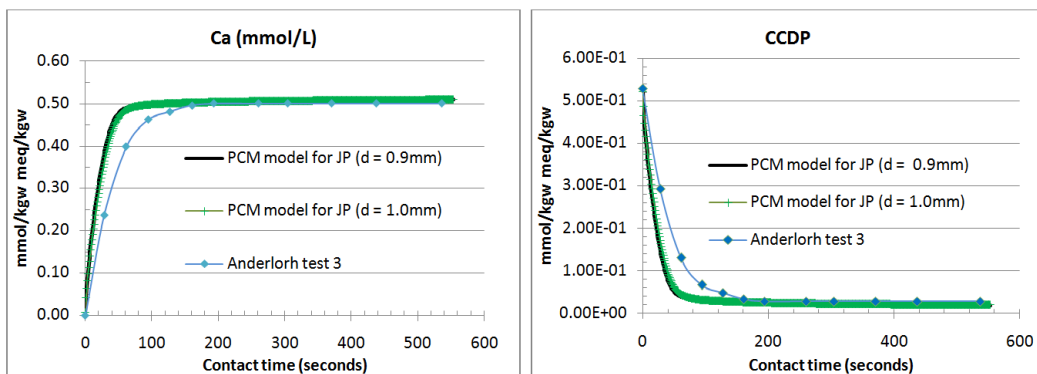
Figure 24: Ca content and solution CCDP of re-simulated Anderlohr test 3 and PCM model simulation
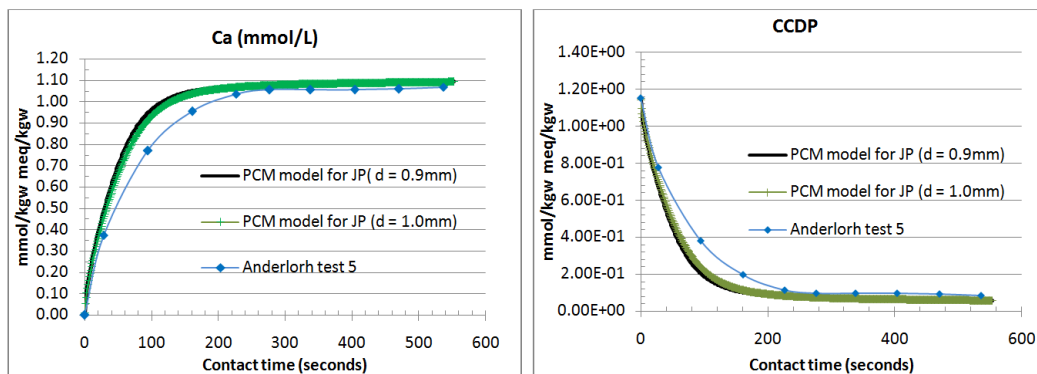
Figure 25: Ca content and solution CCDP of re-simulated Anderlohr test 5 and PCM model simulation

The fact that PCM model simulations have higher dissolution rate compared to Anderlohr tests especially in the first 200 seconds is due to the blockage effects of surface areas occurring in contactor bed of Anderlohr tests but not in Vosbeck experiment type which is represented by PCM model. As previously mentioned, the calcite dissolution rate is proportional to the surface rate and the surface area over solution volume (A/V) ratio. The (A/V) ratio would be much lower in case of contactor bed where calcite grains are packed into layers compared to the batch experiment of Vosbeck where particles are dissolved freely without contacting each other. Thus, a correction factor for (A/V) ratio of PCM model is introduced to compensate (partially) the difference between batch experiment and real limestone contactor condition. The following figures (Figure 26, 27 and 28) show the relative positions of Anderlohr test re-simulated and the corrected PCM model results. Besides, the surface rate could also have a certain influence on the difference between Anderlohr test and PCM simulation since it depends on the diffusion of Alkalinity, Ca^{2+} ions in the solution as well as solution temperature which might not be exactly the same for both contactor bed and batch experiment case. However, these effects are expected to generate minor differences

between two cases compared to the surface area blockage effect which leads to significant differences in (A/V) ratio. Besides, if the filtering water has some other precipitations such as iron or manganese, these products could possibly form in the practical marble filter for some types of extracted water. Consequently, if the forming amount is considerable in the filter, inhibition effects could take place, thus, further decrease the contact surface of the calcite grains. Under these circumstances, the inhibition effect should be taken into account by a lower correction factor for (A/V).
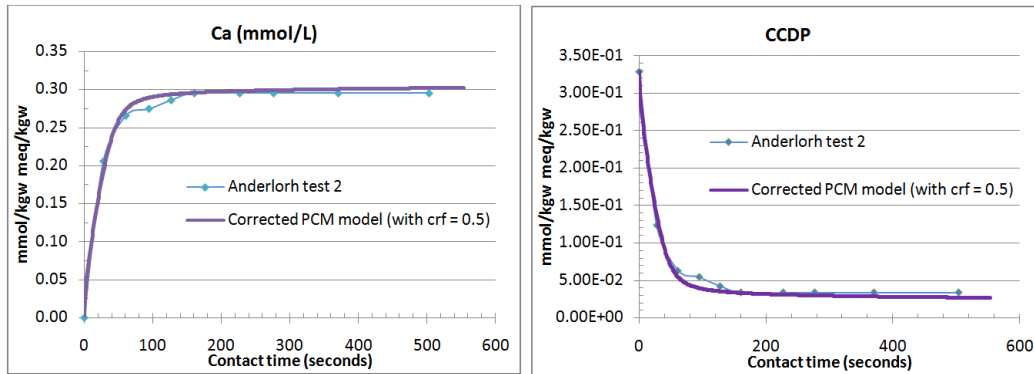
Figure 26: Ca content and CCDP of re-simulated Anderlohr test 2 and corrected PCM model simulation (applying average grain size of 0.95mm)
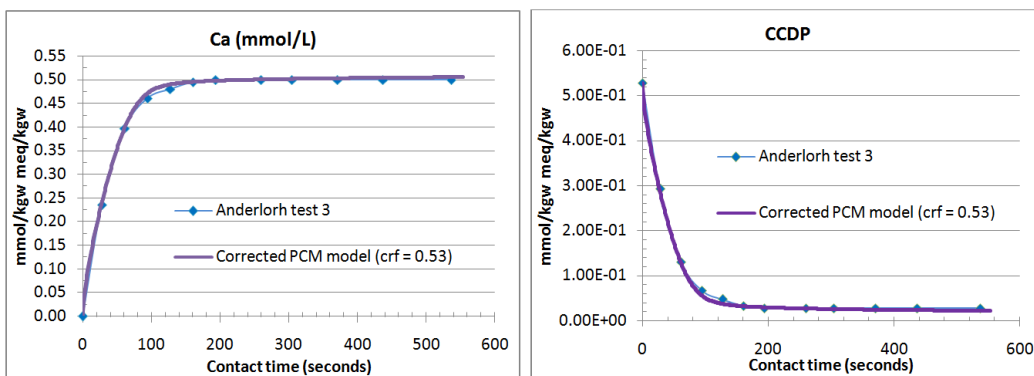
Figure 27: Ca content and CCDP of re-simulated Anderlohr test 3 and corrected PCM model simulation (applying average grain size of 0.95mm)
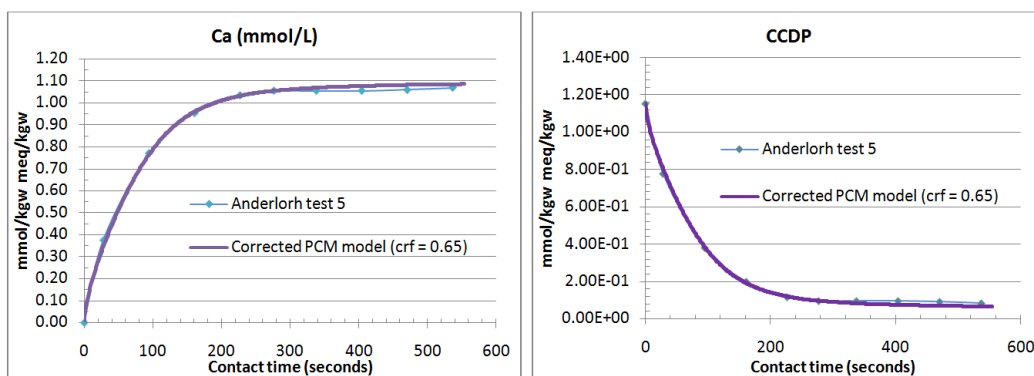
Figure 28: Ca content and CCDP of re-simulated Anderlohr test 5 and corrected PCM model simulation (applying average grain size of 0.95mm)

With the (A/V) correction factor as listed in Table 12, the above figures (Figure 26, 27, 28) show that the PCM model would be improved to closely simulate the result of water solution going through a contactor bed such as in Anderlohr tests. Although there is still a minor difference at the plateau parts, it could be explained by the assumption of the end-point

38

CCDP$_e$ of Anderlohr as well as the possible differences of surface rates between batch experiment and real limestone contactor bed.

Due to the different initial contents of CO_2, the influent water would have different driving force which affects the dissolution process of calcite grains in the contactor bed. Consequently, the dissipated shapes of calcite grains would be affected as well which leads to different blockage effects. Thus, (A/V) correction factor is the not the same for different initial CO_2 content water. Based on Anderlohr test comparison, the (A/V) correction factor for other initial pCO_2 within the concerned range could be read from the plotted graph as shown in Figure 29.

Table 12: (A/V) correction factor for PCM model to simulate different Anderlohr tests

Anderlohr test	pCO$_2$ (mmol/L)	pCO$_2$ (atm) at 10ºC	(A/V) CRF
2	0.297	0.005518	0.50
3	0.509	0.009466	0.55
5	1.231	0.022886	0.75
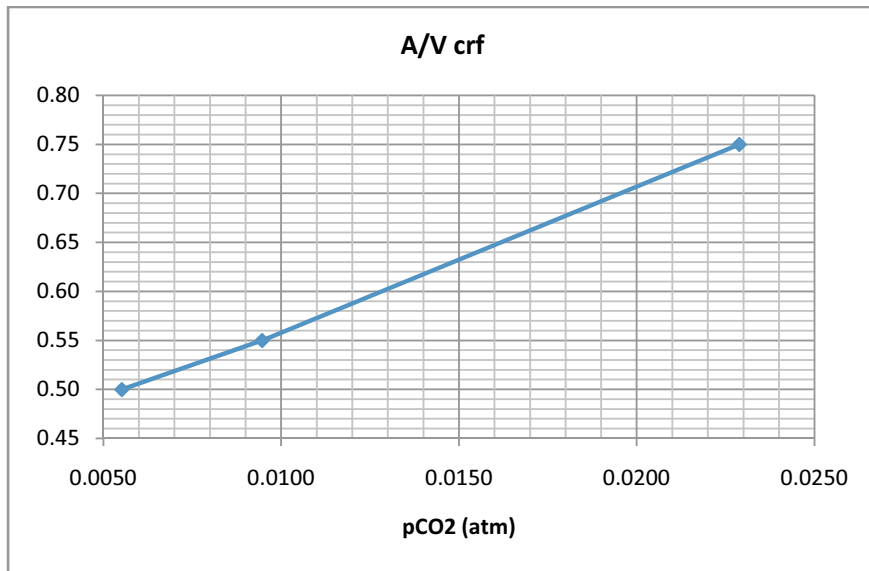
Figure 29: (A/V) correction factor for PCM model to simulate contactor bed condition in different initial pCO_2 at $10^{\circ}C$

3.4. Computer based layer model

3.4.1. General layer model concept

Although the corrected PCM model for natural limestone could be used to simulate the contactor bed as Anderlohr experiments, the model is only valid for a contactor system with narrow range of calcite grain diameters so that the average grain size could be use as PCM model input. A real limestone contactor in practice would have large range of grain sizes (typically from 0.2 to 2.0mm), which always distribute from the smallest to largest in the downward direction. Therefore, a computer based layer model needs to be developed in order to closely simulate the water quality as well as the limestone grain size distribution throughout the contactor bed.
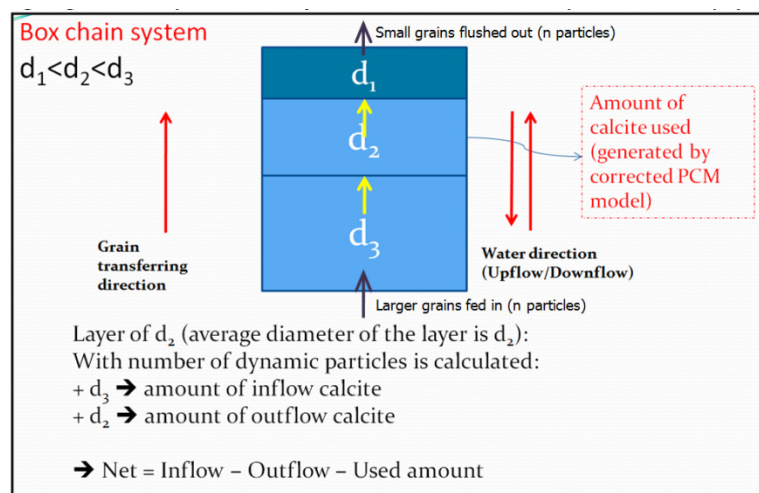
Figure 30: General highlights of layer model (based on box series system concept)

The general concept of the layer model is the box series model with each box represents for a layer of calcite grains with a certain average diameter as shown in Figure 30. When the system is in stable operating condition, the number of dissolved calcite grains transferring from one layer to the next layer just upon it would be approximately a constant number which is also equal to the number of feeding or discharged grains. By firstly assuming a certain average diameter for each layer together with the known bed porosity and the number of particles, calculations could be made for the (A/V) ratio, layer height and contact time and total calcite mol of that layer. Consequently, corrected PCM could be simulated for each layer to achieve how much calcite is used for each layer when a water flow is passing by. In each layer, together with the used amount, the inflow and outflow of amount calculated from the number of transferring particles from layer to layer would help deducing the net (extra or lacking) amount of calcite in that layer. This net amount could then be used to re-calculate the grain size in that layer given the total number of particles in each layer is constant over time. By specifying a small enough time step, the system could be iterated over a number of this time step and approach the balance state. When the system reaches the balanced state, the total net amount is extremely small (almost zero) which leads to no further changes in the diameter distribution of the layer model which is the expected distribution of calcite grains in an equivalent limestone contactor in practice. The sample layout of the input and output interface in Excel with PHREEQC embedded is shown in Annex C.2. This layer model concept is mainly based on the assumptions of ideal filtering bed model with fully classified grain size distribution over bed thickness as well as continuously feeding and backwashing process for every simulation time step.

3.4.2. Downflow layer model

For downflow layer model, the water solution is instructed to travel downwards from the smaller grain size layer at the top to the larger one at the bottom (Figure 31). An important notice in this model is that the top and bottom layer grain size are assumed to be equal to the discharged and feeding grain size respectively. These assumptions are totally valid in the downflow case because de-mineralized water first comes into the top layer with very high driving force for dissolution then traveling through the whole calcite bed and reaching the bottom when the water is almost fully re-mineralized with extremely low driving force for further calcite dissolution. Thus, the top layer grains are strongly dissolved to end up with the average size of discharged grains while the bottom layer grains are hardly dissolved hence the same size of feeding grains is remained. The number of dynamic transferring particles would be calculated from the calcite used amount within the top layer to dissolve the inflow grain size from the lower layer to the discharged size in the top layer.
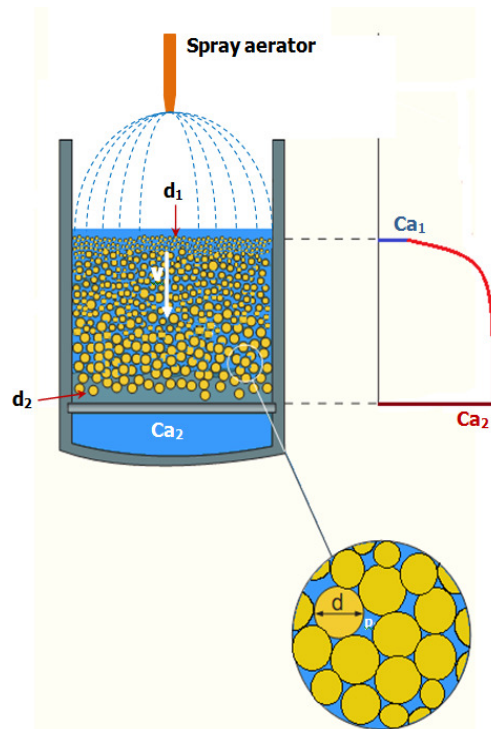
Figure 31: Simple sketch of an downflow contactor model with the calcium concentration over the bed thickness

The downflow model is first applied to simulate the Anderlohr tests in order to test its accuracy before applying for more practical cases. The simulated (Ca, CCDP, SI and pH) results of downflow model are shown in relative to the Anderlohr test 3 results (Figure 32). Similar comparative graphs for the downflow model are also plotted for the case of Anderlohr test 2 and 6 as shown in Annex C.3. Notice that the simulated SI (and pH) values are not very close to the experiment data due to the high sensitivity of the log scale. However, the developed downflow layer model has closely captured the practical filtering bed experiment results in general. Therefore, the downflow layer model could now be used as the base to further verify with industrial data as well as develop the upflow model.
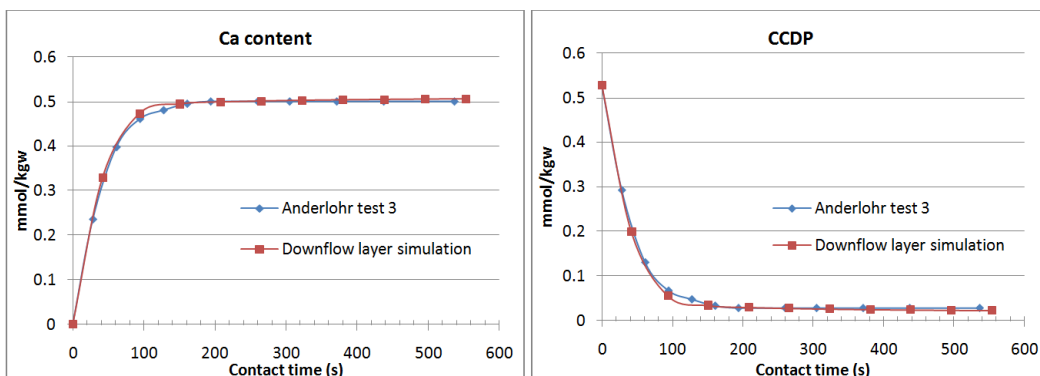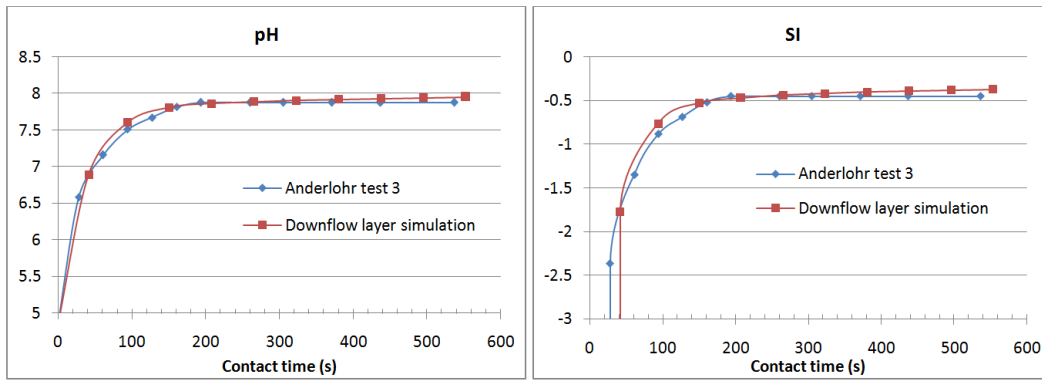
Figure 32: Downflow layer model simulation vs. Anderlohr test 3

On the other hand, the flow-rate influence of the model on the total dissolution process in the filtering bed is another important concern of the developed layer model. In his experiments, Anderlohr also conducted Test 4 and Test 6 which has the same set-up and initial water quality as Test 5 except the filtration flow rate. The flow rates for Test 4 and Test 6 are 5 m/h and 15 m/h respectively. However, the practical filtration load rate in a limestone contactor usually varies from 4 to 8 m/h (Jalil, 2002), is also recommended to be less than 10 m/h (Mackintosh, 2003). Consequently, only Anderlohr's Test 4 would be used for validation of the flow rate influence on the developed downflow layer model. Figure 33 shows the measured test results as well as the model simulation. Obviously, both measured and simulated curves show good consistencies with each other except at the saturation level. The saturated calcium amount measured by Anderlohr is higher than the model simulation which is due to the unknown theoretical saturation level. Although an exact comparison at the saturated level is not possible, the pre-saturated simulation shows a high agreement with the measured data. Therefore, the developed layer model captures closely the calcite dissolution in practical contactor bed within the range of 5 to 10 m/h flow rates.
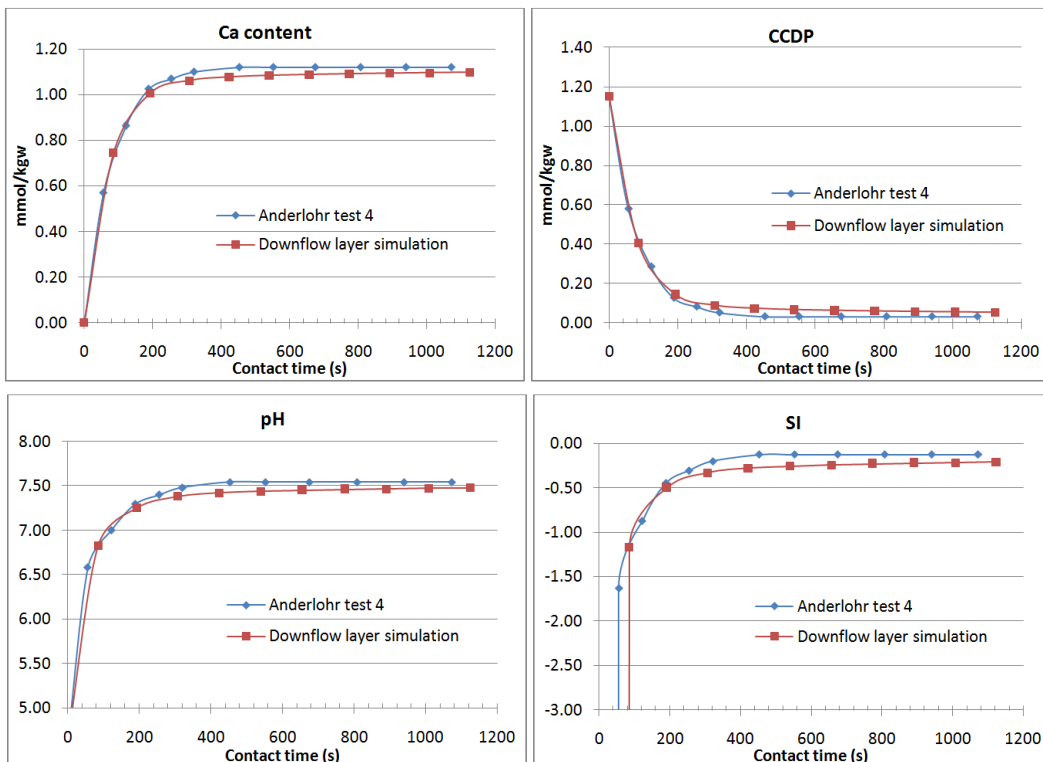
Figure 33: Downflow layer model simulation vs. Anderlohr test 4 (filtration flow rates of 5 m/h)

3.4.3. Upflow layer model

The main difference between upflow and downflow model is obviously the opposite water flowing direction. Other modeling concepts of downflow model could be applied the same for the upflow case except the assumptions of boundary's grain sizes. This is due to the fact that now de-mineralized water first comes into the bottom layer with very high driving force for dissolution then traveling upwards through the whole calcite bed and reaching the top when the water is almost fully re-mineralized with extremely low driving force for further calcite dissolution. Thus, the bottom layer grain average size is much lower than the feeding grain size while the top layer grains would be dissolved until reaching the discharged/washed–away grain size. As a result, the grain sizes at the top layer would be specified the same as the discharged grain size while the ones at the bottom layer would be specified lower than the feeding grain sizes. Figure 34 shows a simple sketch of an upflow limestone contactor with a typical calcium concentration variation over
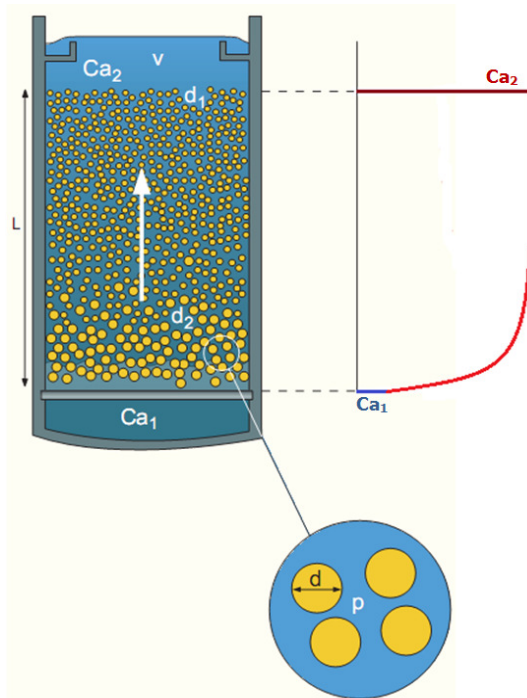
Figure 34: Simple sketch of an upflow contactor model with the calcium concentration over the bed thickness

the bed thickness. Besides in upflow model with high upflow rate, there could be a significant expansion of bed thickness. In other words, the filter bed is always fluidized during operation hence calcite grains in the contactor would always be classified from the smallest and lightest at the top to the largest and heaviest at the bottom. On the other hand, when the flow rate is not strong enough to have a fluidized bed, frequent backwashing of the filter bed with higher rate is required in order to keep the bed layers in classified mood generally. If no backwashing is conducted frequently, over time the upflow model would be indifferent from the downflow model with smaller particles are trapped at the lower depth of the bed.

In order to roughly validate the upflow layer model's reliability, it is first used to simulate Anderlohr test 3 to generate calcium content, solution CCDP, SI and pH. These are then plotted in the same graphs with the downflow model results for the ease of comparison as shown in Figure 35. For the first 120 seconds when the water quality is far from saturation level, the downflow layer model presents a higher dissolution rate compared to downflow model because of the smaller first water- contacting particle size of the downflow model which also means higher (A/V) ratio compared to upflow. While reaching the saturation point, the remineralized water qualities of these two models are almost identical (actually the upflow model dissolves slightly more calcite which is proved in section 5.5, however, the difference is not so obvious in this case due to the small range of pellet size (0.9 – 1.0mm)). This is understandable since the two upflow and downflow models are specified with the same bed thickness, porosity and flow rate which lead to the same total contact time, hence, the same amount of dissolved calcite.

The details of comparison between upflow and downflow would be discussed in detail later. However, this upflow model might need further enhancement in compliance with any improvement of the downflow model which is going to be verified with industrial data.
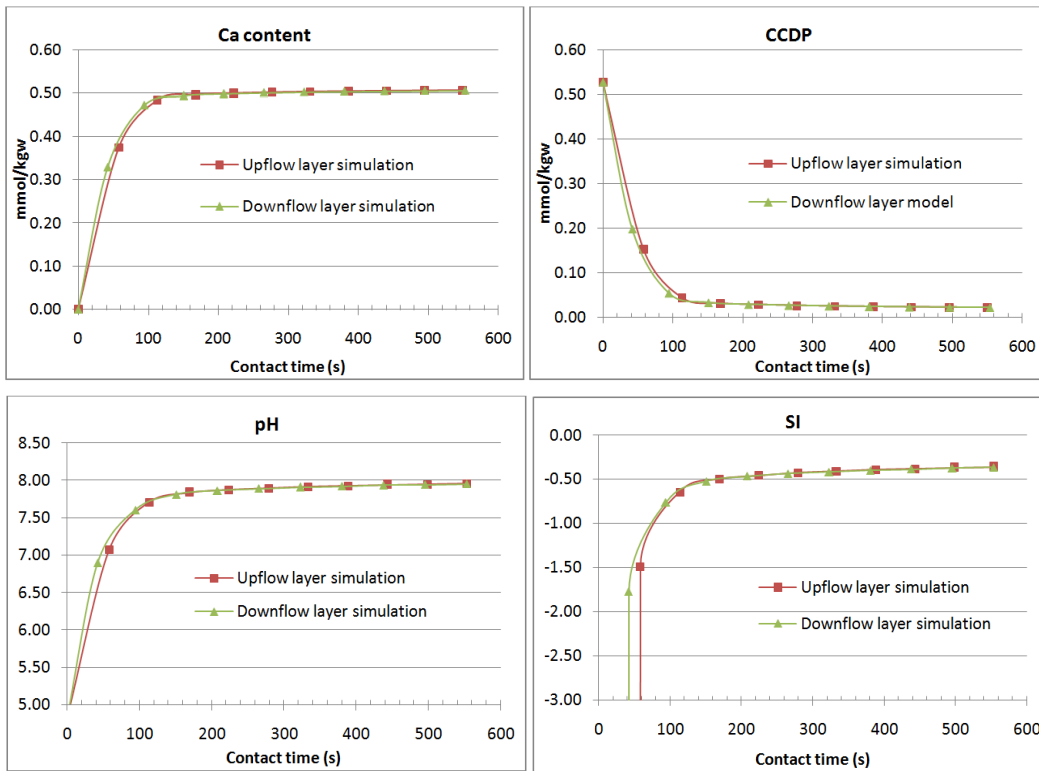
Figure 35: Downflow vs. Upflow layer model simulation for Anderlohr test 3

4. Practice verification & improvements

4.1. Downflow marble filtration at Hoenderloo

The drinking water treatment plant of Vitens at Hoenderloo (Apeldoorn) is one of a few water treatment plants in the Netherlands that has the resource of very pure groundwater. This is due to the soil of the local region consists mainly of sands and low portion of organic matters. Thus, the extracted water from the shallow ground layer is considered soft water with low calcium content and minimal amount of iron, manganese, magnesium as well as nitrate and sulfate.

With a low calcium content as well as pH level, marble filtration is necessary as the first-step after extracting the water from the ground. There are four wells which extract water up from the shallow ground layer. The extracted water would then be sprayed on top of the two limestone marble filter beds with the dropping height of around 1m (Figure 36). This aeration step is to reduce the content of CO_2 as well as to increase the O_2 level dissolved in the water. With the introduction of more oxygen into the raw water, the minor amount of iron, manganese and ammonium could be stripped off in the filter. The detail information on the filter bed is shown in Table 13.

Figure 36: Spraying aeration on top of marble filter bed at Hoenderloo pumping station

Table 13: Technical information on Hoenderloo marble filtration

Technical measurement	Unit	Measured data
Influent capacity	m^3/h	100
Number of filters	-	2
Surface area per filter	m^2	23.8
Flow rate	m/h	2.1
Average bed thickness	m	2.07
Newly filled grain size range	mm	2-3
Bed porosity	%	40
EBCT	s	3540
Real water contact time	s	1415

The marble calcite is a high quality Juraperle limestone imported from Germany. About 25 tons of new marble grains (2-3 mm) would be filled up in the two filters every six months. Therefore, the bed thickness of the filters would be in a decreasing stage from the filled up moment (2.27 m) to 6 months later (1.86 m) for the total bed of around 48m^2 bed (24m^2 each filter). Thus, the total volume of calcite consumption is around 20 m^3 for both filters in half a year. With approximately 25 tons feeding grains every 6 months, the bed porosity is calculated to be around 40 to 50% (adopting the common bed porosity of 40% for this study).The average quality of the raw water as well as the effluent from the marble filters over the past 15 months (February 2011 till May 2012 – see Annex D.1) is shown in Table 14.

Table 14: Average data of the raw water quality at Hoenderloo pump station (Vitens, 2011-2012)

Parameter	Symbol	Unit	Raw water	Effluent
Temperature		^oC	10.2	9.9
pH		-	6.39	8.04
Conductivity at 20^oC		ms/m	21.8	27.9
Oxygen	O_2	mg/L	4.4	8.2
Carbon dioxide	CO_2	mg/L	29.3	1.4
Calcium	Ca	mg/L	21.2	36.3
Magnesium	Mg	mg/L	4.9	4.9
Sodium	Na	mg/L	17.1	*(no record)*
Potassium	K	mg/L	1.62	*(no record)*
Iron	Fe	mg/L	0.03	<0.01
Manganese	Mn	mg/L	0.14	<0.005
Ammonium	NH4	mg/L	0.02	*(no record)*
Bicarbonate	HCO_3	mg/L	39.5	82.7
Chloride	Cl	mg/L	21	*(no record)*
Nitrate	NO_3	mg/L	25	*(no record)*
Sulfate	SO_4	mg/L	24	*(no record)*
Phosphate	PO_4	mg/L	0.08	*(no record)*
Silicate	Si	mg/L	6.3	*(no record)*
Total organic carbon	TOC	mg/L	0.25	*(no record)*

It is important to recognize that the Hoenderloo case is a practical model of marble filter. Unlike the ideal model, Hoenderloo marble bed is not fully classified and only fed or backwashed every half or quarter of the year respectively. Figure 37 shows the relative size of the top layer calcite grains taken from the Hoenderloo marble filter compared to the feeding size in the reference of a 10 cent Euro coin size. From the sample of filtering grains, there is still a number of feeding size grains at the top of the filter tank in addition to the miniature pellets sticking in the colloidal paste. Since the bed is not fully classified, the grain size distribution would vary over time especially at the top layers. With different average grain size, different A/V ratio would vary as well, hence, varying effluent quality generated over time is understandable at Hoenderloo marble filter. On the other hand, the dark brownish colour and colloidal state of the filtering pellets indicates the accumulation of a small amount of iron (III), manganese oxide in the filter bed due to infrequent backwash.

Figure 37: The relative sizes of the top layer filtering marble grains and feeding grains in the reference of a 10 cent Euro coin

4.2. Computer based modelling

With the provided data of Hoenderloo marble filtration, the corrected PCM model could now be further established as the kinetics model for this practical case. Subsequently, this kinetics model will be used for developing the downflow contactor model based on the downflow layer model concept as discussed in 3.4.2.

4.2.1. Kinetics model for Hoenderloo marble filtration

From the raw water and effluent quality data, the amounts of carbon dioxide, calcium decreased by aeration and filtration could be implied. Thus, the aeration efficiency on O2 addition and CO2 removal are found to be 86% and 45% respectively. As a result, the influent quality just after spraying aeration could be deduced. Applying that water quality and a really small grain size (0.2mm < D_3) in the corrected PCM model for contactor bed, the generated data is shown in Table 15 in comparison with Hoenderloo recorded data.

Table 15: Water quality data of Hoenderloo vs. Single layer model simulation for grain size of 0.2mm

Parameter	Symbol	Unit	Raw water	Effluent water	Simulated effluent
Temperature		°C	10.2	9.9	10.20
pH		-	6.39	8.04	7.76
SI			-2.29 (*)	-0.12	-0.42
Oxygen	O_2	mmol/L	0.14	0.26	0.26
Carbon dioxide	CO_2	mmol/L	0.67	0.03	0.06
Calcium	Ca	mmol/L	0.53	0.91	0.87
Magnesium	Mg	mmol/L	0.20	0.20	0.20
Sodium	Na	mmol/L	0.74	*(no record)*	0.74
Potassium	K	mmol/L	0.04	*(no record)*	0.04
Iron	Fe	mmol/L	<0.001	<0.001	5.37E-04
Manganese	Mn	mmol/L	<0.005	<0.005	2.53E-06
Ammonium	NH4	mmol/L	<0.001	*(no record)*	8.14E-04
Bicarbonate	HCO_3	mmol/L	0.65	1.36	1.31
Chloride	Cl	mmol/L	0.59	*(no record)*	0.59
Nitrate	NO_3	mmol/L	0.40	*(no record)*	0.40
Sulfate	SO_4	mmol/L	0.25	*(no record)*	0.23
Phosphate	PO_4	mmol/L	<0.001	*(no record)*	3.08E-08
Silicate	Si	mmol/L	0.22	*(no record)*	0.19

(*): calculated figure

From the tabulated data, the simulated effluent is further from equilibrium compared to the recorded data by comparing the four important indices: pH, SI, Ca, HCO_3^-, and CO_2 content. Even by using acceptable variances in all technical figures such as average grain size, porosity, bed thickness and flow rate as compensations, the simulated results could never be so highly boosted up to match the recorded level. Therefore, given that our model kinetics is correctly verified by Vosbeck and Anderlohr data, the key cause for this difference must be the Vosbeck Juraperle quality adopted in the simulated model and the one used at Hoenderloo. This is confirmed by applying PCM model for Baker calcite to simulate the Hoenderloo effluent. The closer result between Baker calcite model and recorded data implies that the Hoenderloo Juraperle quality is higher than Vosbeck and close to pure calcite.

In fact, the calcite quality strongly depends on the calcite purity which is the proportion of calcium carbonate in a certain weighted amount. The analysis (see detail in Annex D.2) on Hoenderloo, Anderlohr and Vosbeck Juraperle purity clearly shows that Hoenderloo and Anderlohr Juraperle quality are close to each other and both are much purer than Vosbeck Juraperle. The purity of each calcite type is listed in Table 16. Thus, a change in our model

kinetics parameters must be made in order to correctly simulate the dissolution process of Hoenderloo high quality calcite. Similar change could also be made for Anderlohr but does not really affect the previous findings of correction factor for (A/V).

Table 16: Maximum mass percentage of calcium and magnesium carbonate in different calcite types

Calcite type	% CaO	% CaCO$_3$ (equivalent)
Vosbeck Juraperle	52.6%	93.9%
Anderlohr Juraperle	55.9%	99.8%
Hoenderloo Juraperle(*)		98.1%
Baker		100%

(*): supplier's chemical analysis result

According to Chou experiment (section 2.6.3), the dissolution kinetics of magnesite is 1000 times lower than calcite and other carbonates. Therefore, based on the maximum portion of magnesite, the relative dissolution rate between these calcite types could be deduced (detail calculation in Annex D.3). By changing n to a lower value, the main parameter controlling the calcite saturation level in dissolution process, a more accurate kinetics model for the Hoenderloo Juraperle dissolution could be presented. With a 3.3 times smaller n, the simulated effluent data for three different grain sizes (0.2, 1.5 and 3.0mm) is now in a close proximity to the recorded effluent as shown in Table 17.

Table 17: Water quality data of Hoenderloo vs. kinetics model simulations for different grain sizes

Parameter	Symbol	Unit	Raw water	Effluent water	Simulated kinetics model		
					0.2 mm	1.5 mm	3mm
Temperature		°C	10.2	9.9	10.20	10.20	10.20
pH		-	6.39	8.04	8.10	8.06	8.03
SI			-2.29 (*)	-0.12	-0.04	-0.08	-0.11
Oxygen	O$_2$	mmol/L	0.14	0.26	0.26	0.26	0.26
Carbon dioxide	CO$_2$	mmol/L	0.67	0.03	0.03	0.03	0.03
Calcium	Ca	mmol/L	0.53	0.91	0.91	0.91	0.91
Magnesium	Mg	mmol/L	0.20	0.20	0.20	0.20	0.20
Sodium	Na	mmol/L	0.74	*(no record)*	0.74	0.74	0.74
Potassium	K	mmol/L	0.04	*(no record)*	0.04	0.04	0.04
Iron	Fe	mmol/L	<0.001	<0.001	5.37E-04	5.37E-04	5.37E-04
Manganese	Mn	mmol/L	<0.005	<0.005	2.53E-06	2.53E-06	2.53E-06
Ammonium	NH4	mmol/L	<0.001	*(no record)*	8.14E-04	8.14E-04	8.14E-04
Bicarbonate	HCO$_3$	mmol/L	0.65	1.36	1.37	1.37	1.36
Chloride	Cl	mmol/L	0.59	*(no record)*	0.59	0.59	0.59
Nitrate	NO$_3$	mmol/L	0.40	*(no record)*	0.40	0.40	0.40
Sulfate	SO$_4$	mmol/L	0.25	*(no record)*	0.23	0.23	0.23
Phosphate	PO$_4$	mmol/L	<0.001	*(no record)*	3.08E-08	3.08E-08	3.08E-08
Silicate	Si	mmol/L	0.22	*(no record)*	0.19	0.19	0.19

(*): calculated figure

4.2.2.   Downflow contactor model for Hoenderloo Juraperle

With the developed kinetics model, the practical downflow contactor model for Hoenderloo case could be established based on the downflow layer concept. Ideal contactor model would be assumed with fully classified grain size over bed thickness as well as frequent feed and backwash for every simulation step. Although the filter bed is assumed to be fully classified, the simulated effluent quality could be higher or lower than the practical recorded data. This is due to the fact that the recorded data would vary over time because of constantly changes in grain size distribution in the real contactor.

The kinetics model would be applied for each layer of a certain grain size. The grain size would be distributed from the largest (3.0mm) at the bottom to the smallest (average 0.2mm)

at the top. The simulated effluent qualities are shown in Table 18 in comparison with Hoenderloo data. Overall, the model simulation is considered accurate enough to capture the effluent water quality from Hoenderloo marble filtration.

Table 18: Water quality data of Hoenderloo vs. the developed downflow contactor model simulation

Parameter	Symbol	Unit	Raw water	Effluent water	Simulated contactor model
Temperature		°C	10.2	9.9	10.20
pH		-	6.39	8.04	8.04
SI			-2.29 (*)	-0.12	-0.11
Oxygen	O_2	mmol/L	0.14	0.26	0.26
Carbon dioxide	CO_2	mmol/L	0.67	0.03	0.03
Calcium	Ca	mmol/L	0.53	0.91	0.91
Magnesium	Mg	mmol/L	0.20	0.20	0.20
Sodium	Na	mmol/L	0.74	*(no record)*	0.74
Potassium	K	mmol/L	0.04	*(no record)*	0.04
Iron	Fe	mmol/L	<0.001	<0.001	5.37E-04
Manganese	Mn	mmol/L	<0.005	<0.005	2.53E-06
Ammonium	NH4	mmol/L	<0.001	*(no record)*	8.14E-04
Bicarbonate	HCO_3	mmol/L	0.65	1.36	1.36
Chloride	Cl	mmol/L	0.59	*(no record)*	0.59
Nitrate	NO_3	mmol/L	0.40	*(no record)*	0.40
Sulfate	SO_4	mmol/L	0.25	*(no record)*	0.23
Phosphate	PO_4	mmol/L	<0.001	*(no record)*	3.08E-08
Silicate	Si	mmol/L	0.22	*(no record)*	0.19

By plotting the dissolution process of this practical model in the same graph with the previous kinetics simulations for different grain sizes on the base of SI, the grain size effect on calcite dissolution process could be observed easier. For kinetics model, Figure 38 indicates that the lower the grain size, the closer to calcite equilibrium the effluent water could reach. This is due to the fact that smaller grain would have higher total contact surface area which is directly proportional to the dissolution rate. On the other hand, the downflow model simulated curve goes between those of the kinetics model. Since there are many different layers with different average grain sizes, the dissolution rate of calcite into the downward flowing water depends on the average grain size that the water contacts at that particular moment. Thus, the simulated curve started off with the same (or slightly higher since the top grain is not exactly 0.2mm) dissolution rate as kinetics model of 0.2mm grain size, then continuously diminished to be lower than 1.5mm kinetics model at saturation turning point and ended up slightly higher than 3mm model. Table 19 listed out the detail of two intersections of the practical downflow model curve. Besides, the matching curves of kinetics model and downflow contactor model for the same uniform grain size (3.0mm) also confirms that the kinetics model could be seen as a single layer model with one uniform grain size.

Table 19: SI curve intersection of the downflow contactor model (d=0.2-3.0mm) with the kinetics model

Time (s)	Approximate contacting grain size (mm)	Corresponding kinetics model grain size (mm)	Interaction type	Approximate SI
0.36	0.3	0.2	Intersection	-1.99
195	2.6	1.5	Intersection	-0.34
> 800	> 2.97	3.0	Asymptote	>-0.14
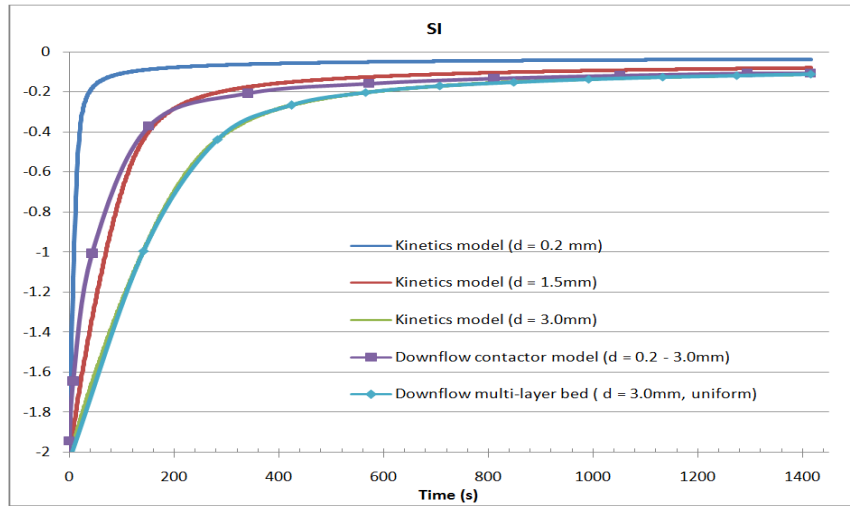
Figure 38: SI increasing process simulation by the kinetics model with different grain sizes and the practical downflow model of Hoenderloo marble filtration

50

5. Application and design for Hoenderloo marble filtration

By comparing with Drinkwaterbesluit standard, the generated remineralized water from Hoenderloo filtration fully satisfies all the requirements as shown in Table 20. Thus, the effluent amount of alkalinity, SI, pH level is not required to be improved at this level although there is still a possibility of more stringent remineralized water standard announcing in future. Notice that Drinkwaterbesluit does not specify minimum or maximum requirement for remineralized water's hardness, Hoenderloo effluent is not constrained on its calcium level.

Table 20: Hoenderloo effluent quality and Drinkwaterbesluit requirements on drinking water in the Netherlands

Quality index	Unit	Drinkwaterbesluit requirement	Hoenderloo effluent
pH		≥ 7.0 and ≤ 9.5	8.04
SI		> -0.2	-0.12
Ca	mmol/L	-	0.91
Alkalinity	meq/L	> 1.0	1.40

Beside the possible raise of the quality standard, it is also wise to look on possible alternative design of Hoenderloo marble filters to reduce operating costs while still producing the qualified remineralized water with respect to Drinkwaterbesluit standard. The developed contactor model for Hoenderloo would be applied with different set-up conditions in order to test the importance of each parameter on the final generated effluent quality. Based on these analyzed results, optimal design in terms of economical wise could be recommended for future development or reformation of Hoenderloo marble filtration process.

5.1. Initial CO_2 removal efficiency

Initial CO_2 content plays an important role in marble filtration process since it is the main reactant to dissolve calcite into water. Thus, more CO_2 dissolved in water initially would result in more calcite dissolved in water given the same filtering conditions. However, carbon dioxide reduction by more efficient aeration could help increasing the level of pH hence less calcite is required for the remineralization process to reach calcite saturation.

Table 21: Drinkwaterbesluit requirements for drinking water in the Netherlands and Hoenderloo effluent quality with different aeration efficiency in CO_2 removal (assumed no changes in O_2 addition)

Quality index	Unit	Drinkwaterbesluit requirement	Hoenderloo effluent with different aeration efficiency in CO2 removal							
			0% (no aeration)		45% (existing)		75%		90%	
			In[1]	Out[2]	In	Out	In	Out	In	Out
pH		≥ 7.0 and ≤ 9.5	6.39	7.76	6.65	8.04	6.99	8.29	7.37	8.46
SI		> -0.2	-2.29	-0.14	-2.04	-0.12	-1.69	-0.09	-1.31	-0.08
Ca	mmol/L	-	0.53	1.17	0.53	0.91	0.53	0.71	0.53	0.62
Alkalinity	meq/L	> 1.0	0.65	1.92	0.65	1.40	0.65	1.02	0.65	0.82
CO_2	mmol/L	-	0.72	0.09	0.40	0.03	0.18	0.01	0.07	0.01
O_2	mmol/L	-	0.14	0.14	0.26	0.26	0.26	0.26	0.26	0.26

(1): the water quality when first entering the marble filter
(2): the water quality of the effluent from marble filter

As shown in Table 21, higher CO_2 removal efficiency would lead to better effluent quality with higher SI and pH level but less alkalinity introduced. However, in order to satisfy the Dutch requirement on alkalinity level (1.0 meq/L), the CO_2 removal efficiency of the pre-filtering aeration Hoenderloo must be not higher than 75%. Higher efficiency would limit the amount of bicarbonate level hence alkalinity in water. For instances, at 90% efficiency of CO_2 removal, the alkalinity level is below 1.0 meq/L and no longer satisfies the Dutch requirement. At 75%

aeration efficiency in CO_2 removal, the amount of feeding calcite would be lower compared to lower aeration efficiency cases since there is less calcite dissolved in lower CO_2 water. Thus, with high aeration efficiency in carbon dioxide removal would be a more economical alternative.

On the other hand, completely removing of aeration step does not significantly lower the effluent quality. In fact, the outlet water still qualifies for Drinkwaterbesluit requirement and requires no extra-post treatment. Therefore, while considering for developing a new filter at Hoenderloo, high efficiency requirement for pre-filtering aeration could be neglected given that the current drinking water standard is still preserved. However, if there is such a requirement to achieve the same SI (-0.12) as the existing system, a common post treatment such as NaOH dosage could be considered. The NaOH (25%) dosage amount would be around 1.80 L/day given the filtering capacity is 100m³/h as existing condition. Moreover, without aeration step to remove CO_2, more alkalinity could be introduced to the water due to higher amount of calcite will be dissolved. By focusing on the non-aeration case, the maximum amount of calcite and alkalinity dissolved in Hoenderloo water would be investigated.

5.2. Smaller size of feeding calcite grains

The grain size is inversely proportional to the contact surface area which is directly proportional to the dissolution rate. Therefore, in order to dissolve more calcium into water for a given contact time, smaller average grain size would be preferred. The improvement in water quality is clearly shown in Table 22 with smaller feeding calcite grains in the original system with contact time of 1415 seconds.

Table 22: Drinkwaterbesluit requirements for drinking water in the Netherlands and Hoenderloo effluent quality with different feeding grain sizes

Quality index	Unit	Drinkwaterbesluit requirement	Filter influent	Hoenderloo effluent with different feeding grain size		
				3mm (existing)	2mm	1mm
pH		≥ 7.0 and ≤ 9.5	6.65	8.04	8.05	8.07
SI		> -0.2	-2.04	-0.12	-0.09	-0.07
Ca	mmol/L	-	0.53	0.906	0.908	0.910
Alkalinity	meq/L	> 1.0	0.65	1.40	1.41	1.41
CO_2	mmol/L	-	0.40	0.03	0.03	0.03
O_2	mmol/L	-	0.26	0.26	0.26	0.26

With smaller feeding grains, the pH and SI level clearly increase even though there is very marginal increase in the amount of calcium and alkalinity in the effluent. Thus, feeding smaller calcite grains could be a compensation for other cost-saving remedies that could lower the water quality.

5.3. Controlling contact time through flow rate and bed thickness

One of the most important parameters in calcite dissolution process is the contact time of the calcite grains with the soft water. The longer the contact time, the higher amount of calcite would be dissolved and vice versa. Contact time could be adjusted through the influent flow rate or the bed thickness. Clearly, slower flow rate or thicker bed would elongate the contact time and otherwise. However, increasing the flow rates or reducing the bed thickness could also be considered for economical concerns.

5.3.1. Flow rate

The current flow rate in Hoenderloo filters is 2.1 m/h which is correspondent to a maximum capacity of 100m^3/h for two operating marble filters at Hoenderloo. There are two test cases on which the capacity is half and double the existing capacity.

Table 23: Drinkwaterbesluit requirements for drinking water in the Netherlands and Hoenderloo effluent quality with different influent flow rate

Quality index	Unit	Drinkwaterbesluit requirement	Filter influent	Hoenderloo effluent with different flow rate		
				1.05 m/h	2.1 m/h (existing)	4.2 m/h
pH		≥ 7.0 and ≤ 9.5	6.65	8.06	8.04	7.99
SI		> -0.2	-2.04	-0.08	-0.12	-0.16
Ca	mmol/L	-	0.53	0.909	0.906	0.901
Alkalinity	meq/L	> 1.0	0.65	1.41	1.40	1.39
CO$_2$	mmol/L	-	0.40	0.032	0.033	0.040
O$_2$	mmol/L	-	0.26	0.26	0.26	0.26

With half the existing flow rate, the water quality is clearly increasing with SI is now above -0.1. However, if the plant is to operate with a double capacity (200 m^3/h), the effluent from the case of 4.2 m/h flow rate is still in the acceptable zone, thus, no extra treatment is required. However, if there is such a requirement to achieve the same SI (-0.12) as the existing system, a common post treatment such as NaOH dosage could be considered. The NaOH (25%) dosage amount would be around 2.40 L/day for the new filtering capacity of 200m^3/h.

5.3.2. Bed thickness

Similar to flow rate, the developed limestone contactor model for Hoenderloo would be applied with two different bed thicknesses (half and double the current one) for investigating the changes in effluent quality.

Table 24: Drinkwaterbesluit requirements for drinking water in the Netherlands and Hoenderloo effluent quality with different bed thickness

Quality index	Unit	Drinkwaterbesluit requirement	Filter influent	Hoenderloo effluent with different bed thickness		
				1.033 m	2.065 m (existing)	4.130
pH		≥ 7.0 and ≤ 9.5	6.65	7.99	8.04	8.06
SI		> -0.2	-2.04	-0.16	-0.12	-0.08
Ca	mmol/L	-	0.53	0.901	0.906	0.909
Alkalinity	meq/L	> 1.0	0.65	1.39	1.40	1.41
CO$_2$	mmol/L	-	0.40	0.040	0.033	0.032
O$_2$	mmol/L	-	0.26	0.26	0.26	0.26

Obviously, the water qualities of 1.033 m and 4.130 m bed are the same as the ones of 4.2 m/h and 1.05 m/h flow rate case respectively because of the same contact time. However, doubling the existing bed thickness would require a higher concrete filter tank, hence, reducing the inflow rate to 1.05 m/h should be a better alternative. Thus, for the case of bed thickness reducing to half the existing bed, the amount of NaOH (25%) used as post treatment step would be approximately 2.40 L/day in order to keep the calcite SI at -0.12 as the current system.

5.4. Optimal design for Hoenderloo downflow contactor

The operating costs of Hoenderloo marble filter could be significantly reduced by cutting half the current bed thickness to 1.05 m and double the flow rate to 4.2 m/h. Besides, a highly efficient aeration is also unnecessary. However, the effluent quality would no longer satisfy the Drinkwaterbesluit requirement as shown in design A, Table 25. The amount of caustic soda (25%) dosage is also really high (90.3 L/day) in order to raise the SI level to the Drinkwaterbesluit standard. Alternatively, an aeration method with CO_2 removal efficiency of 34% could also help raising the SI level to meet the standard. Thus, a smaller feeding grain size would be chosen as the compensation to raise the effluent quality. With 2.0mm feeding grain size (design B), the effluent SI is still lower than the requirement, even though higher than design A. In consequence, the required amount of NaOH 25% dosage is significantly reduced (28.2 L/day) compared to design A and so is the CO_2 removal efficiency (18%).
Overall, design C is the optimal downflow design for Hoenderloo with the average feeding grain size of 1mm. This design doubles the filter operating capacity as well as requiring only half of the current bed thickness. Most importantly, the effluent water quality is well above the Drinkwaterbesluit standard. Besides, the dosage amount of caustic soda 25% or CO_2 removal efficiency in aeration is also really low: 15.4 L/day or 12% respectively if it is required to achieve the same effluent quality as the existing system.

Table 25: Drinkwaterbesluit requirements for drinking water in the Netherlands and different designs for Hoenderloo marble filter

Set-up parameters	Unit		Hoenderloo effluent	Design A	Design B	Design C
Aeration CO_2 removal efficiency	%		45%	0% (no aeration)		
Flow rate	m/h		2.1	4.2		
Bed thickness	m		2.065	1.033		
Contact time	s		1416	354		
Total capacity	m^3/h		100	200		
Feeding grain size	mm		3.0	3.0	2.0	1.0
Number of feeding grains		per m^2	$1.27*10^6$	$3.88*10^6$	$1.38*10^7$	$1.16*10^8$
Quality index		**DWB requirement**				
pH		≥ 7.0 and ≤ 9.5	8.04	7.51	7.63	7.73
SI		> -0.2	-0.12	-0.43	-0.29	-0.17
Ca	mmol/L	-	0.91	1.11	1.14	1.16
Alkalinity	meq/L	> 1.0	1.40	1.80	1.87	1.91
CO_2	mmol/L	-	0.03	0.19	0.13	0.10
O_2	mmol/L	-	0.26	0.14	0.14	0.14
Drinkwaterbesluit qualified		-	✓	X	X	✓
Extra treatment						
Required NaOH (25%) dosage to achieve SI = -0.2	L/day	-	0.0	90.3	28.2	0.0
Required CO_2 removal efficiency in aeration	%	-	0.0%	34%	18%	0.0%

5.5. Upflow vs. downflow limestone contactor

5.5.1. Equivalent contactor simulations of upflow and downflow model

In order to compare the effluent qualities generated by the equivalent upflow and downflow model simulations, a calibrating case must be carried out. The current influent water and set up conditions in Hoenderloo marble filtration would be applied for an upflow contactor model with a bed thickness of 1.48 m, hence the total contact time would be approximately 1014 seconds. This upflow contactor model is built based on the upflow layer model concept in the previous section (3.4.3). Table 26 shows the generated quality of this upflow model.

Table 26: Simulated effluent results of the calibrated upflow contactor model and the equivalent downflow model (influent quality & set-up are based on the existing Hoenderloo filters except bed thickness and number of feeding grains)

Set-up parameter	Unit	Calibrated upflow model	Equivalent downflow model
Bed thickness	m	1.48	10.25
Contact time	s	1014	7033
Number of feeding grains	per m^2	1.55*10^5	
Quality index	**Unit**		
pH		8.086	8.085
SI		-0.053	-0.054
Ca	mmol/L	0.912	0.912
Alkalinity	meq/L	1.413	1.412
CO$_2$	mmol/L	0.031	0.031
O$_2$	mmol/L	0.26	0.26

Subsequently, an equivalent downflow layer model would be created in order to produce the same quality as the upflow model. The equivalent downflow model is found to have an approximately 7 times thicker bed (10.25 m) or longer contact time (7033 seconds) than the upflow case. The first graph in Figure 39 shows the diameter distribution over the bed thickness of the two equivalent models. In general, the average grain size of upflow model is much smaller than the downflow one; hence, a much higher contact surface area is expected in the upflow contact. With those distributions, it is easier to understand why the upflow model could generate the same water quality within a very short contact time compared to the downflow model. For other graphs of water quality parameters, there is a sharp rise in downflow model results for the first 24 seconds which is due to the fact that first two layers are very thin and contains of minuscule marble grains, while the rather uniform size layers at the bottom of the upflow model keeps the water quality rising in the first 500 seconds. It is important to notice that there is not enough data in both models in the pre-saturation stage to exactly describe in detail the dissolution process of calcite in this first stage. After 500 seconds, both models are more or less reaching the equilibrium proximity, thus, the driving forces are now significantly decreased. With the original feeding grain size (hence lowest A/V) at the lower layers, the downflow model needs much more time to achieve the same water quality end point as the upflow model. Overall, for the same inlet water and filter set-up, upflow limestone contactor is noticeably more superior in terms of technical as well as economical wise compared to downflow model.
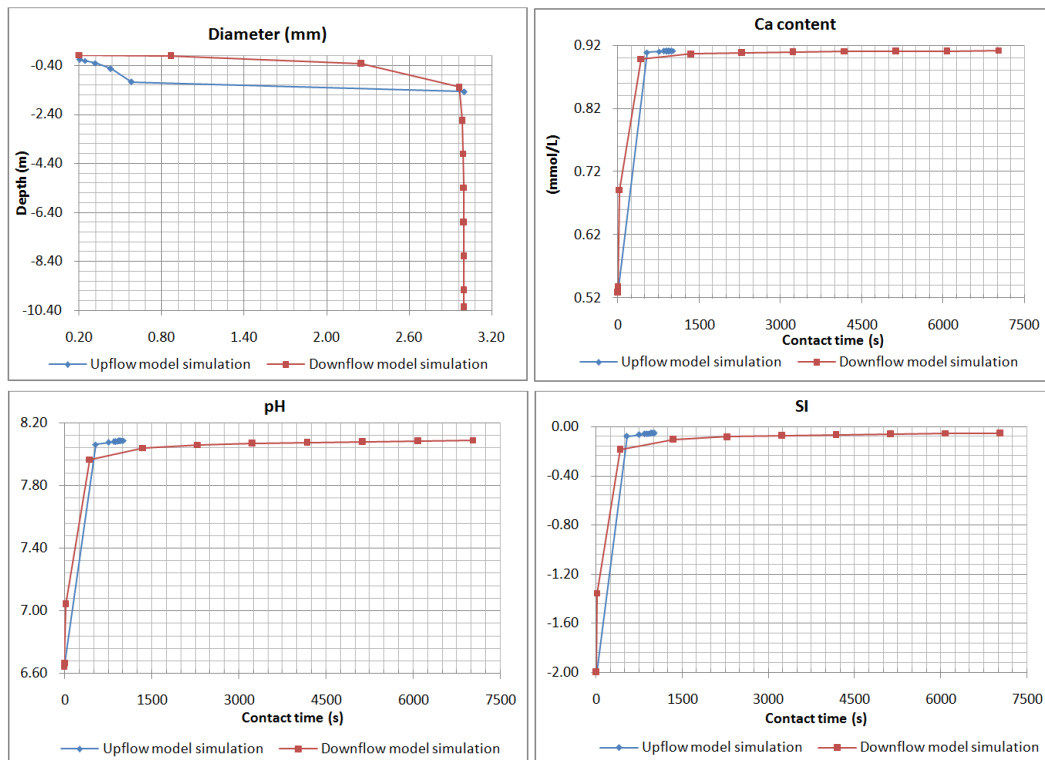
Figure 39: Calibrated simulations of equivalent upflow and downflow contactor model

5.5.2.   Hoenderloo upflow limestone contactor

Optimal upflow design

Since design C is the optimal downflow design for Hoenderloo marble filtration, the most superior design would be the upflow version of the same design given only the influence is now flowing upward instead. At equilibrium balance state, the grain size distribution over the bed thickness of the upflow model would be certainly different from the downflow case as shown in Figure 40. Other graphs on important remineralization quality index including calcium, pH and SI undoubtedly points out that the correspondent upflow model of design C produces a better effluent quality. The main reason for this difference is the much smaller mean diameter of the upflow model (hence higher A/V) compared to the one of downflow model. At the pre-saturation stage, the kinetics of downflow model seems faster than upflow model, however, this may not completely accurate for the whole 80 seconds of this stage due to the shortage of data in the upflow model in this range. In order to accurately describe the kinetics in the pre-saturation stage of upflow model, more layers need to be included in order to generate more data at this stage to be plotted. However, the developed models are aim to focus more on the near equilibrium range and effluent water quality which the current existing simulations satisfies adequately for further analysis. The difference might not be huge on the graph, but may require a seven-time thicker bed and eight-time higher number of feeding particles for design C to achieve the similar quality. Figure 41 shows a simple illustration of the relative grain size, porosity and layer distribution between two models. The detail figures could be found in Table 27 together with the existing effluent quality of Hoenderloo marble filter. It is important to notice with the upflow model, the effluent quality is also higher than the existing effluent even though the flow rate is doubled and the bed thickness is half the existing conditions. Furthermore, the effluent quality is also well above Drinkwaterbesluit requirement, thus, no further treatment is required.

56
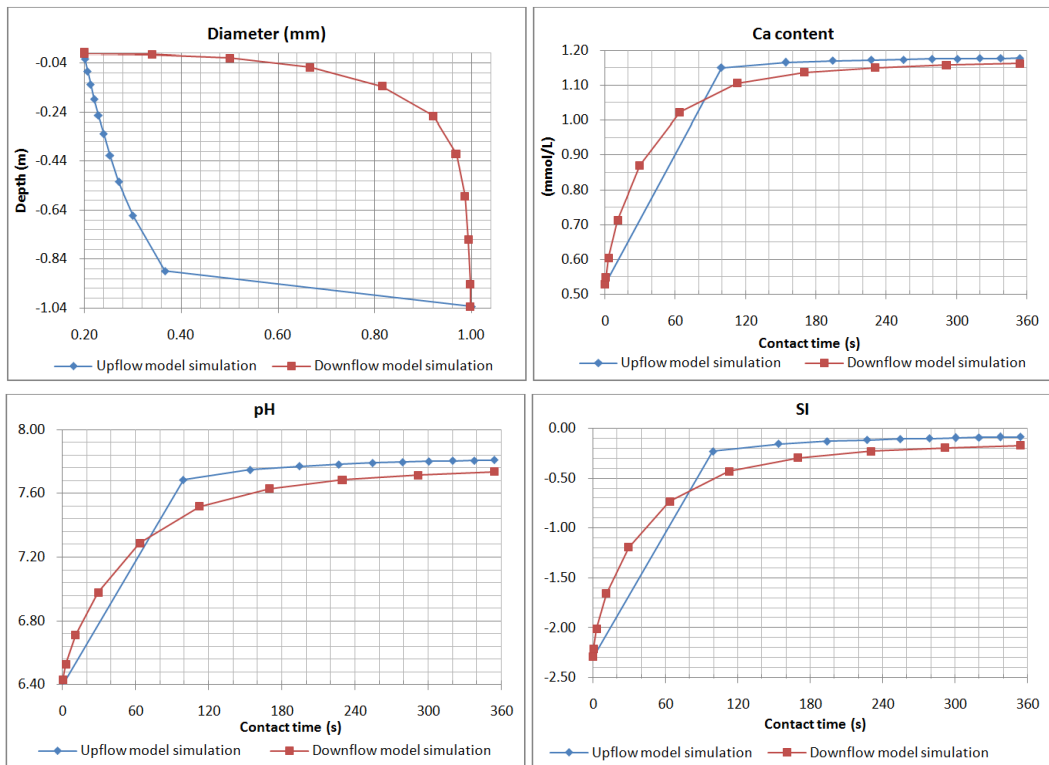
Figure 40: Simulations of the optimal downflow model design for Hoenderloo marble filtration and its upflow correspondent model
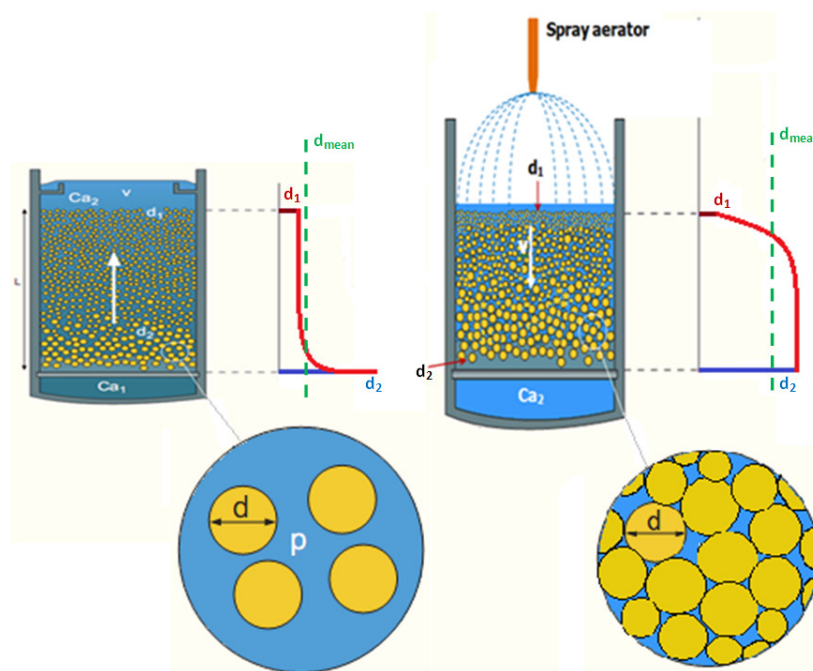
Figure 41: Simple sketch (not to scale) of the upflow vs downflow contactor model

Table 27: The optimal downflow and upflow designs in comparison with the existing Hoenderloo marble filtration model

Set-up parameters	Unit	Hoenderloo effluent	Best downflow design (Design C)	Optimal design (Upflow contactor)
Aeration CO$_2$ removal efficiency	%	45%	0% (no aeration)	
Flow rate	m/h	2.1	4.2	
Bed thickness	m	2.065	1.033	
Contact time	s	1416	354	
Total capacity	m^3/h	100	200	
Feeding grain size	mm	3.0	1.0	
Number of feeding grains	per m^2	1.27*10^6	1.16*10^8	1.19*10^8
Quality index				
pH		8.04	7.73	7.81
SI		-0.12	-0.17	-0.09
Ca	mmol/L	0.91	1.16	1.18
Alkalinity	meq/L	1.40	1.91	1.95
CO$_2$	mmol/L	0.03	0.10	0.08
O$_2$	mmol/L	0.26	0.14	0.14
Drinkwaterbesluit qualified		✓	✓	✓

In summary, the optimal design for Hoenderloo future reformation or development is the upflow design as shown in Table 27.

Testing to the extreme water demand condition

In long term, the water demand from Hoenderloo pumping station would gradually increase and possibly overcome the optimal design specification (200 m^3/h). However, that specified designed capacity could be further increased if a higher flow rate is applied. With higher flow rate, the bed would become fluidized and the small particles are susceptible to being washed out of the filter tank. Since the filter tank is around 3.5m deep, the optimal design bed thickness is only 1.033m, thus, there is a considerable depth for bed expansion in case of high flow rate. Assume that the smallest grain size that still remains in the tank is 0.2mm with the biggest possible bed expansion is approximately 2.0m. Under that circumstance, the bed porosity would be increased to 80% instead of 40%. Taking into account all of those conditions, the highest possible flow rate for Hoenderloo filter tank is 25.1 m/h which means a filtering capacity of 1195 m^3/h (see calculation method in Annex E). The effluent quality is then simulated as shown in Table 28.

Table 28: The optimal upflow design for Hoenderloo in comparison with its results when operating in extreme water demand condition

Set-up parameters	Unit	Optimal design (Upflow contactor)	Extreme operating condition
Aeration CO_2 removal efficiency	%	0% (no aeration)	
Flow rate	m/h	4.2	25.1
Bed thickness (during operation)	m	1.033	3.098
Contact time	s	354	355
Total capacity	m^3/h	200	1195
Feeding grain size	mm	1.0	
Number of feeding grains		$1.19*10^8$	$6.38*10^7$
Quality index			
pH		7.81	7.27
SI		-0.09	-0.76
CCDP		0.015	0.178
Ca	mmol/L	1.18	1.01
Alkalinity	meq/L	1.95	1.62
CO_2	mmol/L	0.08	0.24
O_2	mmol/L	0.14	0.14
Drinkwaterbesluit qualified		✓	**X**
Extra treatment alternatives			
Required NaOH (25%) dosage to achieve SI = -0.2	L/day	0.0	594
Required CO_2 removal efficiency in aeration	%	0.0%	75%

Thus, with the maximum flow rate, the effluent quality no longer satisfies Drinkwaterbesluit requirement on calcite SI. In order to increase the SI value to the minimal accepted range (-0.2), the required caustics soda (25%) dosage would be extremely high with 594 L on average per operating day. Otherwise, a highly efficient aeration must be implemented after marble filtration. The minimal efficiency required for carbon dioxide removal is 75% in order to boost up the SI level to meet the standard.

Possible disadvantages of upflow model

Although the upflow design is generally more superior than downflow in terms of generated quality, the system also has a few technical drawbacks. In upflow limestone contactor with fluidized bed, small particles are uplifting to the top, hence, susceptible to be washed out of the contactor. When the grain is small enough, the difference between the uplifting force caused by the upflow rate and the downward gravity force of the pellet would become large enough to discharge the grain out of the contactor. Consequently, unlike the downflow system, a limit upflow rate must be specified in upflow contactor to avoid washing away particles which are actually larger than the allowable discharged grain size. Besides, upflow system is also susceptible to being clogged at the bottom nozzles with unfamiliar compounds such as iron or manganese in case the influent water contains high amounts of iron and manganese. The clogging effect could also happen if backwashing process is conducted infrequently. Once the bed has been significantly clogged with high amount of exotic ingredients, the calcite dissolution process could be significantly inhibited; consequently, the developed contactor model could not predict accurately the effluent quality. However, in case of desalinated water, the content of iron and manganese is insignificant hence no clogging effect if upflow limestone contactor is utilized.

6. Conclusion & recommendation

6.1. Conclusion

On the basis of the initial theoretical models for surface dissolution rate R such as PWP and Chou which generally overestimate the calcite dissolution rate, this study has developed them into a more practically valuable PCM model which is cooperated by three important models: PWP, Chou and Morse models by verifying the simulated results with Vosbeck measured data.

Corrected PCM model for limestone contactor:

$$\frac{dC}{dt} = R * \left(\frac{A}{V}\right)^*$$

Where $R = (a_1 * [H^+] + a_2 * [CO_2] + a_3 * [H_2O]) * (1 - 10^{SI})^n$
$n = n_0 * (1 + q * b)$
$\left(\frac{A}{V}\right)^* = crf * \left(\frac{A}{V}\right)$
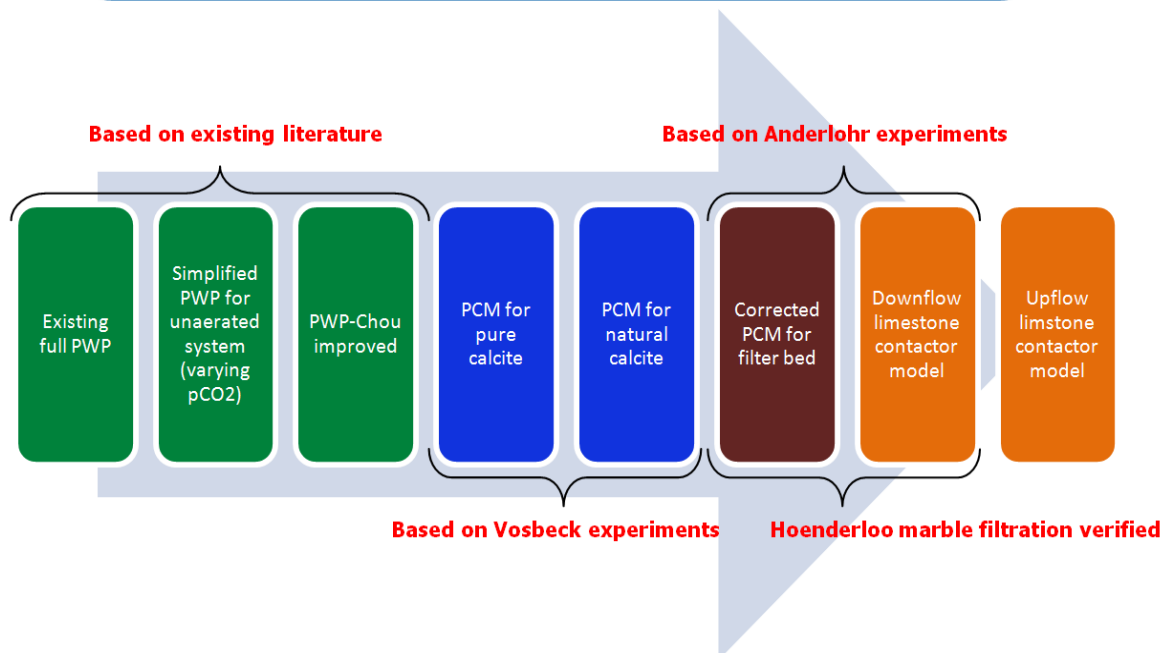
Figure 42: Final corrected PCM model of calcite dissolution kinetics and the improvement process from the original theoretical model (PWP)

The primary stage of the improvement is the combination of PWP (simplified) model and the Chou measurement data to formulate the PWP-Chou model which is one step closer to practice cases. On this basis, the PCM model for pure calcite has been further developed with new rate constants (a_1, a_2, a_3) and Morse's rate order n, which fully capture the dissolution kinetics of the Baker calcite in Vosbeck experiments. Introducing n (n>1.0) into the model could help capturing the low dissolution kinetics near equilibrium which PWP model is incapable of as proven by verifying with Vosbeck measured data. Subsequently, a discrete function for rate order n is further introduced to produce a more complete version - the PCM model for natural limestone. This PCM model is capable of capturing the dissolution rate of

the common used calcite (Juraperle) in practice which usually contains a certain percentage of extraneous matters.

Table 29: Parameters for PWP, Chou and PCM models at 25ºC, initial pCO_2 = 0.01 atm i.e. initial n_{CO2}= 0.54 mmol/L

Parameters	PWP	Chou	PCM
Temperature dependent:			
log k_1 or log a_1	100%	81%	83%
log k_2 or log a_2	100%	96%	88%
log k_3 or log a_3	100%	104%	100%
Temperature independent:			
n_0	1.00		3-7.5 (from high to low quality limestone)
b	0.00		0.13

However, the practice marble filtration would present different effluent quality from the predicted simulation due to the blockage of contacting surface area and possibly the different diffusion effects of Ca^{2+}, Alkalinity ions which is considered insignificant compared to the blockage effect. As a result, the corrected PCM model for contactor bed is accomplished with a correction factor for (A/V) embedded which varies from 0.5 for low initial CO_2 content (0.3 mmol/L) to 0.75 for higher initial content (1.2 mmol/L). The full corrected PCM model is presented in Figure 42 with the correction factors (α_1, α_2, α_3, η, β) for parameters (a_1, a_2, a_3, n, b) over different initial CO_2 content could be approximately predicted from the provided graph in 3.2.5. The constant q has a different value (q = {0, 1, 2, 3}) for different stages which depend on the saturation level (Ca/Ca_e) of the solution. This corrected PCM model has been verified with the measured data from Anderlohr experiments. Based on the corrected PCM model which is utilized as a basic kinetics model for commercial calcite dissolution in filtering bed, the layer model has been developed to closely simulate the marble-filtering bed in practice with stratified grain size layer assumption. Figure 43 shows the improvement achieved on the base of simulated SI from the original model PWP to the PCM model for natural limestone and then to the final corrected PCM model.
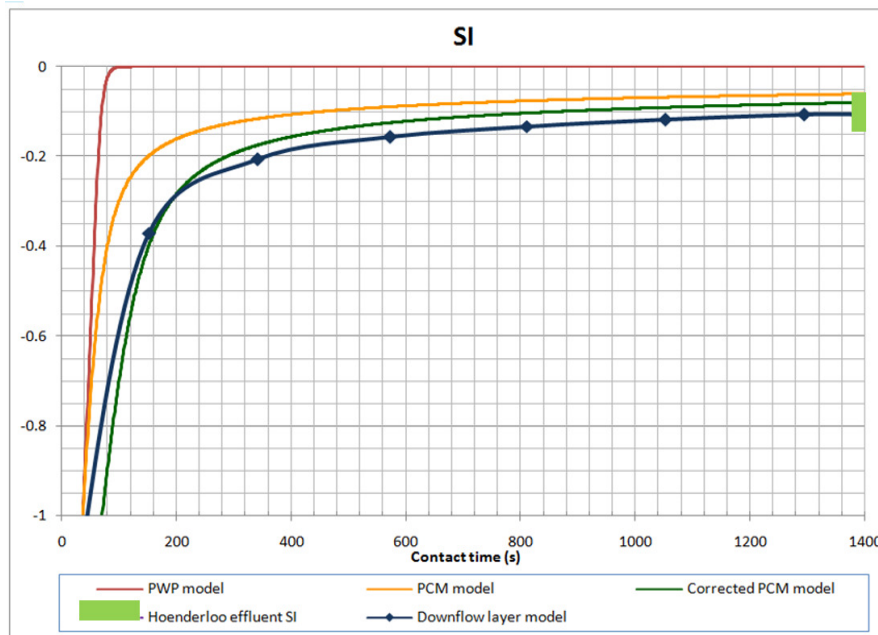
Figure 43: Simulated SI over time of different models (PWP, PCM, corrected PCM and downflow layer) for the same initial conditions of Hoenderloo water and the mean A/V (average gain diameter = 1.5mm for the kinetics models) and the real Hoenderloo filter effluent SI level

On the other hand, the kinetics of calcite dissolution significantly depends on the calcite pellet's purity which is implicitly included by the rate order n of the PCM model. This is seen clearly by the difference between Hoenderloo recorded data and the corrected PCM model simulation which is developed on the base of Vosbeck's Juraperle. In fact, chemical analysis shows that Vosbeck's Juraperle consist of approximately 5% more impurities than the one using in Hoenderloo filters. The higher purity of Hoenderloo calcite could be described in the kinetics by a lower rate order n which is closer to 1.0 whom describes the kinetics of the synthetic pure calcite. With a more precise rate order, the downflow contactor model certainly has a better accuracy in predicting the effluent quality of Hoenderloo.

By applying the developed PCM model to investigate the influence of different conditional parameters such as initial CO_2 content, feeding grain sizes and contact time which is controlled by bed thickness and influent flow rate. Smaller feeding grains and higher contact time are the possible factors to generally increase the effluent quality including higher pH, SI, alkalinity and water hardness level. In contrast, lower initial CO_2 content does produce higher SI and pH, but also lower Alk and water hardness level which could fall below the Drinkwaterbesluit requirement especially with a highly efficient aeration process. Based on the studied influence by different conditional parameters, an optimally economical downflow design is proposed for Hoenderloo marble filtration with a bed height reduced by half and filter's capacity increased by five times.

In another analysis, upflow models are proved to be more superior to the equivalent downflow by producing the same water quality with a seven-time thinner bed thickness and requiring eight-time lower number of feeding particles. An upflow version of the optimal downflow design is suggested to be the optimal design for future development or reformation at Hoenderloo pumping station with better effluent quality compared to the equivalent downflow model (Figure 44). Nevertheless, there are still a number of technical draw-backs or difficulties for applying upflow limestone contactor. One of them is the risk of washing off calcite particles that are still well above the discharged size while the other is the system's susceptibility to clogging effect at the bottom nozzle locations due to heavy extraneous matter deposit which is caused by infrequent filter's backwash.
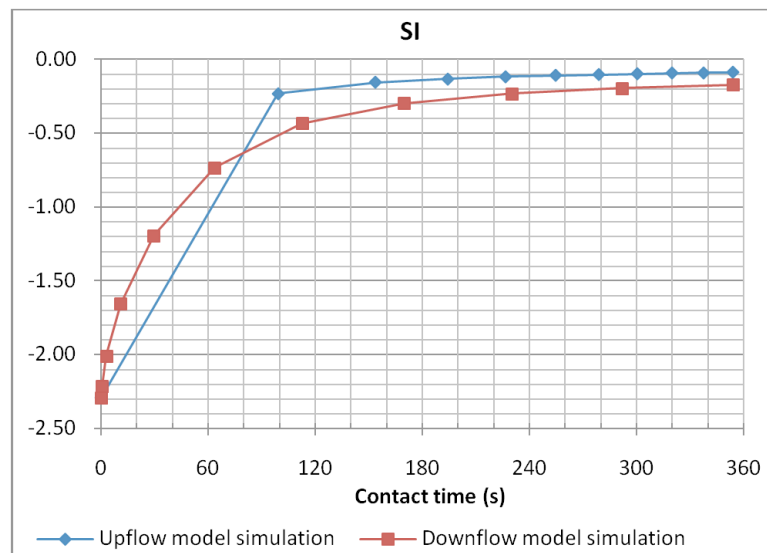
Figure 44: Simulated SI of the optimal downflow model design for Hoenderloo marble filtration and its upflow correspondent model

62

6.2. Recommendation for future research

The accuracy of the developed PCM model could be further improved by verifying with more laboratory experiments and practical data in order to achieve more complete indicator graphs of rate parameters (a_1, a_2, a_3, n, b) over different conditions of temperature and initial pCO_2. Moreover, the expression of rate order n in case of natural limestone near saturation point could be revised and possibly further developed into a simpler yet more precise function to simulate the real dissolution process at the final dissolution stage. The PCM model could be used as the base for further experimental research which focuses on a diversified range of different limestone quality especially the one collected from softening reactor which could help cutting off a huge amount of material costs of the imported Juraperle. The possibility of re-using pellets from softening is therefore practically very promising in both economical and environmental terms. However, the effects of extraneous ingredients such as magnesium, iron and manganese should be cautiously studied. Iron is not desirable to be introduced into the remineralized water during marble filtration process while magnesium with a thousand times lower dissolution kinetics could inhibit or retard the calcite dissolving process in general. These effects might also be encountered in case of the natural soft water contains high amount of magnesium or iron in the water. Besides, the inhibition effect should be noticeably emphasized on at close proximity to equilibrium when the calcite dissolution rate has dropped significantly.

On the other hand, the degree of grain size classification in the upflow contactor should also be studied. It is important to see what are the advantages and disadvantages between a fluidized bed over an equivalent static bed with frequent backwashing attempts. From the SI graph in Figure 40, it is clear that the calcium level in water reaches 95% of saturation amount only after approximately 110 seconds in the optimal upflow design for Hoenderloo water. Thus, there is a possibility to further minimize the contact time (to around 110 to 150 seconds) by increasing the upflow rate to even higher than the extreme case in a higher tank. It is important to take into account the minimum grain size that is designed to be remaining in the contactor at a given high fluidized rate. In fluidized bed, the blockage effects can also be ignored due to the high flow rate which up lifts most particles in the contactor. Besides, with a much shorter contact time in the contactor, the overall remineralization capacity would increase significantly. The small gap from equilibrium or acceptance level in terms of generated SI and CCDP could be closed up by post-treatment method with caustic soda dosage.

Reference list

Anderlohr, A., Sontheimer, Spindler. (1975). *Experimentelle Untersuchungen zur Auflösung von Calciumkarbonat durch Kohlensäurehaltige Wässer in Schüttungen* MSc., Institut der Universität Karlsruhe

AWWA Research Foundation., & DVGW-Technologiezentrum Wasser. (1996). *Internal corrosion of water distribution systems* (2nd ed.). Denver, CO: The Foundation.

Barbeau, B., Huffman, D., Mysore, C., Desjardins, R., Prevost, M. (2004). Examination of discrete and counfounding effects of water quality parameters during the inactivation of MS2 phages and Bacillus subtilis spores with free chlorine *Journal of Enviromental Engineering and Science 3 (4)*.

Beltran F.J., R. E. M., Romero M.T. (2006). Kinetics of the ozonation of muconic acid in water. *Journal of Hazardous Materials 138 (3)*, 534-538.

Bernadi, D., Dini, F.L., Azzarelli, A., Giaconi, A., Volterrani, C. and Lunardi, M. (1995). Sudden cardiac death rate in an area characterized by high incidence of coronary artery disease and low hardness of drinking water. *Angiology 46*, 145-149.

Birnhack, L., Voutchkov, N., & Lahav, O. (2011). Fundamental chemistry and engineering aspects of post-treatment processes for desalinated water-A review. *Desalination, 273*(1), 6-22. doi: 10.1016/j.desal.2010.11.011

Buhmann, D., & Dreybrodt, W. (1985). The kinetics of calcite dissolution and precipitation in geologically relevant situations of karst areas: 1. Open system. *Chemical Geology, 48*(1–4), 189-211. doi: 10.1016/0009-2541(85)90046-4

Chou, L., Garrels, R. M., & Wollast, R. (1989). Comparative study of the kinetics and mechanisms of dissolution of carbonate minerals. *Chemical Geology, 78*(3–4), 269-282. doi: 10.1016/0009-2541(89)90063-6

Colombani, J. (2008). Measurement of the pure dissolution rate constant of a mineral in water. *Geochimica et Cosmochimica Acta, 72*(23), 5634-5640. doi: 10.1016/j.gca.2008.09.007

Dawoud, M. A. (2005). The role of desalination in augmentation of water supply in GCC countries. *Desalination 186 (1-3)*, 187-198.

Delion, N., Mauguin, G., Corsin, P. (2004). Importance and impact of post treatments on design and operation of SWRO plants. *Desalination 165 (1-3)*, 323-334.

Dreybrodt, W., Lauckner, J., Zaihua, L., Svensson, U., & Buhmann, D. (1996). The kinetics of the reaction CO2 + H2O → H+ + HCO3− as one of the rate limiting steps for the dissolution of calcite in the system H2O·CO2·CaCO3. *Geochimica et Cosmochimica Acta, 60*(18), 3375-3381. doi: 10.1016/0016-7037(96)00181-0

Durlach, J., Bara, M. and Guiet-Bara, A. (1989). Magnesium level in drinking water: its importance in cardiovascular risk. In Y. I. a. J. Durlach (Ed.), *Magnesium in Health and Disease* (pp. 173-182). London: J.Libbey & Co Ltd.

Eisenberg, M. J. (1992). Magnesium deficiency and sudden death *Am. Heart J.124*, 544-549.

EU. (1980). *Council Directive 80/778/EEC of 15 July 1980 relating to the quality of water intended for human consumption*.

EU. (1998). *Council Directive 98/83/EC on the quality of water intended for human consumption : calculation of derived activity concentrations*. Roma: Istituto superiore di sanità.

Garzon, P. a. E., M.J. (1998). Variation in the mineral content of commercially available bottled waters: implication for health and disease. *Am. J. Med. 105*, 125-130.

Golubev, I. M. a. Z., V.P. . (1994). On the standard of total hardness in drinking water (in Russian). *Gig. Sanit. No.3/1994*, 22-23.

Greenlee L.F., L. F., Freeman B.D., Marrot B., Moulin P. (2009). Reverse osmosis desalination: Water sources, technology, and today's challenges. *Water Research 43 (9)*, 2317-2348.

Gyurek L.L., F. G. R., Belosevic M. (1997). Modeling chlorine inactivation requirements of Cryptosporidium parvum oocysts. *Journal of Enviromental Engineering - Asce 123 (9)*.

Hernandez-Suárez. (2005). Short guideline for limestone contactor design for large desalination plants Canary Islands Water Center.

Imran, S. A., Dietz, J.D., Mutoti, G., Xiao, W., Taylor, J.S. and Desai, V. (2005). *Effects of blending on distribution system water quality*. Denver, Colo.: AWWA Research Foundation and Tampa Bay Water.

Iwami, O., Watanabe, T., Moon, Ch.S., Nakatsuka, H. and Ikeda, M. (1994). Motor neuron disease on the Kii Peninsula of Japan: excess manganese intake from food coupled with low magnesium in drinking water as a risk factor. *Sc. Total Environ. 149*.

Jacqmin, H., Commenges, D., Letenneur, L., Barberger-Gateau, P. and Dartigues, J.F. . (1994). Components of drinking water and risk of cognitive impairment in the elderly. *Am. J. Epidemiol., 139*, 48-57.

Jalil, A., Robinson, R. B., Letterman, R. D., Mackintosh, G. S. . (2002). Small public water system technology guide - Limestone contactors. *Volume II*. Retrieved from New England Water Treatment Technology Assistance Center website:

KG, E. M. G. C. (2011). Technical data sheet on Juraperle: Eduard Merkle GMBH & CO. KG.

Kozisek, F. (1992). *Biogenic value of drinking water (in Czech).* Doctoral, National Institute of Public Health, Praha.

Kozisek, F. (2003). Health significance of drinking water calcium and magnesium. Retrieved from Available from: https://www.szu.cz/chzp/voda/pdf/haardness.pdf website:

Lutai, G. F. (1992). Chemical composition of drinking water and the health of population (in Russian). *Gig. Sanit. No.1/1992*, 13-15.

Mackintosh, G. S., De Souza, P.F. and De Villiers, H. A. (2003). Design and operation guidelines for fixed bed limestone contactors.

Melles, Z. a. K., S.A. . (1992). Influence of the magnesium content of drinking water and of magnesium therapy on the occurence of preeclampsia. *Magnes. Res. 5*, 277-279.

Moel, P. J. d., Verberk, J. Q. J. C., & Dijk, J. C. v. (2006). *Drinking water : principles and practices*. New Jersey ; Hong Kong: World Scientific.

Morse, J. W., & Arvidson, R. S. (2002). The dissolution kinetics of major sedimentary carbonate minerals. *Earth-Science Reviews, 58*(1–2), 51-84. doi: 10.1016/s0012-8252(01)00083-6

Muzalevskaya, L. S., Lobkovskii, A.G. and Kukarina, N.I. . (1993). Incidence of chole - and nephrolithiasis, osteroarthrosis, and salt arthropathies and drinking water hardness (in Russian). *Gig. Sanit. No. 12/1993*, 17-20.

Novikov, J. V., Plitman, S.I., Levin, A.I. and Noarov, J.A. (1983). Hygienic regulation for the minimum magnesium level in drinking water (In Russian). *Gig. Sanit. No.9/1983*.

Plummer, L. N., Busenberg, E. (1999). Data on the crystal growth of calcite from calcium bicarbonate solutions at 34°C and CO_2 partial pressures of 0.101, 0.0156 and 0.00102 atmospheres. Reston, Virginia U.S. Geological Survey.

Plummer, L. N., Wigley, T. M. L., & Parkhurst, D. L. (1978a). Critical-Review of Kinetics of Calcite Dissolution and Precipitation. *Abstracts of Papers of the American Chemical Society, 176*(Sep), 84-84.

Plummer, L. N., Wigley, T. M. L., & Parkhurst, D. L. (1978b). Kinetics of Calcite Dissolution in Co2-Water Systems at 5-Degrees-C to 60-Degrees-C and 0.0 to 1.0 Atm Co2. *American Journal of Science, 278*(2), 179-216.

Rakhmanin, Y. A., Bonasevskaya, T. I., Lestrovoy, A.P., Michailova, R.I., Guscina, L. M. (1976). Coll.: Public Health Aspects of Environmental Protection (In Russian). *Acad. Med. Sci. USSR*(fasc. 3), 68-71.

Rakhmanin, Y. A., Fillippova, A.V., Michailova, R.I., Belyaev, N.N., Lamentova, T.G., Kumpan, N.B. and Feldt, E.G. (1990). Hygienic assessment of mineralizing lime materials used for the correction of mineral composition of low-mineralized water (in Russian). *Gig. Sanit. No.8/1990*, 4-8.

Rakhmanin, Y. A., Lycnikova, T. D., Michailova, R.I. (1973). Coll.: Water Hygiene and the Public Health Protection of Water Bodies (in Russian) *Acad. Med. Sci. USSR*(fasc. 3), 44-51.

Rubenowitz, E., Molin, I., Axelsson, G., and Rylander, R. . (2000). Magnesium in drinking water in relation to morbidity and mortality from acute myocardial infarction. *Epidemiology 11*, 416-421.

Sjöberg, E. L., & Rickard, D. T. (1985). The effect of added dissolved calcium on calcite dissolution kinetics in aqueous solutions at 25°C. *Chemical Geology, 49*(4), 405-413. doi: 10.1016/0009-2541(85)90002-6

Sontheimer, H., Kolle, W., & Snoeyink, V. L. (1981). The siderite model of the formation of corrosion-resistant scales. *Journal American Water Works Association, 73*(11), 572-579.

Svensson, U., & Dreybrodt, W. (1992). Dissolution kinetics of natural calcite minerals in CO2-water systems approaching calcite equilibrium. *Chemical Geology, 100*(1–2), 129-145. doi: 10.1016/0009-2541(92)90106-f

Tang, Z., Hong, S., Xiao, W., & Taylor, J. (2006). Characteristics of iron corrosion scales established under blending of ground, surface, and saline waters and their impacts on iron release in the pipe distribution system. *Corrosion Science, 48*(2), 322-342. doi: 10.1016/j.corsci.2005.02.005

UNEP. (2008). Vital water graphics 2nd edition. from www.unep.org

Verd Vallespir, S., Domingues Sanches, J., Gonzales Quintial, M., Vidal Mas, M., Mariano Soler, A. C., de Roque Company, C. and Sevilla Marcos, J. M. (1992). Association between calcium content of drinking water and fractures in children (in Spanish). *An. Esp. Pediatr., 37*, 461-465.

Vitens. (2010). Gelderland Kwaliteit en Zuivering: Vitens.

Wen, Y. S., Sutherland, J., Mackey, E., Walker, W.S. (2012). *Upflow calcite contactor study.* Master of Science, University of Texas at El Paso University of Texas at El Paso

WHO. (1980). *Guidelines on health aspects of water desalination*. Geneva: World Health Organization.

WHO. (1996). *Guidelines for drinking-water quality* (2nd ed.). Geneva: World Health Organization.

WHO. (2011). *Guidelines for drinking-water quality* (4th ed.). Geneva: World Health Organization.

Withers, A. (2005). Options for recarbonation, remineralization and disinfection for desalination plants. *Desalination 179 (1-3)*, 11-24.

Yang, C. Y., Cheng, M.F., Tsai, S.S. and Hsieh, Y.L. (1998). Calcium, magnesium and nitrate in drinking water and gastric cancer mortality. *Jpn. J. Cancer, Res. 89*, 124-130.

Yang, C. Y., Chiu, H.F., Chang, Ch. Ch.,, Wu T.N. and Sung, F. Ch. . (2002). Association of very low birth weight with calcium levels in drinking water. *Environ. Research, Section A 89*, 189-194.

Yang, C. Y., Chiu, H.F., Cheng, M.F., Tsai, S.S., Hung, Ch.F. and Lin, M.Ch. (1999a). Esophageal cancer mortality and total hardness levels in Taiwan's drinking water *Environ. Research, Section A 81*, 302-308.

Yang, C. Y., Chiu, H.F., Cheng, M.F., Tsai, S.S., Hung, Ch.F. and Tseng, Y.T. . (1999b). Pancreatic cancer mortality and total hardness level in Taiwan's drinking water. *J. Toxicol. Environ. Health, A 56*, 361-369.

Yang, C. Y., Chiu, H.F., Cheng, M.F., Hsu, T.Y., and Wu, T.N. (2000). Calcium and magnesium in drinking water and the risk of death from breast cancer. *J. Toxicol. Environ. Health, Part A 60*, 231-241.

Yang, C. Y., Chiu, H.F., Chiu, J.F., Tsai, S.S. and Cheng, M.F. . (1997). Calcium and magnesium in drinking water and risk of death from colon cancer. *Jpn. J. Cancer, Res. 88*, 928-933.

Yang, C. Y., Tsai, S.S., Lai, T. Ch., Hung, Ch.F., and Chiu, H.F. . (1999c). Rectal cancer mortality and total hardness level in Taiwan's drinking water. *Environ. Research Section A 80*, 311-316.

Annexes

Table of contents

Annex A Summary on development of hardness and bicarbonate requirements on human health, corrosion and legal regulations

Annex A.1. Relevant studies on hardness level of drinking water in terms of human-health

Calcium and magnesium intakes were proved to be critical to human health over the last century. Specific knowledge about changes in calcium metabolism in a population supplied with desalinated water (i.e., distilled water filtered through limestone) low in TDS and calcium, was obtained from studies carried out in the Soviet city of Shevchenko. The local population showed decreased activity of alkaline phosphatase, reduced plasma concentrations of calcium and phosphorus and enhanced decalcification of bone tissue. The changes were most marked in women, especially pregnant women and were dependent on the duration of residence in Shevchenko (Y. A. Rakhmanin, Lycnikova, T. D., Michailova, R.I., 1973). The importance of water calcium was also confirmed in a one-year study of rats on a fully adequate diet in terms of nutrients and salts and given desalinated water with added dissolved solids of 400 mg/l and either 5 mg/l, 25 mg/l, or 50 mg/l of calcium (Y. A. Rakhmanin, Bonasevskaya, T. I., Lestrovoy, A.P., Michailova, R.I., Guscina, L. M., 1976). The animals given water dosed with 5 mg/l of calcium exhibited a reduction in thyroidal and other associated functions compared to the animals given the two higher doses of calcium.

Throughout the last two decades, many other studies had been carried out and suggest that the intake of soft water, i.e. water low in calcium, may be associated with higher risk of fracture in children (Verd Vallespir, 1992), certain neurodegenerative diseases (Jacqmin, 1994), pre-term birth and low weight at birth (C. Y. Yang, Chiu, H.F., Chang, Ch. Ch.,, Wu T.N. and Sung, F. Ch. , 2002) and some types of cancer (C. Y. Yang, Cheng, M.F., Tsai, S.S. and Hsieh, Y.L., 1998; C. Y. Yang, Chiu, H.F., Chiu, J.F., Tsai, S.S. and Cheng, M.F. , 1997). In addition to an increased risk of sudden death (Bernadi, 1995; Eisenberg, 1992; Garzon, 1998), the intake of water low in magnesium seems to be associated with a higher risk of motor neuronal disease (Iwami, 1994), pregnancy disorders (so-called preeclampsia) (Melles, 1992), and some types of cancer (C. Y. Yang, Chiu, H.F., Cheng, M.F., Tsai, S.S., Hung, Ch.F. and Lin, M.Ch., 1999a; C. Y. Yang, Chiu, H.F., Cheng, M.F., Tsai, S.S., Hung, Ch.F. and Tseng, Y.T. , 1999b; C. Y. Yang, Chiu, H.F., Cheng, M.F., Hsu, T.Y., and Wu, T.N., 2000; C. Y. Yang, Tsai, S.S., Lai, T. Ch., Hung, Ch.F., and Chiu, H.F. , 1999c).

Some studies even recommended a minimum level of magnesium, calcium and total hardness in drinking water:

- For magnesium, a minimum of 10 mg/l (Novikov, 1983; Rubenowitz, 2000) and an optimum of about 20-30 mg/l (Durlach, 1989; F. Kozisek, 1992);
- For calcium, a minimum of 20 mg/l (Novikov, 1983) and an optimum of about 50 (40-80) mg/l (F. Kozisek, 1992; Y. A. Rakhmanin, Fillippova, A.V., Michailova, R.I., Belyaev, N.N., Lamentova, T.G., Kumpan, N.B. and Feldt, E.G., 1990);
- For total water hardness, the sum of calcium and magnesium should be 2 to 4 mmol/l (Golubev, 1994; Lutai, 1992; Muzalevskaya, 1993)

At these concentrations, minimum or no adverse health effects were observed. The maximum protective or beneficial health effects of drinking water appeared to occur at the estimated desirable or optimum concentrations. The recommended magnesium levels were based on cardiovascular system effects, while changes in calcium metabolism and ossification were used as a basis for the recommended calcium levels. The upper limit of the hardness optimal range was derived from data that showed a higher risk of gall stones, kidney stones, urinary stones, arthrosis and arthropathies in populations supplied with water of hardness higher than 5 mmol/L.

Annex A.2. Corrosion concerns from hardness and bicarbonate level in supplied water

Pure water, as produced with reverse osmosis membrane filtration or flash evaporation, cannot be distributed as drinking water because of its corrosivity towards pipe material in distribution systems and in-house plumbing. Pure water needs a certain minimum alkalinity and a high pH in order to prevent corrosion. The relation between alkalinity, pH and iron corrosion is shown in Figure 45 (Tang, Hong, Xiao, & Taylor, 2006). Although the theoretical siderite model did not consider particulate release of which forms iron dissolves, the model predicts correctly iron will decrease as pH and alkalinity increase.
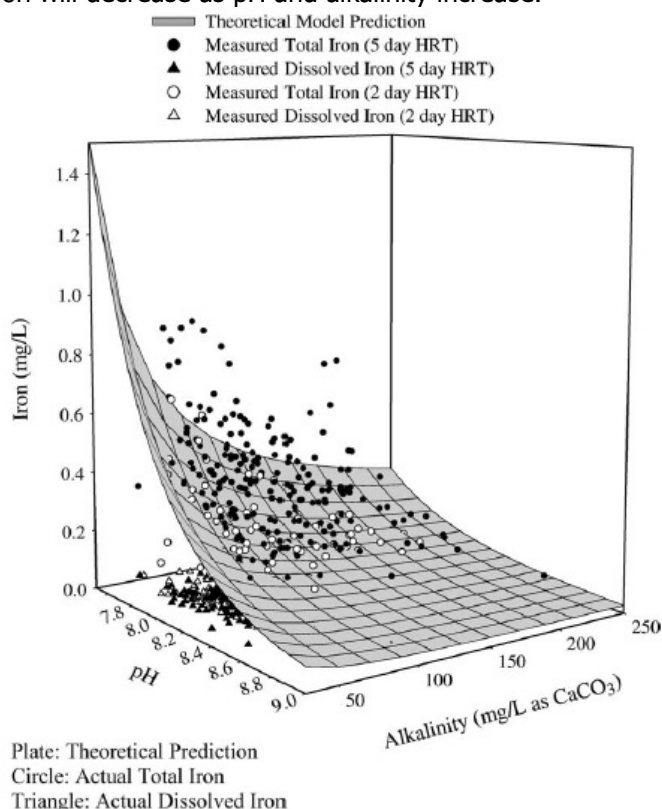
Fig. 9. Actual and predicted total and dissolved iron versus pH and alkalinity using the siderite model. Data taken from hybrid pilot distribution lines receiving blended waters over one year.

Figure 45: Actual and predicted total and dissolved iron vs pH and alkalinity using siderite model (Corrosion Science 48 (2006) 322–342)

Similar relations have been found for other pipe materials. In Effects of Blending on Distribution System Water Quality (Imran, 2005), it has been shown that higher alkalinity would reduce the colour release which also which also represents the release of iron corrosion product into water. A strong relationship existed between the total iron (Fe) concentration (mg/L) and apparent color (cpu) is shown (Imran et al, 2005b; Imran, 2003):

Fe = 0.0132 x Apparent Color

Moreover, the adverse effect of increased chlorides in the reverse osmosis (RO) water on color release is also mitigated by a higher alkalinity in the groundwater source (Imran et al, 2005b) because a higher chloride and sodium level could be expected in case of membrane deterioration. However, Imran (2005) also indicated that higher alkalinity would increase the lead release into RO water. The fact is that ground water with high alkalinity is beneficial for controlling iron release but detrimental to copper and lead release. The author hence recommends increasing pH level in the water of high alkalinity to a certain range could help controlling copper and lead release although calcium scaling and deposition may occur in the

70

distribution system. A decrease in hydraulic retention time (HRT) could also decrease the level of iron release in the pipe system.

There are also a few other studies around the world tackle the corrosion problem in water distribution system by adjusting to suitable range of pH and alkalinity level. One of the most prominent cases was Seattle severe corrosion problems in distribution system due to the water source from Cascade Mountain range which provides soft, low to neutral pH, poor buffering capacity and low mineral content according to Internal corrosion of water distribution systems each(AWWA Research Foundation. & DVGW-Technologiezentrum Wasser., 1996). Corrosion of the galvanized steel resulted in reduced flow and blockage of pipe as well as dissolving heavy metals from plumbing systems into "standing" water which caused a potential health concern. The main causes of corrosion were found to be the acidity of the water with low pH due to chlorination process, the insufficiency of calcium and bicarbonate alkalinity as well as high halogen-alkalinity ratio (above 0.6). Therefore, raising pH and alkalinity in the water is the chosen solution for the problem. Since 1982, lime and soda ash has been added into the water supply of Seattle and that has significantly improved the situation from then on. On the other hand, in the water systems of Yanbu and Medina city in Saudi Arabia, pipe corrosion was also found just a few weeks after first installation built between 1979 and 1980 (AWWA Research Foundation. & DVGW-Technologiezentrum Wasser., 1996). Although the steel pipe was lined with an epoxy coating, pieces of lining had peeled off the pipe walls are easily found at the screens protecting the pumps of the Medina line. Causes of corrosion were implied as too high levels of sodium and chloride compared to bicarbonate and calcium contents and the water was not saturated with calcium carbonate so no protective layer could be formed on the pipe inner walls. Consequently, the remedies adopted were to increase the calcium hardness to near 60 mg CaCO3/L and pH to above 8.0 to protect the entire pipe wall, which were found to be effective after six months. Similar corrosion situation also happened at Al Khobar the eastern town in Saudi Abrabia where the mains, made of steel with an epoxy lining between 1979 and 1981. The same treatment method was applied here as calcium hardness was increased to 60 mg CaCO3/L as well as pH to obtain calcifying water. These case studies clearly shows the relations between pH, alkalinity and calcium hardness to the corrosion possibility in the distribution system which causes harm in both economics and human health terms.

These relations have resulted in water quality regulations and recommendations giving a minimum alkalinity value which varies by different legislations and also changes over time. The requirements and recommendations for pH are also less restrictive, because of its complicated relation with other water quality parameters. Nowadays, corrosion risk in water distribution pipeline is considered as the main governing factor in controlling pH, total hardness and bicarbonate level in the supplied drinking water especially in the global and local standards of drinking water quality. This is partially due to the lack of direct and convinced evidences for the effects of total hardness, bicarbonate level on health base concern which will be discussed in the following part.

Annex A.3. WHO – Guidelines for drinking water quality

Because adverse effects such as altered water-salt balance were observed not only in completely desalinated water but also in water with total dissolved solids (TDS) between 50 and 75 mg/l, the WHO report (1980) recommended that the minimum TDS in drinking water should be 100 mg/l. The composing team also recommended that the optimum TDS should be about 200-400 mg/l for chloride-sulphate waters and 250-500 mg/l for bicarbonate waters. In addition to the TDS levels, the minimum calcium content of desalinated drinking water around 30 mg/l is also recommended. These levels were based on health concerns with the most critical effects being hormonal changes in calcium and phosphorus metabolism and reduced mineral saturation of bone tissue. Also, when calcium is increased to 30 mg/l, the corrosive activity of desalinated water would be appreciably reduced and the water would be more stable. The team (WHO, 1980) also recommended a bicarbonate ion content of 30 mg/l as a minimum essential level needed to achieve acceptable organoleptic characteristics, reduced corrosion, and an equilibrium concentration for the recommended minimum level of calcium.

From the second edition (WHO, 1996) onwards, WHO no longer specified either minimum or maximum limits concerning public health for calcium, manganese or total hardness in drinking water. There are insufficient data to suggest either minimum or maximum concentrations of minerals at this time, as adequate intake will depend on a range of other factors. Therefore, no guideline values are proposed.

In the fourth edition (WHO, 2011), WHO provides some remarks on the acceptability aspects including taste, odour and appearance in which states that public acceptability of the degree of hardness of water may vary considerably from one community to another. The taste threshold for the calcium ion is in the range of 100–300 mg/l, depending on the associated anion, and the taste threshold for magnesium is probably lower than that for calcium. In some instances, consumers tolerate water hardness in excess of 500 mg/l. Depending on the interaction of other factors, such as pH and alkalinity, water with a hardness level above approximately 200 mg/l may cause scale deposition in the treatment works, distribution system and pipeline network and tanks within buildings. Soft water, but not necessarily cation exchange softened water, with a hardness of less than 100 mg/l may, in contrast, have a low buffering capacity and so be more corrosive for water pipes.

Although no certain health base guideline is proposed for hardness in drinking water, WHO (2011) does discuss on the corrosion aspect of supplied drinking water which might greatly affect the final quality where human consume. However, most corrosion could be overcome or limited under control of the water pH before supplying. Depending on the material of the piping distribution system, a different appropriate pH level range should be selected for the supplying drinking water.

Table 30: Recommended pH ranges for corrosion control

Corrosive material	Controlled pH range
Brass	< 8.3
Cement	≥8.5
Copper[1]	8.0 – 8.5
Iron [2]	6.8 – 7.3
Lead[3]	8.0 – 8.5
Zinc[3]	≈ 8.5

(1): less than 60mg CaCO3/L and pH<6.5 → very aggressive to copper
(2): Besides pH control, hardness & Alkalinity must be adjusted to at least 40 mg/L (CaCO3), super-saturation with CaCO3 of 4 -10 mg/L.
(3): for low Alkalinity water

Annex A.4. EU regulations on the quality of water intended for human consumption

The first European Directive (EU, 1980) established a requirement for minimum hardness for softened or desalinated water ($\geq$ 60 mg/L as calcium or equivalent cations). The alkalinity level of water was also required to be not lower than 60 mg HCO_3^-/L while the guide range of water pH is between 6.5 and 8.5 with the maximum admissible value of 9.5.

However, the new Directive (EU, 1998) does not contain a requirement for calcium, magnesium, water hardness or bicarbonate levels. Moreover, it does not prevent member states from implementing such a requirement into their national legislation. The guide level of pH was also simplified to be from 6.5 to 9.5. EU (1998) also suggests that the supplied drinking water should not be aggressive.

Annex B   Kinetics models for calcite dissolution with PHREEQC simulation

Annex B.1. PWP model with Chou improvement on rate constants

Since Chou only provided a set of measured rate constants (k_1, k_2, k_3 and k_4) at 25°C which are more accurate than those constants in PWP model (Plummer, 1999), relations between Chou rate constants and temperature are missing. Consequently, in order to bring the model closer to the accurate values measured by Chou, PWP's relation between rate constants and temperature could be adopted. However, there are generally two alternatives to express Chou rate constant over temperature range following PWP relation: by correction factor and by direct shift of the logarithm curve of the rate constants.

General form of PWP rate constant: $k_i = 10^{(A + B/TK)}$ or $\log(k_i) = A + B/TK$

i   = 1,2 or 3
A, B   = constants in PWP relation
TK   = Kelvin temperature = t ($^{\circ}$C) + 273.15
At 25°C, $\log(k_i) = C_i$ = Chou measured value for k_i

Correction factor:

Assume α_i is the correction factor for PWP model.

⇨ $C_i = \alpha_i [A + B/(25 + 273.15)] = \alpha_i (A + B/298.15)$

⇨ $\alpha_i = C/(A + B/298.15)$

From this follow that, the following table of correction factor α_i is achieved:

Table 31: Summary of rate constants of PWP and Chou with the correction factor for PWP model ($mmol/cm^2 s$)

Rate constant	Calcite		Correction factor
Formula	$CaCO_3$		α_i
Models	Chou	PWP	
log k_1	-1.05	-1.29	0.814
log k_2	-4.30	-4.47	0.962
log k_3	-7.19	-6.92	1.039

Direct shift of the logarithm curve:

Assume δ_i is the difference between PWP and Chou rate constants

⇨ $C_i = A + B/298.15 + \delta_i$

⇨ $\delta_{i\_} = C_i - (A + B/298.15)$

Hence at temperature T other than 298.15°K:

⇨ $\log k_i = A + B/T + \delta_i = A + B/T + C_i - (A + B/298.15) = C_i - B*(1/298.15 - 1/T)$

This method could also be seen as the Van't Hoff relation for two rate different measured rate constants k_{iPWP} and k_{iChou}:

⇨ $\ln k_{iPWP-Chou(T)} - \ln k_{iChou(25)} = \ln(k_{iPWP-Chou(T)} / k_{iChou(25)}) = 2.3026*\log(k_{iPWP-Chou(T)} / k_{iChou(25)})$

   $= \Delta H*[1/T - 1/(273.15 + 25)]$

⇨ $\log k_{iPWP-Chou(T)} - \log k_{iChou(25)} = (\Delta H/2.3026)*(1/T - 1/298.15) = - B*(1/298.15 - 1/T)$

⇨ $\log k_{iPWP-Chou(T)} = \log k_{iChou(25)} - B*(1/298.15 - 1/T) = C_i - B*(1/298.15 - 1/T)$

With the following graphs comparing the rate constant variations over temperature for two alternatives, it is easy to recognize that the method of direct shifting δ provide the same rate constant's gradient as the original PWP model hence the original variation is reserved while the correction factor method does not have the same quality.

Therefore, the direct shift δ method would be accepted to improve the PWP model's rate constant based on the Chou measured values. Hence the Chou's rate constant could be expressed as a function of temperature as followed (in terms of $mmol/cm^2s$):

$$\log k_1 = -1.05 + 444*(1/298.15 - 1/T)$$

$$\log k_2 = -4.30 + 2177*(1/298.15 - 1/T)$$

$$\log k_3 = -7.19 + 317*(1/298.15 - 1/T) \quad \text{for} \quad T \leq 273.15 + 25 = 298.15^oK$$

$$= -7.19 + 1737*(1/298.15 - 1/T) \quad \text{for} \quad T > 298.15^oK$$
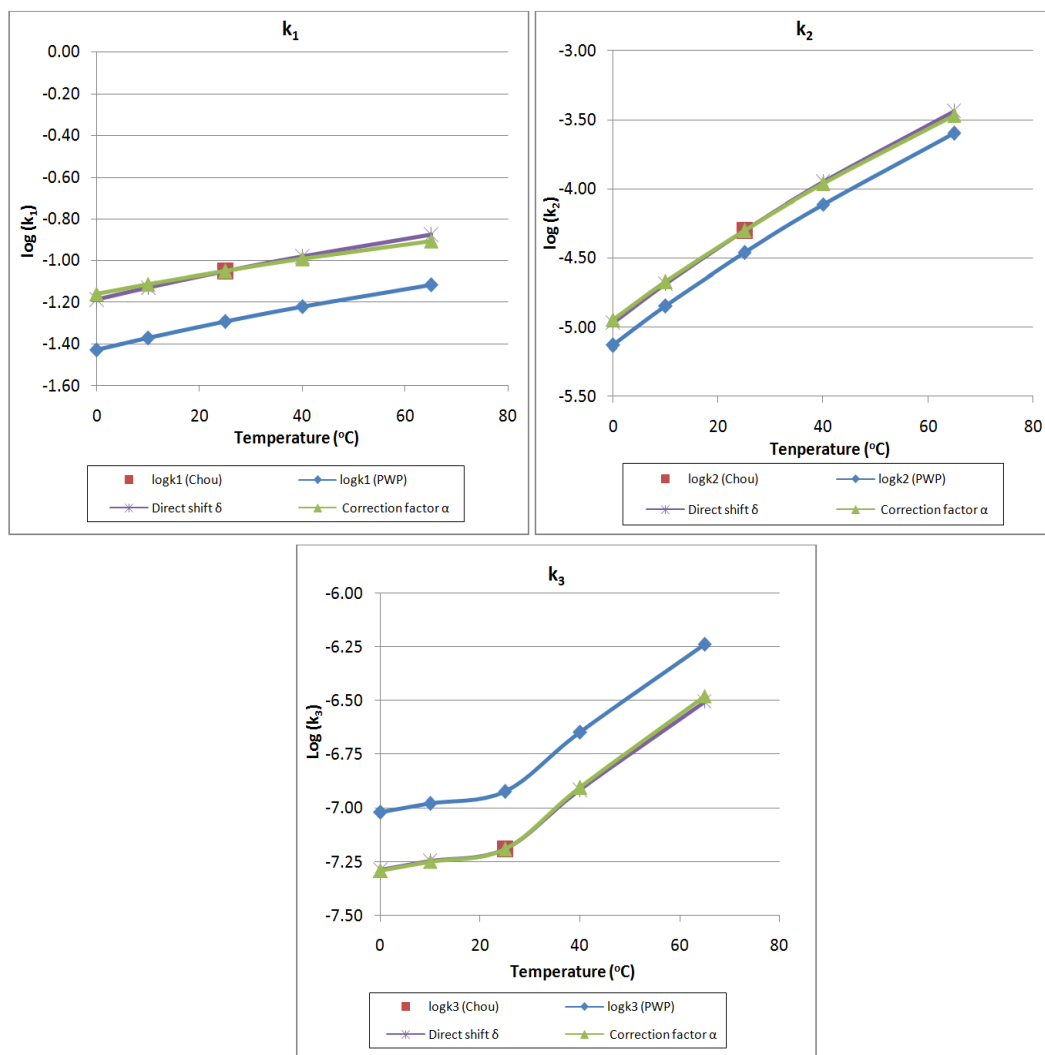
Figure 46: Rate constant vs. temperature for different models

Annex B.2. A brief introduction of PHREEQC & PHREEQC built in Excel

PHREEQC is one of the most popular water-chemistry modelling software nowadays especially in geohydrology. Starting in 1980, it has been developed over time by the US Geological Survey (USGS). Although being widely applied in geohydrology, PHREEQC is hardly applied in water treatment. Due to its powerful ability in simulating complicated chemical reaction processes, PHREEQC has a large potential in water treatment area. It is a broad language program which allows users flexibility to manipulate the simulation of treatment process which could be different from a traditional problem. This is also a limitation in many existing modelling software used in water treatment currently such as Stimela.

Since it is a broad language program, the user of PHREEQC must be able to write codes and commands that to simulate the real process. After the codes and commands are ready, data should be inputted in for the simulation process to generate output. However, writing programming codes and commands is usually not familiar to the practice engineering in water treatment. Thus, the simulation codes could be pre-programmed to be a fix application for a certain simulations. The universal interface of Excel could be used as an excellent user-friendly base to develop the PHREEQC codes on. The user only needs to input the required data and trigger the simulation process.
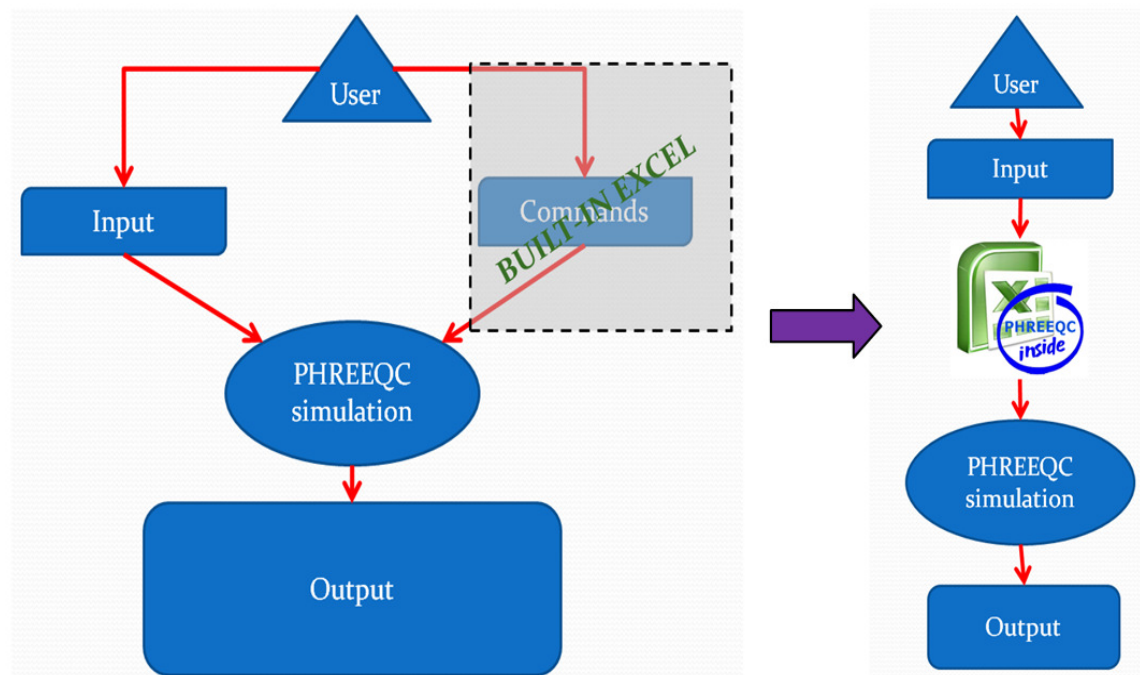
Figure 47: Processing chart of PHREEQC and PHREEQC built in Excel

Annex B.3. Extra code lines inputted for the full PWP model and simplified unaerated system model in PHREEQC

Full PWP model:

```
RATES
Calcit_PWP_k4
      -start
        1    REM                        Modified from Plummer and others, 1978
        2    REM                        M = current moles of calcite
        3    REM                        M0 = initial moles of calcite
        4    REM                        parm(1) = Area/Volume, cm^2/L    (or cm^2 per cell)
        5    REM                        parm(2) = exponent for M/M0 for surface area correction
       10    REM                        rate = 0 if no calcite and undersaturated
       20    si_cc = SI("Calcite")
       30    if (M <= 0  and si_cc < 0) then goto 300
       40    k1 = 10^(0.198 - 444.0 / TK )
       50    k2 = 10^(2.84 - 2177.0 / TK )
       60    if TC <= 25 then k3 = 10^(-5.86 - 317.0 / TK )
       70    if TC > 25 then k3 = 10^(-1.1 - 1737.0 / TK )
       74    K2_ = 10^(-LK_SPECIES("HCO3-"))
       75    Ks_ = 10^(LK_PHASE("Calcite"))
       76    k4 = ( k1 + ( k2 * ACT("CO2")  + k3 * ACT("H2O") ) / ACT("H+") ) * K2_ / Ks_
       80    REM                        surface area calculation
       90    t = 1
      100    if M0 > 0 then t = M/M0
      110    if t = 0 then t = 1
      120    area = PARM(1) * (t)^PARM(2)
      130    rf = k1 * ACT("H+") + k2 * ACT("CO2") + k3 * ACT("H2O") - k4 * ACT("Ca+2") * ACT("HCO3-")
      140    REM                        1e-3 converts mmol to mol
      150    rate = area * 1e-3 * rf
      160    moles = rate * TIME
      170    REM                        do not dissolve more calcite than present
      180    if (moles > M) then moles = M
      190    if (moles >= 0) then goto 300
      200    REM                        do not precipitate more Ca or C(4) than present
      210    temp = TOT("Ca")
      220    mc  = TOT("C(4)")
      230    if mc < temp then temp = mc
      240    if -moles > temp then moles = -temp
      300    SAVE moles
      310    PUT(rf*10, 1)
      -end
```

Simplified model for unaerated system:

```
RATES
Calcit_closed
      -start
        1    REM                        Modified from Plummer and others, 1978
        2    REM                        M = current moles of calcite
        3    REM                        M0 = initial moles of calcite
        4    REM                        parm(1) = Area/Volume, cm^2/L    (or cm^2 per cell)
        5    REM                        parm(2) = exponent for M/M0 for surface area correction
       10    REM                        rate = 0 if no calcite and undersaturated
       20    si_cc = SI("Calcite")
       30    if (M <= 0  and si_cc < 0) then goto 300
       40    k1 = 10^(0.198 - 444.0 / TK )
       50    k2 = 10^(2.84 - 2177.0 / TK )
       60    if TC <= 25 then k3 = 10^(-5.86 - 317.0 / TK )
       78    if TC > 25 then k3 = 10^(-1.1 - 1737.0 / TK )
       80    REM                        surface area calculation
       90    t = 1
      100    if M0 > 0 then t = M/M0
      110    if t = 0 then t = 1
      120    area = PARM(1) * (t)^PARM(2)
      130    rf = k1 * ACT("H+") + k2 * ACT("CO2") + k3 * ACT("H2O")
      140    REM                        1e-3 converts mmol to mol
      150    rate = area * 1e-3 * rf * (1 - 10^(si_cc))            # new code: 2/3 removed for closed systems
      160    moles = rate * TIME
      170    REM                        do not dissolve more calcite than present
      180    if (moles > M) then moles = M
      190    if (moles >= 0) then goto 300
      200    REM                        do not precipitate more Ca or C(4) than present
      210    temp = TOT("Ca")
      220    mc  = TOT("C(4)")
      230    if mc < temp then temp = mc
      240    if -moles > temp then moles = -temp
      300    SAVE moles
      -end
```

Annex B.4. Simplified PWP model (PHREEQC default) vs. Full PWP model for aerated (open) systems

In order to investigate the differences of the PHREEQC default model and the full PWP model, a set of initial conditions is inputted in PHREEQC and each model would be applied to generate the rate of calcite dissolution over time. The initial conditions consists of demineralised water with insignificant mineral and bicarbonate content, constant pCO_2 of 0.01 atm and A/V ratio of 90 000 cm^2/L.

The results of two simulations are plotted on the same graphs as shown below. It is obvious that the PHREEQC default model (with SI) would take more time to reach equilibrium compared to the full PWP model with k_4 in the formula. This could be due to the assumption that the bicarbonate activity must be twice the calcium activity of the PHREEQC default model. In fact, the bicarbonate activity is not approximately twice the calcium activity by checking PHREEQC output file of the default model simulation at any state which might be due to the calculation sequences of PHREEQC. Consequently, the assumption is invalid and the PHREEQC default model is not very accurate for aerated system. Thus, the full PWP model is recommended in case of aerated system.
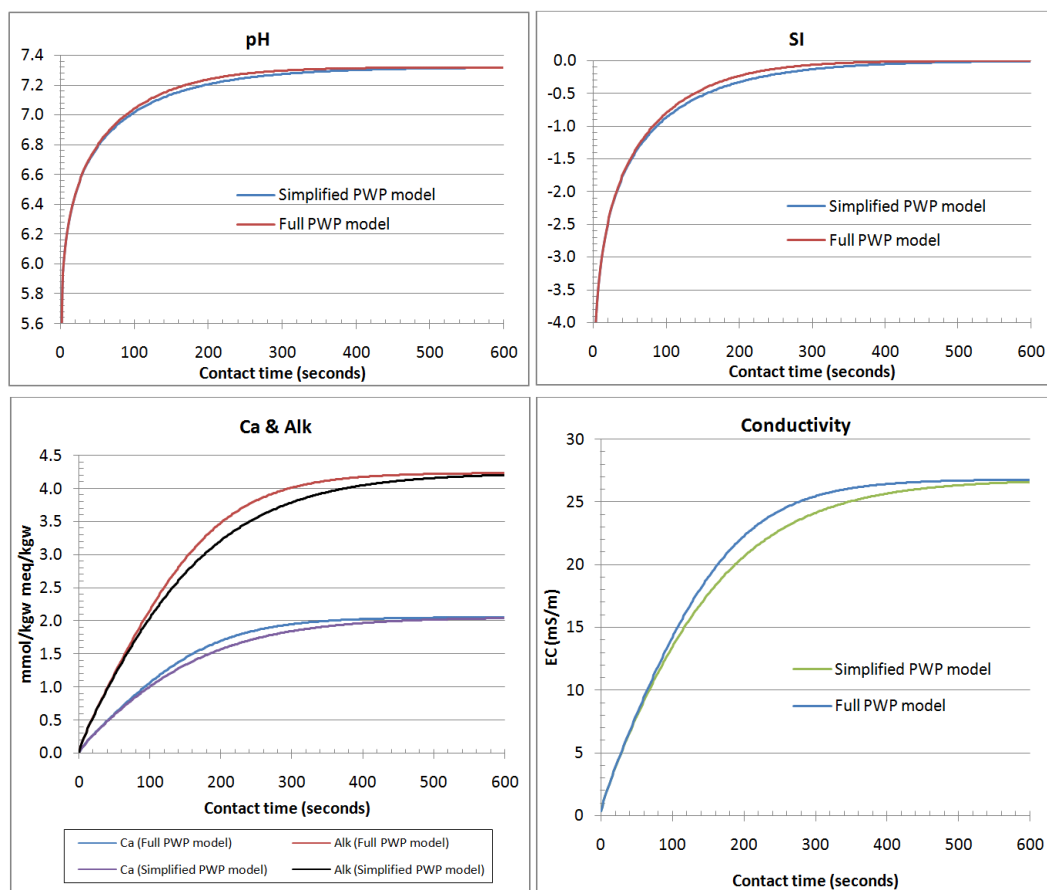
Figure 48: Simulation results for aerated systems (Simplified PWP model vs full PWP model)

Annex B.5. Simplified PWP model vs. Full PWP model for unaerated (close) systems

Similar to Annex B.7, sampling simulations are carried out in order to investigate the difference between simplified and full PWP model for the case of unaerated systems such as limestone contactor where CO_2 content in water would vary over time. The initial conditions for sampling simulation consists of demineralised water with insignificant mineral and bicarbonate content, constant pCO_2 of 0.01 atm and A/V ratio of 90 000 cm^2/L.

The results of two simulations are plotted on the same graphs as shown below. It is obvious that the PHREEQC default model is approximately the same as the full PWP model with k_4 in the formula. Thus, the simplified PWP model could replace the full PWP model in case of unaerated systems.
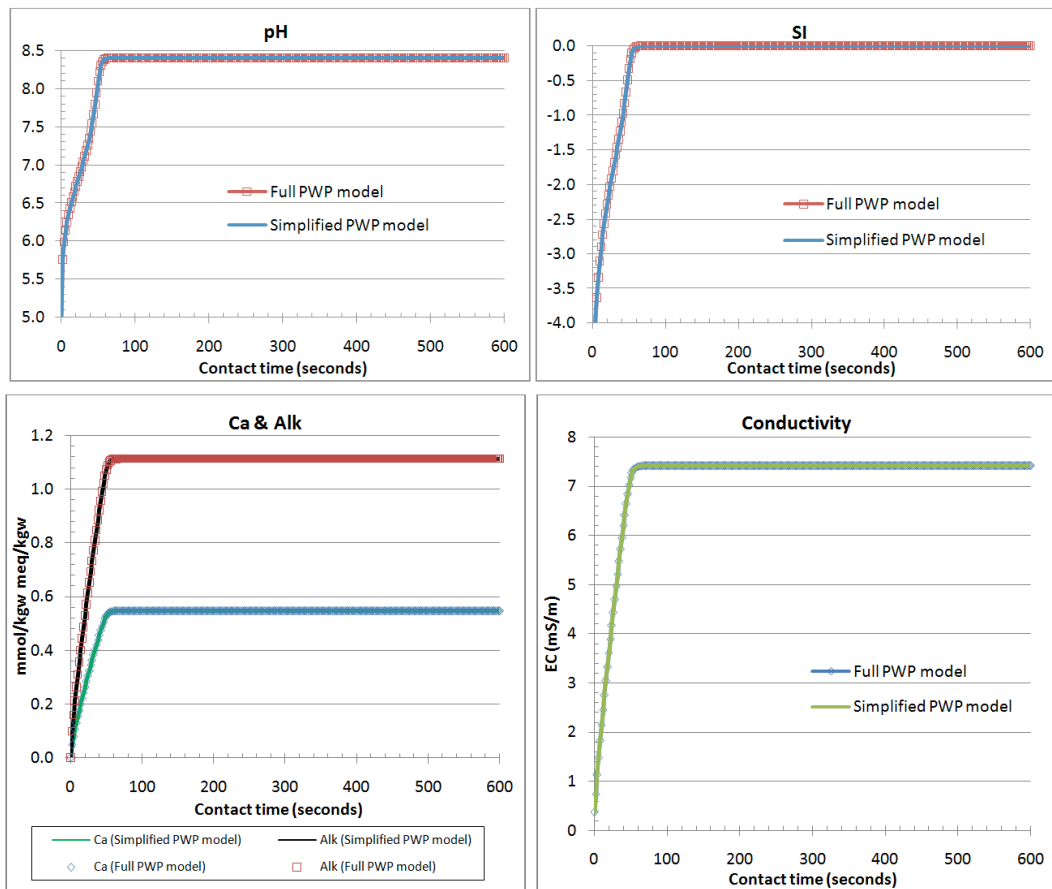
Figure 49: results for unaerated system (Simplified PWP model vs full PWP model)

Annex B.6. Vosbeck recorded data on Baker calcite and Acidized Juraperle dissolution

1. *Baker calcite*
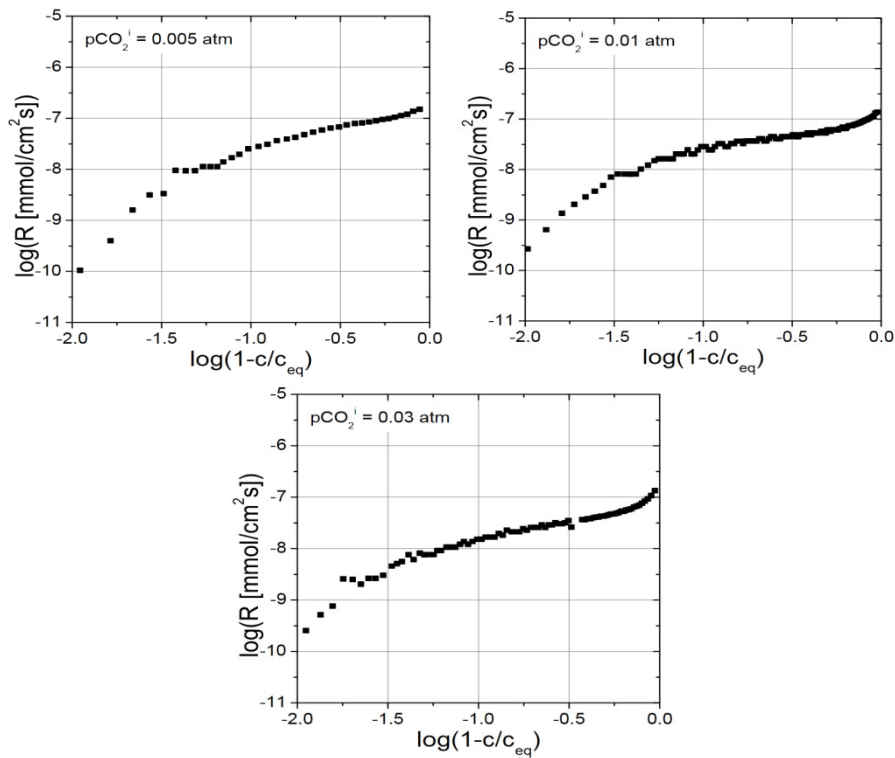
Figure 50: Vosbeck recorded data of Baker calcite dissolution rate vs. Ca content in water

2. *Acidized Juraperle*
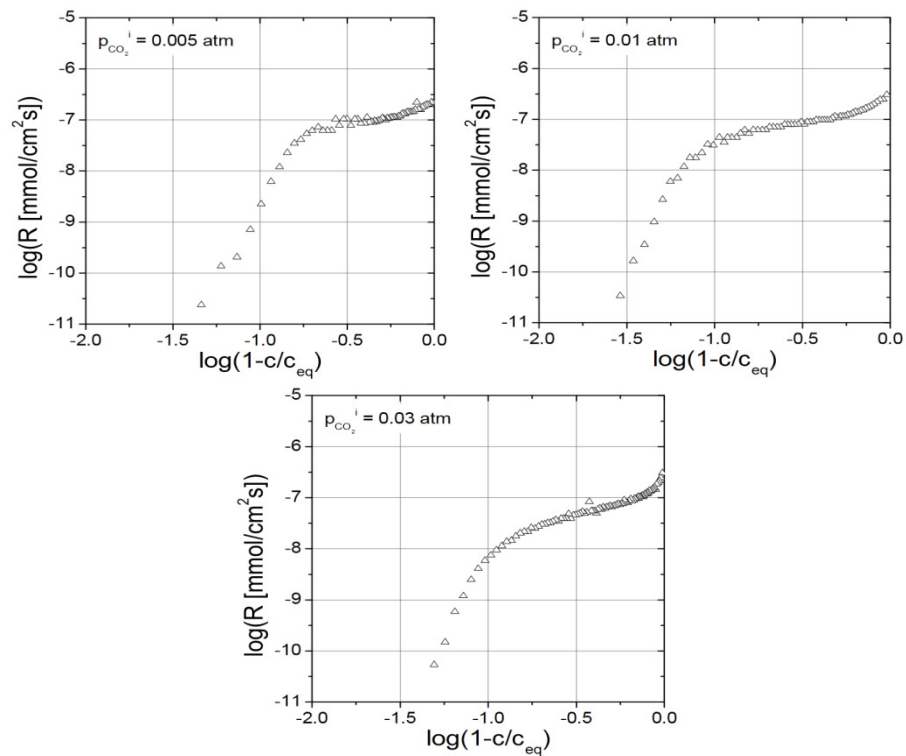
Figure 51: Vosbeck recorded data of acidized Juraperle dissolution rate vs. Ca content in water

Annex B.7. Failed approaches for optimizing best fits for Juraperle calcite dissolution

Adopting Lasaga model

Lasaga model: $r = [a_1*(H^+) + a_2*(H_2CO_3) + a_3*(H_2O)]*(1 - 10^{SI*n})$
With this adjustment, by varying n, the simulated pH curve over time could only shift left or right without improving the gradient problem. Thus, the fully matched fit on the measured data could not be achieved with Lasaga model.
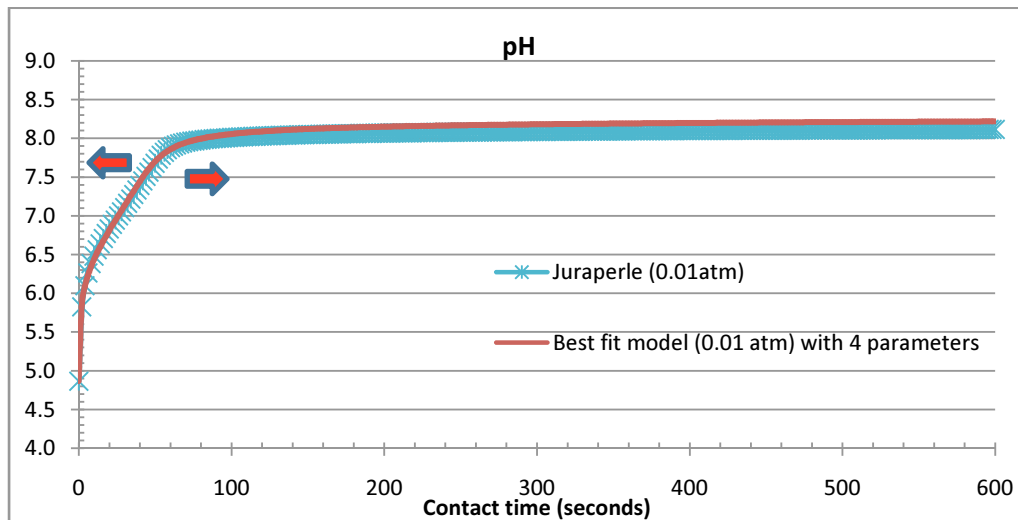
Figure 52: Vosbeck data on Juraperle (0.01 atm) vs. best fit improved model with Lasaga adjustment (curve shifted left and right when varying n)

Assuming pseudo equilibrium SI_e

Pseudo equilibrium SI_e or $CCPP_e$ could be introduced due to the fact that the dissolution process could be seen as virtually ceasing after a certain level of SI_e or $CCPP_e$ is reached (Figure 53). At this stage, the dissolution rate is significantly dropping compared to previous stage and very close to zero. When SI_e or $CCPP_e$ is introduced to the kinetics model, the dissolution curve would be limit to reach SI_e or $CCPP_e$ as the end point instead of the theoretical equilibrium (zero).
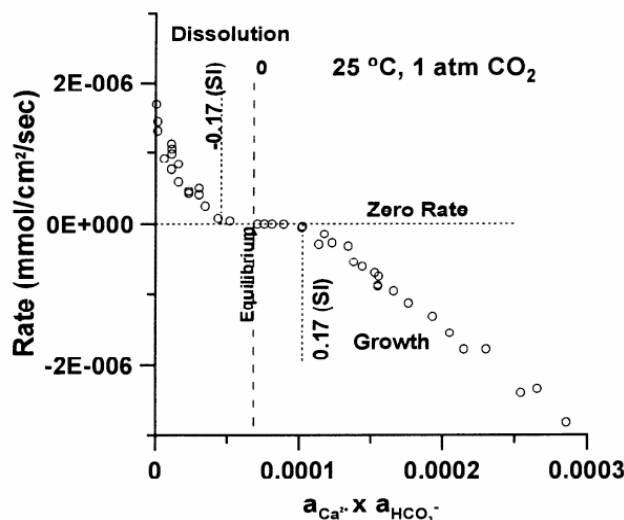
Figure 53: Calcite dissolution (precipitation) rate vs. product of calcium and bicarbonate content in water (Plummer and Busenberg, 1999)

In order to define SI_e or $CCPP_e$, the following graph of SI and CCPP of the solution over time could be plotted based on the recorded data. Now assuming a threshold of differential change over time compared to the plotted trend-line curve (Figure 54) would be chosen for instance, the first drop in the order of 100 (or log scale of 2).
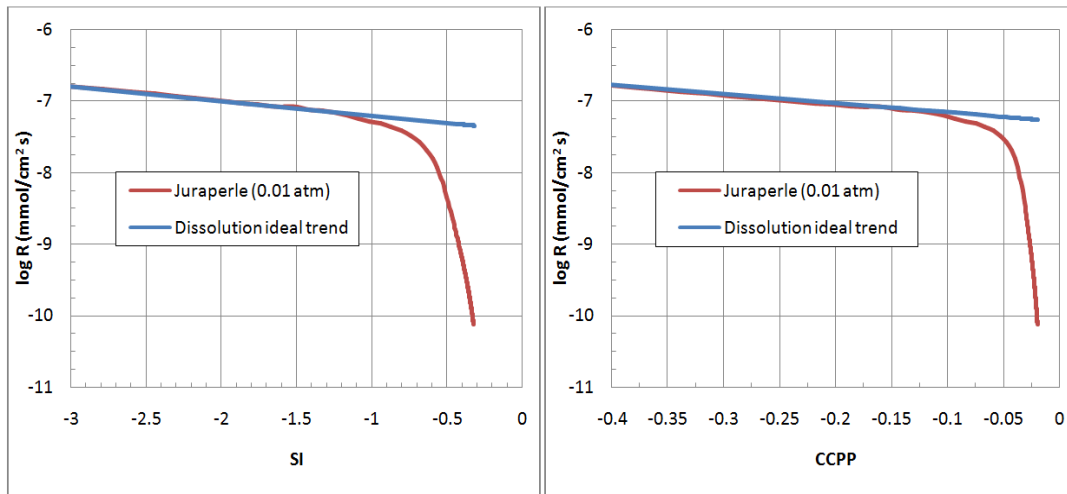
Figure 54: Dissolution rate vs. solution SI and CCPP (Vosbeck measured data against ideal trend line)

With the selected SI_e, the adjusted model could be used:
Adjusted model: $r = [a_1*(H^+) + a_2*(H_2CO_3) + a_3*(H_2O)]*(1 - 10^{(SI-SIe)})$
With the introduced pseudo equilibrium SIe (a negative value), the rate would be decreased hence lower gradient curve could be achieved. Thus, best fit for 0.01 atm case could be achieved.
However, if the case of Juraperle $pCO_2 = 0.005$atm is considered, it is obvious the measured curve here has a high gradient curve at equilibrium. A negative SI_e would make the curve even more flat. Only a positive SI_e, which does not make sense as pseudo equilibrium, could improve the problem but the best fit is still impossible to achieve (if possible with an enormous value of n). Meanwhile, similar problems are encountered when $CCPP_e$ is applied. Therefore, introducing pseudo equilibrium could not help achieving the best fit for Juraperle calcite dissolution.
Besides, if the last measured data of Vosbeck curves is taken as the SI_e, it is clear that the assumption of SI_e =-0.17 of Plummer and Busenberg (1999) is not really accurate since the real end point of SI_e could be much closer to zero.
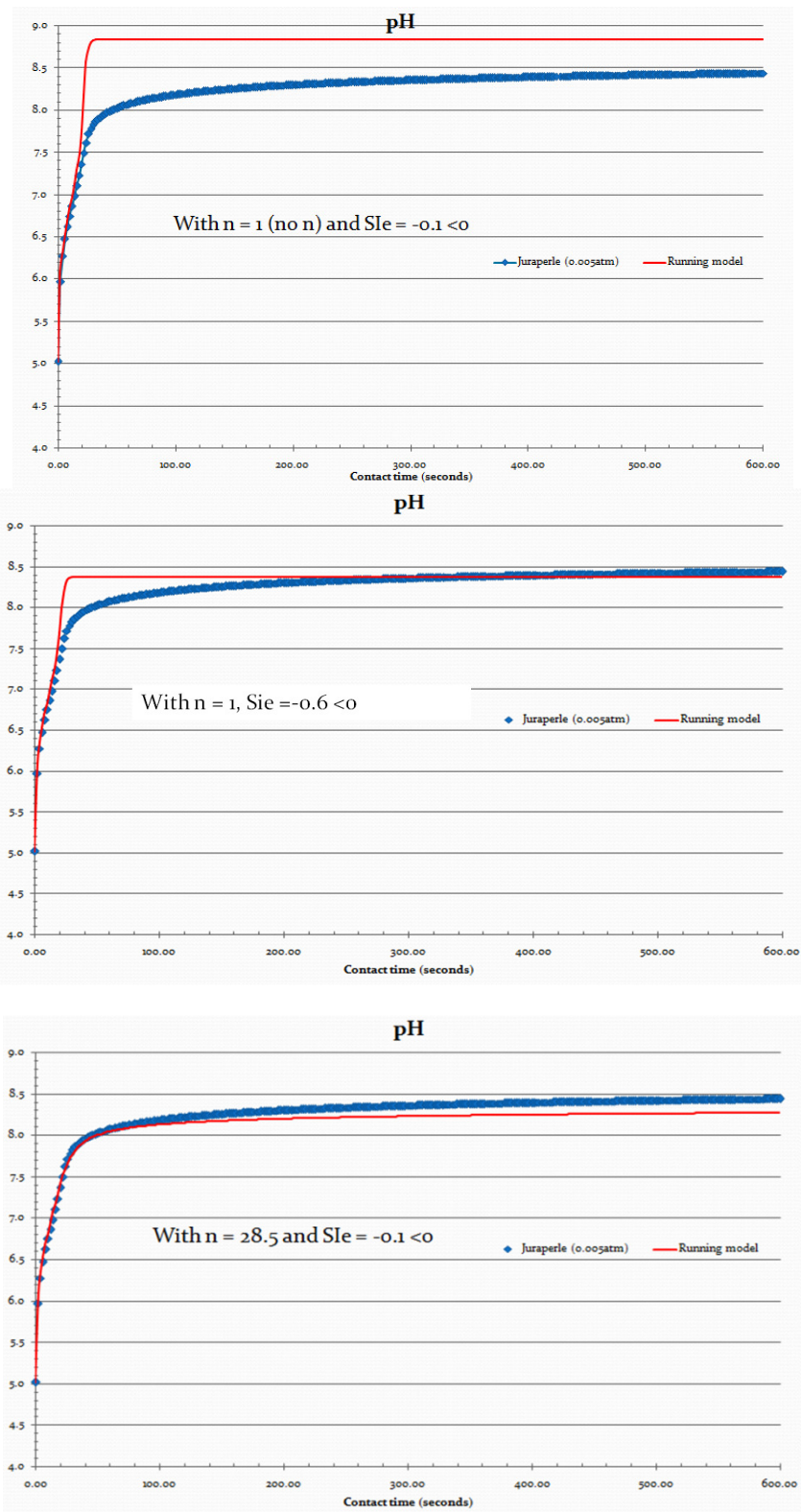
Figure 55: Vosbeck's Juraperle data and simulated pH curve of different combination of n and SIe for the developed model
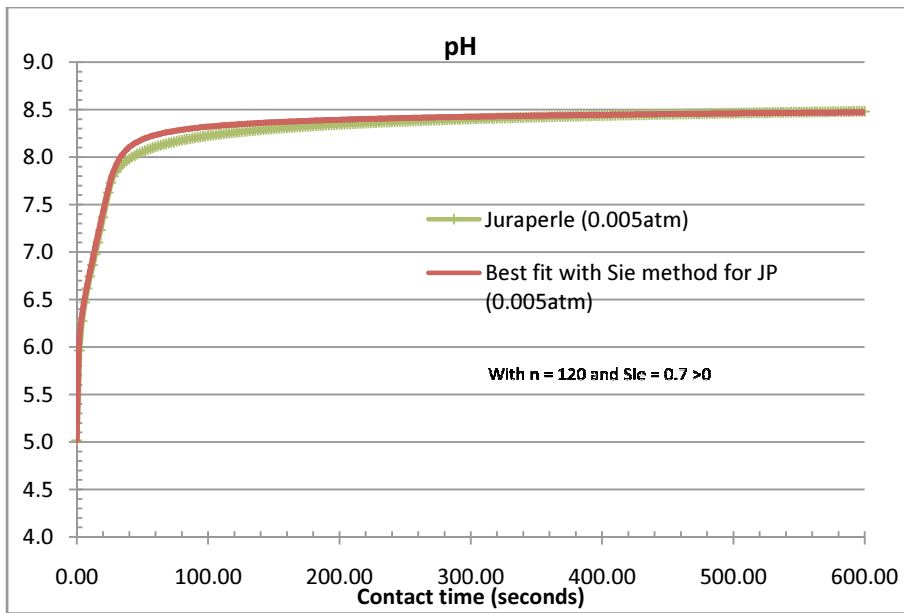
Figure 56: Vosbeck data on Juraperle (0.005 atm) vs. best fit improved model with applied pseudo equilibrium SIe

Annex B.8. Code lines inputted for the PCM model of pure and natural calcite in PHREEQC

PCM model for pure calcite:

```
Calcit_PCM_Baker                                              # copied from phreeqc.dat, ID 4842 2010-09-27 17:17:44Z dlpark
        -start
                        1 REM                                 Modified from Plummer and others, 1978
                        2 REM                                 M = current moles of calcite
                        3 REM                                 M0 = initial moles of calcite
                        4 REM                                 parm(1) = Area/Volume, cm^2/L   (or cm^2 per cell)
                        5 REM                                 parm(2) = exponent for M/M0 for surface area correction
                        6 REM                                 parm(3) = correction factor for a1
                        7 REM                                 parm(4) = correction factor for a2
                        8 REM                                 parm(5) = correction factor for a3
                        9 REM                                 parm(6) = correction factor for n
                       10 REM                                 parm(7) = possibly dissoluted calcium amount (mmol/kgw)
                       11 REM                                 parm(8) = Saturated level decrement (> 0 : flatenning) (< 0 : increasing)
                       12 REM                                 parm(9) = pseudo equilibrium Sie
                       13 REM                                 rate = 0 if no calcite and undersaturated
                       20 si_cc = SI("Calcite")
                       30 if (M <= 0  and si_cc < 0) then goto 300
                       40 a1 = parm(3)*0.65*10^(0.438 - 444.0 / TK )
                       50 a2 = parm(4)*1.1*10^(3.01- 2177.0 / TK )
#                      51 if (TOT("Ca")<= 0.00026) then x = parm(5)
#                      52 if (TOT("Ca")> 0.00026) then x = parm(5)*0.1
                       60 if TC <= 25 then  a3 = parm(5)*0.75*10^(-6.127 - 317.0 / TK )
                       70 if TC > 25 then a3 = parm(5)*0.75*10^(-1.376 - 1737.0 / TK )
                       75 Ks_ = 10^(LK_PHASE("Calcite"))
                       76 a4 = ( a1*ACT("H+") +  a2 * ACT("CO2")  + a3*ACT("H2O"))/ Ks_
                       80 REM                                 surface area calculation
                       90 t = 1
                      100 if M0 > 0 then t = M/M0
                      110 if t = 0 then t = 1
                      120 area = PARM(1) * (t)^PARM(2)
                      125 rf = a1 * ACT("H+") + a2 * ACT("CO2") + a3*ACT("H2O")
#                     130 rf = a1 * ACT("H+") + a2 * ACT("CO2") + a3* ACT("H2O") - a4* ACT("Ca+2") * ACT("CO3-2")
                      140 REM                                 1e-3 converts mmol to mol
                      141 if (TOT("Ca")*1000/parm(7) < 0.89) then x = parm(6)
                      142 if (TOT("Ca")*1000/parm(7)>= 0.89) then x = parm(6)+1*0.13*parm(8)*abs(parm(6))
                      143 if (TOT("Ca")*1000/parm(7) > 0.91) then x = parm(6)+2*0.13*parm(8)*abs(parm(6))
                      144 if (TOT("Ca")*1000/parm(7) >= 0.92) then x = parm(6)+3*0.13*parm(8)*abs(parm(6))
#                     150 rate = area * 1e-3 * rf
                      150 rate = area * 1e-3 * rf *(1 - 10^(si_cc-parm(9)))^(3*x)
                      160 moles = rate * TIME
                      170 REM                                 do not dissolve more calcite than present
                      180 if (moles > M) then moles = M
                      190 if (moles >= 0) then goto 300
                      200 REM                                 do not precipitate more Ca or C(4) than present
                      210 temp = TOT("Ca")
                      220 mc  = TOT("C(4)")
                      230 if mc < temp then temp = mc
                      240 if -moles > temp then moles = -temp
                      300 SAVE moles
                      310 PUT(rate*1000*10, 1)                # rate in mol/m2/s
        -end
```

PCM model for natural limestone (Juraperle):

```
Calcit_PCM_Juraperle                                      # copied from phreeqc.dat, ID 4842 2010-09-27 17:17:44Z dlpark
          -start
                    1 REM                                  Modified from Plummer and others, 1978
                    2 REM                                  M = current moles of calcite
                    3 REM                                  M0 = initial moles of calcite
                    4 REM                                  parm(1) = Area/Volume, cm^2/L   (or cm^2 per cell)
                    5 REM                                  parm(2) = exponent for M/M0 for surface area correction
                    6 REM                                  parm(3) = correction factor for a1
                    7 REM                                  parm(4) = correction factor for a2
                    8 REM                                  parm(5) = correction factor for a3
                    9 REM                                  parm(6) = correction factor for n
                   10 REM                                  parm(7) = possibly dissoluted calcium amount (mmol/kgw)
                   11 REM                                  parm(8) = Saturated level decrement (> 0 : flatenning) (< 0 : increasing)
#                  12 REM                                  parm(9) = pseudo equilibrium Sie
                   13 REM                                  rate = 0 if no calcite and undersaturated
                   20 si_cc = SI("Calcite")
                   30 if (M <= 0  and si_cc < 0) then goto 300
                   40 a1 = parm(3)*0.95*10^(0.438 - 444.0 / TK )
                   50 a2 = parm(4)*2.3*10^(3.01- 2177.0 / TK )
#                  51 if (TOT("Ca")<= 0.00026) then x = parm(5)
#                  52 if (TOT("Ca")> 0.00026) then x = parm(5)*0.1
                   60 if TC <= 25 then  a3 = parm(5)*1.8*10^(-6.127 - 317.0 / TK )
                   70 if TC > 25 then a3 = parm(5)*1.8*10^(-1.376 - 1737.0 / TK )
                   75 Ks_ = 10^(LK_PHASE("Calcite"))
                   76 a4 = ( a1*ACT("H+") +  a2 * ACT("CO2")  + a3*ACT("H2O"))/ Ks_
                   80 REM                                        surface area calculation
                   90 t = 1
                  100 if M0 > 0 then t = M/M0
                  110 if t = 0 then t = 1
                  120 area = PARM(1) * (t)^PARM(2)
                  125 rf = a1 * ACT("H+") + a2 * ACT("CO2") + a3*ACT("H2O")
#                 130 rf = a1 * ACT("H+") + a2 * ACT("CO2") + a3* ACT("H2O") - a4* ACT("Ca+2") * ACT("CO3-2")
                  140 REM                                        1e-3 converts mmol to mol
                  141 if (TOT("Ca")*1000/parm(7) < 0.89) then x = parm(6)
                  142 if (TOT("Ca")*1000/parm(7)>= 0.89) then x = parm(6)+1*0.13*parm(8)*abs(parm(6))
                  143 if (TOT("Ca")*1000/parm(7) > 0.909) then x = parm(6)+2*0.13*parm(8)*abs(parm(6))
                  144 if (TOT("Ca")*1000/parm(7) >= 0.919) then x = parm(6)+3*0.13*parm(8)*abs(parm(6))
#                 150 rate = area * 1e-3 * rf
                  150 rate = area * 1e-3 * rf *(1 - 10^(si_cc))^(7.5*x)
                  160 moles = rate * TIME
                  170 REM                                  do not dissolve more calcite than present
                  180 if (moles > M) then moles = M
                  190 if (moles >= 0) then goto 300
                  200 REM                                  do not precipitate more Ca or C(4) than present
                  210 temp = TOT("Ca")
                  220 mc  = TOT("C(4)")
                  230 if mc < temp then temp = mc
                  240 if -moles > temp then moles = -temp
                  300 SAVE moles
                  310 PUT(rate*1000*10, 1)                         # rate in mol/m2/s
          -end
```

Annex C   Anderlohr test and the developed contactor layer model

Annex C.1. Logical range of ending point CCDP$_e$ in Anderlohr tests

Unlike Vosbeck's batch experiments, Anderlohr conducted marble filtration tests to investigate the calcite dissolution process of natural limestone (Juraperle). Assumed the same quality of Jurperle used in Vosbeck and Anderlohr's experiments, the dissolution rate in Anderlohr tests is thus expected to be lower than Vosbeck data due to the non-ideal conditions for free-contacted calcite grain dissolving. As developed earlier, the Vosbeck experiments on natural calcite dissolution could be well simulated by the PCM model for Juraperle. Therefore, given the same contact time, A/V ratio and initial water quality, the PCM model for natural calcite would generate dissolution curves that reach closer to the equilibrium end.

Notice that in most of Anderlohr measured data, at a certain point along the tube, the water quality becomes invariable with unchanged Ca content and CCDP which is then called CCDP$_e$. For instances, in test 2, the water content of Ca stays still at 0.295 mmol/L from measured point 14 towards the bottom. This point could represent for a perceptible saturation point of the solution while approaching the real equilibrium point. In order to reach this point in the filtration bed, the water must have travelled through a certain bed thickness; hence, there must be a certain contact time which is 161 seconds for the Test 2 case. With the same contact time, A/V ratio, initial inlet water, the calcite dissolution simulated by PCM model for natural calcite would reach closer to equilibrium hence the PCM's CCDP at this time would be smaller (closer to zero) compared to Anderlohr test. Consequently, that CCDP could be seen as a lower boundary for CCDP$_e$ of Anderlohr experiment since the real CCDP$_e$ of Anderlohr could never be equal or lower than this as shown in Figure 57. By trials and errors with different initial CO_2 content in the inlet water for both PCM model and Anderlohr re-simulation to achieve same CCDP at the chosen time, a better value (closer to the real amount) of CO_2 would be achieved hence the lower-boundary CCDP$_e$.

Figure 57: CCDP curves of the (imaginary) Anderlohr Test 2 and the simulation by PCM model together with the lower boundary CCDPe for Anderlohr experiment

At the saturation turning point in Vosbeck dissolution experiment, the calcite dissolution rate in the Vosbeck free-contacted conditions is impending to drop significantly. The water quality in Anderlohr test at the constant stage in the end must already surpass this turning point. In other words, the $CCDP_e$ of Anderlohr could not be equal or higher than the CCDP at the turning point in PCM model. For upper boundary, the CCDP extracted at this turning point in PCM model for natural calcite would be chosen to be the $CCDP_e$ for Anderlohr test as shown in Figure 58.

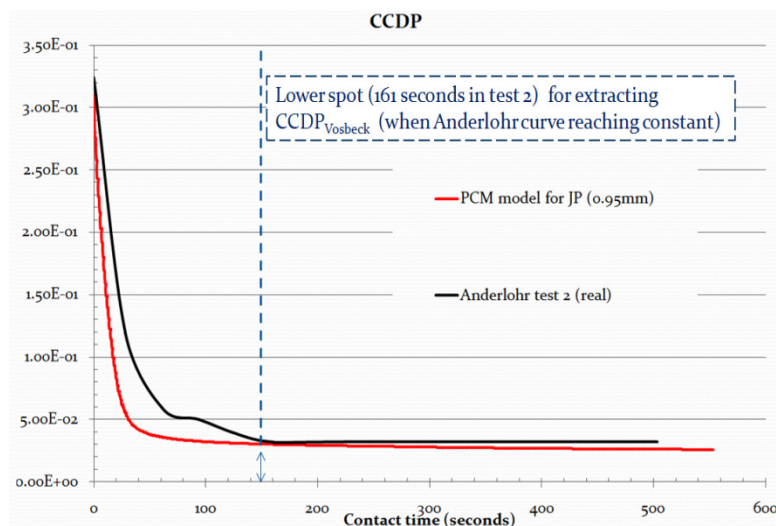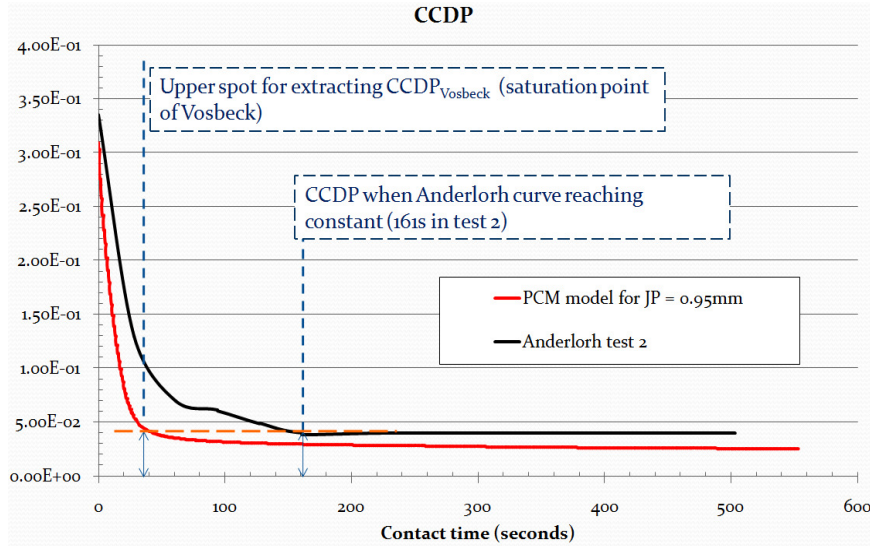Figure 58: CCDP curves of the (imaginary) Anderlohr Test 2 and the simulation by PCM model together with the upper boundary CCDPe for Anderlohr experiment

88

Annex C.2. Sample layout of the input and output of the computer based layer model

Legend

	Caption
	Input
	Excel Generated
	PHREEQC output

Sample description — Vosbeck pCO2 (atm)   0.005724932   nCO2 (mmol/L)   0.308

Assumption: mg/L =mg/kgs =mg/kgw

Basic data

Temperature	t	°C		
Oxygen	O2	mg/L	0.00	mmol/kgw
pH		-		
Conductivity (EC measured, at t °C)		mS/m	0	µS/cm
Total dissolved solids (TDS residue)		mg/L		

Cations

Calcium	Ca	mg/L	0.00	mmol/kgw
Magnesium	Mg	mg/L	0.00	mmol/kgw
Sodium	Na	mg/L	0.00	mmol/kgw
Potassium	K	mg/L	0.00	mmol/kgw
Iron	Fe	mg/L	0.00	mmol/kgw
Manganese	Mn	mg/L	0.00	mmol/kgw
Ammonium	NH4	mg/L	0.00	mmol/kgw
Aluminium	Al	µg/L	0.00	mmol/kgw
Barium	Ba	µg/L	0.00	mmol/kgw
Cadmium	Cd	µg/L	0.00	mmol/kgw
Copper	Cu	µg/L	0.00	mmol/kgw
Lead	Pb	µg/L	0.00	mmol/kgw
Lithium	Li	µg/L	0.00	mmol/kgw
Strontium	Sr	µg/L	0.00	mmol/kgw
Zinc	Zn	µg/L	0.00	mmol/kgw

Anions

Hydrogen carbonate (as Alkalinity)	HCO3	mg/L	0.00	mmol/kgw
Chloride	Cl	mg/L	0.00	mmol/kgw
Nitrate	NO3	mg/L	0.00	mmol/kgw
Sulfate	SO4	mg/L	0.00	mmol/kgw
Fluoride	F	mg/L	0.00	mmol/kgw
Bromide	Br	mg/L	0.00	mmol/kgw
Phosphate	PO4	mg/L	0.00	mmol/kgw
Nitrite	NO2	mg/L	0.00	mmol/kgw

Non-charged

Silicate	Si	mg/L	0.00	mmol/kgw
Boron	B	µg/L	0.00	mmol/kgw

Superficial velocity	v	m/h	10.0
Water load	Q	kgw/m2.s	2.77
Diameter discharged grains	mm	dout	0.90
Diameter feed grains	mm	din	1.00
Total bed height	H	mm	3,340
Total net contact time	t	s	554
Model name Calcite dissolution			Calcit_PCM
Kinetic model time step	dt	s	1
Time step for iteration	dT	days	2.00
Molair mass of dissolved solid	M	g/mol	100.0
Density of dissolved solid	rho	kg/m3	2,650
Correction factor for a1	α1		0.994
Correction factor for a2	α2		2.737
Correction factor for a3	α3		1.887
Initial dissolution rate order	η0		30.000
Increasing factor of n0	β		-0.065
Possibly dissolved calcium amount (mmol/kgw)			0.324
Correction factor of A/V	crf		0.500

Figure 59: Input layout for inlet water quality, contactor conditions, and PCM model parameters of the computer based layer model (sample of Anderlohr Test 2)

diameter	porosity	particles number	particles volume	A/V	layer height	contact time	CaCO3 mass
mm	%	/m2	L/m2	cm2/L	mm	s	mol/m2
0.90	46%	3.6E+08	136.2	78,261	252.2	41.8	3,609
0.91	46%	3.6E+08	140.8	77,401	260.7	43.3	3,731
0.92	46%	3.6E+08	145.5	76,560	269.4	44.7	3,855
0.93	46%	3.6E+08	150.3	75,736	278.3	46.2	3,982
0.94	46%	3.6E+08	155.2	74,931	287.4	47.7	4,112
0.95	46%	3.6E+08	160.2	74,142	296.6	49.2	4,245
0.96	46%	3.6E+08	165.3	73,370	306.1	50.8	4,380
0.97	46%	3.6E+08	170.5	72,613	315.8	52.4	4,519
0.98	46%	3.6E+08	175.8	71,872	325.6	54.0	4,660
1.00	46%	3.6E+08	181.3	71,146	335.7	55.7	4,804
Total					2,928	486	41,898

Figure 60: Input layout for each calcite grain layer

Output generated by PHREEQC corrected PCM model

Used mol = mol used * iteration time step

before timestep diameter	CaCO3 used	CaCO3 used	CaCO3 inflow	CaCO3 outflow	CaCO3 net flow	after CaCO3 mass	after timestep diameter
mm	mmol/kgw	mol	mol	mol	mol	mol/m2	mm
0.90	0.244	117.1	395.3	382.4	-104.2	3,505	0.89
0.91	0.040	19.4	408.5	395.3	-6.2	3,725	0.91
0.92	0.005	2.6	421.9	408.5	10.9	3,866	0.92
0.93	0.002	1.0	435.7	421.9	12.7	3,995	0.93
0.94	0.001	0.6	449.7	435.7	13.5	4,126	0.94
0.95	0.001	0.4	464.1	449.7	13.9	4,259	0.95
0.96	0.001	0.3	478.7	464.1	14.3	4,395	0.96
0.97	0.001	0.3	493.7	478.7	14.6	4,533	0.97
0.98	0.001	0.3	509.0	493.7	15.0	4,675	0.98
1.00	0.000	0.2	524.5	509.0	15.4	4,819	0.99
Total	0.297				3.5	41,898	
Mass balance layer 1		3.78E+07 particles					

Mol used in layer 1/(change in diameter over layer 1)

Figure 61: Output layout for each calcite grain layer with explanations (a)

Net = Inflow – Outflow – Used

Input for the next iteration

Discharged grain (0.9 mm)

before timestep diameter	mass balance in mol / m2 / timestep					after	after
	CaCO3 used	CaCO3 used	CaCO3 inflow	CaCO3 outflow	CaCO3 net flow	CaCO3 mass	timestep diameter
mm	mmol/kgw	mol	mol	mol	mol	mol/m2	mm
0.90	0.244	117.1	395.3	382.4	-104.2	3,505	0.89
0.91	0.040	19.4	408.5	395.3	-6.2	3,725	0.91
0.92	0.005	2.6	421.9	408.5	10.9	3,866	0.92
0.93	0.002	1.0	435.7	421.9	12.7	3,995	0.93
0.94	0.001	0.6	449.7	435.7	13.5	4,126	0.94
0.95	0.001	0.4	464.1	449.7	13.9	4,259	0.95
0.96	0.001	0.3	478.7	464.1	14.3	4,395	0.96
0.97	0.001	0.3	493.7	478.7	14.6	4,533	0.97
0.98	0.001	0.3	509.0	493.7	15.0	4,675	0.98
1.00	0.000	0.2	524.5	509.0	15.4	4,819	0.99
Total	0.297				3.5	41,898	
Mass balance layer 1	3.78E+07 particles						

Feeding grain (1.0 mm)

= zero means system balance

Re-calculated CaCO3 mass = Initial CaCO3 mass + net CaCO3

Figure 62: Output layout for each calcite grain layer with explanations (b)

91

Annex C.3. Downflow layer model simulation of Anderlohr tests

Figure 63: Downflow layer model simulation vs. Anderlohr test 2

Figure 64: Downflow layer model simulation vs. Anderlohr test 5

Annex D   Practice verification and the downflow contactor model

Annex D.1.   Measurements of water quality at Hoenderloo

Figure 65: Measurements of important quality parameters of raw water and filtrated water at Hoenderloo

Figure 66: Measurements of post-filtrated effluent at Honderloo

Annex D.2.   Different Juraperle quality analysis and comparison

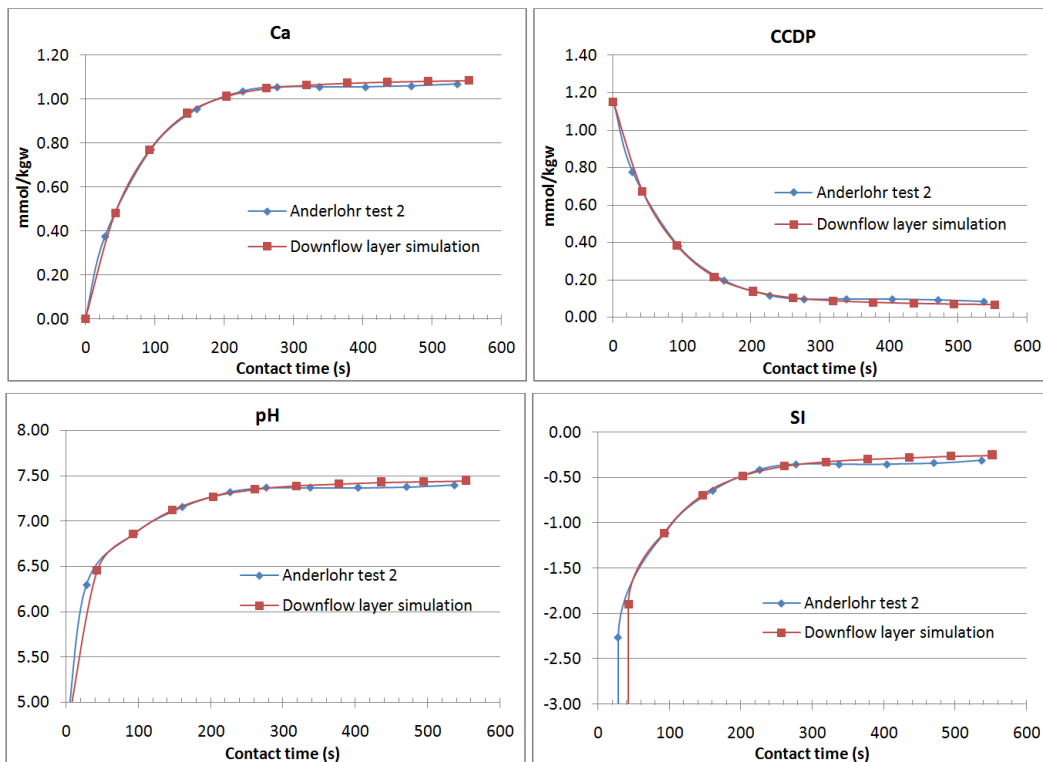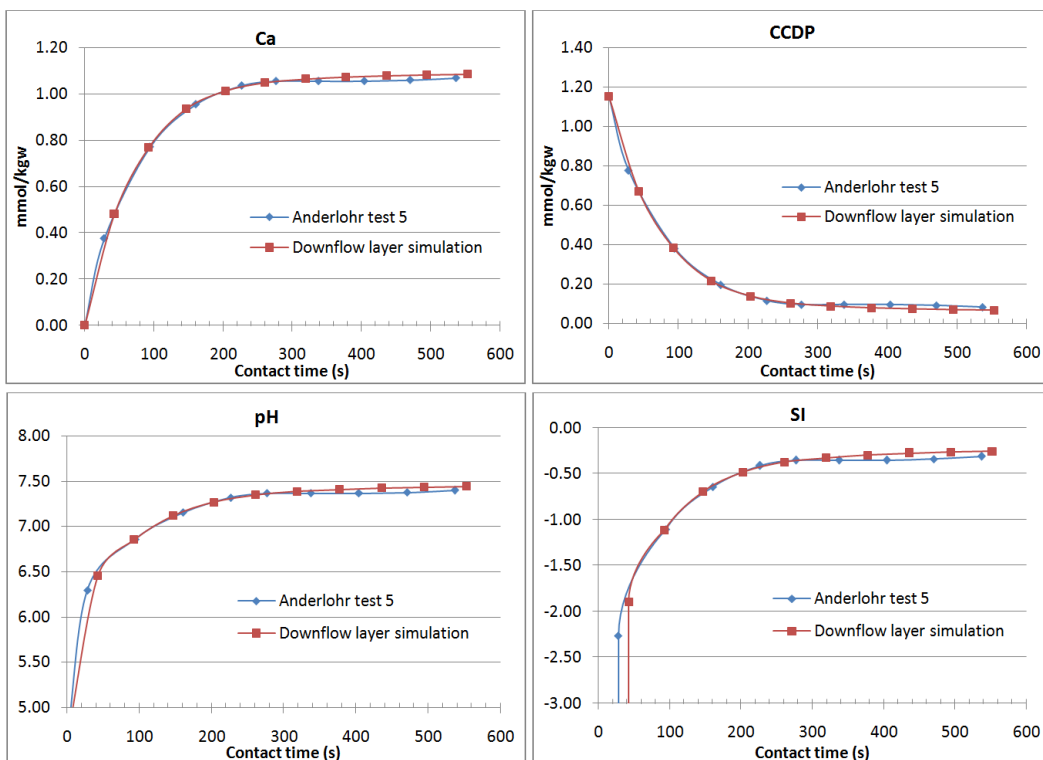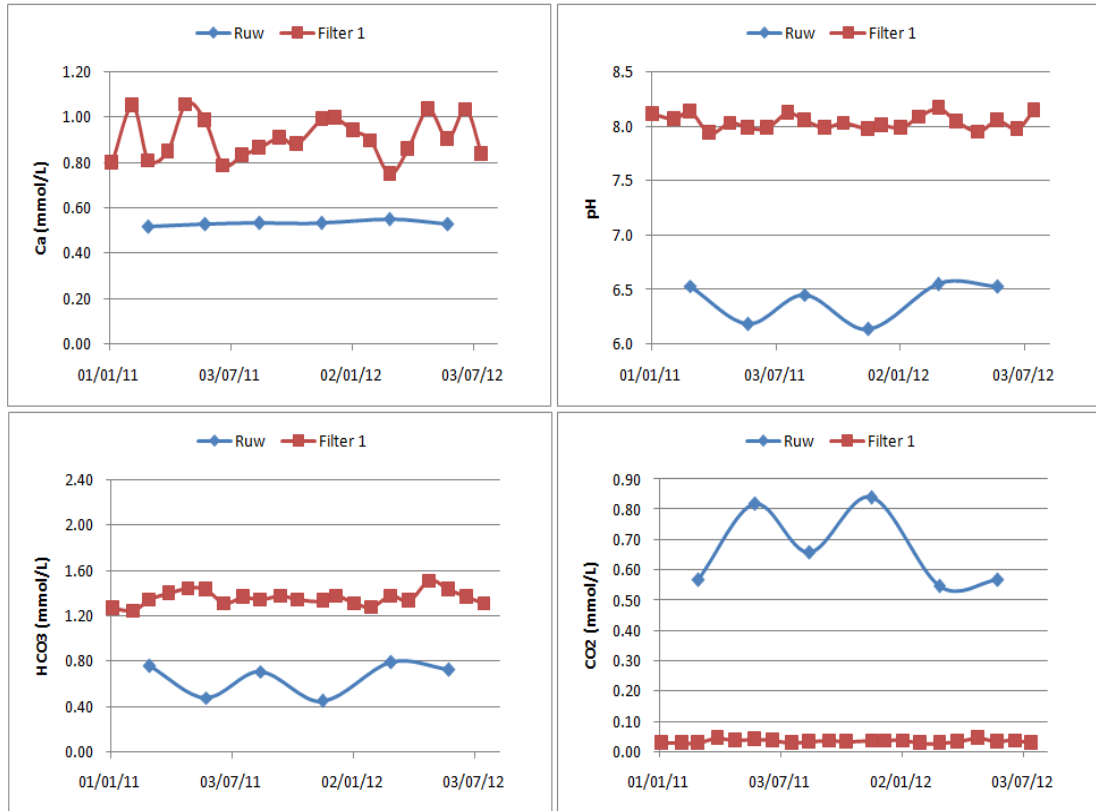The component analysis for Juraperle used in Vosbeck, Anderlohr's experiments as well as in Hoenderloo marble filters are shown in the below figures.

Jura Kalkstein (JL bzw. JLa)

In den Lösungsexperimenten dieser Arbeit wurde Jura Kalkstein in zwei Varianten verwendet: frisch gebrochenes und künstlich angelöstes Material.

Das Material ist von hellbrauner Farbe und weist eine feinkörnige dichte Struktur auf. Die in Abbildung 3-1 und 3-2 dargestellten Rasterelektronenmikrosp (REM)-Aufnahmen zeigen Partikel von Jura Kalkstein bzw. angelöstem Jura Kalkstein sowie Detailaufnahmen der Oberflächen. Darauf sind Poren und Kanäle zu erkennen. Zudem ist die Oberfläche des angelösten Materials rauher als die des frisch gebrochenen Materials.

Die Röntgenfluoreszenzspektralanalyse (RFA) wies neben Calcium, die weiteren "Neben"-Elemente Magnesium, Silicium, Phosphor, Eisen, Natrium und Kalium nach (Tab. 3-1).

Tab. 3-1: RFA-Analyse von Jura Kalkstein.

CaO %	MgO %	SiO$_2$ %	Al$_2$O$_3$ %	P$_2$O$_5$ %	Fe$_2$O$_3$ %	Na$_2$O %	K$_2$O %	Sr ppm	Ba ppm	Sc ppm
52.6	3.06	1.6	0.4	0.021	0.18	0.11	0.13	85	26	60

Figure 67: Vosbeck's Juraperle component analysis

3.1.3   Das Entsäuerungsmaterial

Als Filtermasse diente handelsüblicher Kalkstein der Firmen E. Schwenk/Herrlingen. Die Korngröße wurde durch Aussieben auf 0,9 – 1,0 mm festgelegt. Die Kornform zeigt Abb. 12. Eine Analyse des Materials führte zu folgendem Ergebnis:

SiO$_2$	0,22 %
Glühverlust	3,17 %
Carbonat	40,75 %
Calcium (als CaO)	55,90 %
Magnesium (als MgO)	0,18 %
Natrium (als Na$_2$O)	0,05 %
Fe$_2$O$_3$	0,02 %
Total	100,29 %

Die Dichte wurde in Pyknometerversuchen zu $\varrho_K = 2,668$ kg/l bestimmt. Die Dichte von CaCO$_3$ als Kalkspatkristall

Figure 68: Anderlohr's Juraperle component analysis (Anderlohr, 1975)

EDUARD MERKLE GMBH & CO. KG
KALK-, TERRAZZO- UND STEINMAHLWERKE   89143 Blaubeuren-Altental   Tel. (0 73 44) 96 01-0   Fax (0 73 44) 96 01-11

J U R A P E R L E   L M

Chemical analysis of JURAPERLE

$CaCO_3$		98,1 %
$MgCO_3$		0,9 %
Fe_2O_3		0,08 %
Al_2O_3		0,35 %
SiO_2 (Silicates)		0,55 %
Volatile matter (105°C)	(DIN EN ISO 787-2)	< 0,2 %
Loss on ignition	(DIN EN 459-2)	43,3 %
HCl-insoluble	(DIN 55 918)	0,8 %

Figure 69: Hoenderloo's Juraperle chemical analysis as indicated by the supplier

Besides, according to Vitens report on quality and treatment 2010 (Vitens, 2010), the calcium carbonate portion in Jurapele used at Hoenderloo is reported to be 99.8% average as tested by Vitens (Table 32). By taking the average of Vitens and the supplier chemical analysis results (KG, 2011), the calcium carbonate concentration in Hoenderloo Juraperle is approximately 99.2%.

Table 32: Overview of chemical analysis 2010 of Hoenderloo Juraperle (Vitens, 2010)

Pb. Hoenderloo				O&A	$CaCO_3$	Sb	As	Cd	Cr	Hg	Pb	Ni	Se	D10	D50	D60	D90	DEH	UFC
				-	% m/m	mg/kg	mg/kg	mg/kg	mg/kg	mg/kg	mg/kg	mg/kg	mg/kg	µm	µm	µm	µm	µm	-
		tcetsing	$CaCO_3$		>97%	<3	<3	<2	<10	<0,5	<10	<10	<3						
		tcetsing	Laserdiffractie																<1,5
Monsterpunt	Ber n. datum	Omschrijving																	
Calciumcarbonaat	8-4-2010	Iura Perle		OK	98,8	<3	<1	0,2	1,55	<0,1	<2	1,08	<2	1400	2500	2600	3100	2100	1,9
	8 11 2010			OK	100,8	<3	<1	<0,2	1,12	<0,1	<2	<1	<2	1500	2400	2500	2900	2200	1,6

For a certain weight of Juraperle, if the purity is 100%, the amount of calcium would be 40% or 56% as CaO. As a result, with 52.6% and 55.9% CaO in the component, the purity of Vosbeck and Anderlohr's Juraperle could be deduced to be 93.9% and 99.8% respectively.

Using the same method to apply for finding maximum percentage of magnesite in each calcite type, the results are shown.

Table 33: Maximum mass percentage of magnesite in different calcite types

Calcite type	% MgO	% $MgCO_3$ (equivalent)
Vosbeck Juraperle	3.06%	6.40%
Anderlohr Juraperle	0.18%	0.38%
Hoenderloo Juraperle(*)		0.9%
Baker		0.0%

(*): supplier's chemical analysis result

Notice that for Vosbeck and Anderlohr Juraperle, the maximum total mass percentage of calcite and magnesite is higher than 100% due to the fact that there are not enough carbonate anions for both calcium and magnesium cations. Thus, by assuming there is enough carbonate, the maximum total percentage could exceed 100%.

As mention in Chou experiment (1989), the surface rate of magnesite is 1000 times lower than calcite or other carbonates. Thus:

$r_{magnesite} = r_{diss-MgCO3}(1-10^{SI}) = (r_{diss-CaCO3}/1000)*(1-10^{SI}) = r_{diss-CaCO3}(1-10^{SI})^{n1}$

$r_{Vosbeck} = r_{diss-Vosbeck}(1-10^{SI}) = r_{diss-CaCO3}(1-10^{SI})^{n2}$

$r_{Hoenderloo} = r_{diss-Hoenderloo}(1-10^{SI}) = r_{diss-CaCO3}(1-10^{SI})^{n3}$

$\Rightarrow$ $r_{Vosbeck}/ r_{Hoenderloo} = (1-10^{SI})^{(n2-n3)}$

Assume R is the overall dissolution rate of Baker calcite or pure calcite, the rate of Vosbeck and Hoenderloo Juraperle could be calculated as following:

$r_{Vosbeck} = [R*(100 − 6.40) + 6.40*R/1000]/100 = 0.936R$
$r_{Hoenderloo} = [R*(100 − 0.90) + 0.90*R/1000]/100 = 0.991R$

$\Rightarrow$ $r_{Vosbeck}/ r_{Hoenderloo} = 0.94$

$\Rightarrow$ $(1-10^{SI})^{(n2-n3)} = 0.94$

With SI = -2.04 for influent water.
$\Rightarrow$ $n_2 − n_3 = 7.28$

From the η graph for Vosbeck Juraperle ➔ $n_2 \approx \eta*7.5 \approx 1.4*7.5 \approx 10.5$

$\Rightarrow$ $n_3 = 10.50 -7.28 = 3.22$
$\Rightarrow$ $n_2/n_3 = 3.3$

Hence, the correct n for Hoenderloo Juraperle is around 3.3 times lower than Vosbeck Juraperle.

Annex E   Extreme case calibration for Hoenderloo optimal design

In the Hoenderloo marble filter tank, assume that the maximum expansion for the considerably smallest grain size of 0.2mm is 2.07m from the original bed thickness of the optimal design (1.033m). This could be used for computing the bed expansion percentage:

$$E = \frac{L_e - L_0}{L_0} = \frac{2.07}{1.033} = 200\%$$

With the maximum possible bed expansion E of Hoenderloo marble filter tank, the expanded porosity of the bad could be induced by the following equation:

$$p_e = \frac{p_0 + E}{1 + E} = 0.8 = 80\%$$

where p_0 is the initial bed porosity (40%). Next, the maximum flow rate could be deduced as followed:

$$v^{1.2} = \frac{g}{130\vartheta^{0.8}} \left(\frac{\rho_f - \rho_w}{\rho_w} \right) \frac{p_e{}^3 d^{1.8}}{(1 - p_e)^{0.8}}$$

$$\Rightarrow \quad v = 25.1 \, m/h$$

With the found flow rate, the filtering capacity could be achieved by multiplying the flow rate with the total bed area of two filters (2*23.81 = 47.62 m^2):

$$Filter \; bed \; capacity = 25.1 m/h \times 47.62 m^2 \simeq \; 1195 \, m^3/h$$

Annex F Brief manual instructions for the developed computer based model application for calcite dissolution kinetics

Before using the CalciteDissolutionKinetics_Do_Peter.xlsm application, make sure PHREEQC has been installed on your computer and PHREEQC.dat file is copied to the same location with this application.

The developed application is built with the codes and commands of PHREEQC on the base of Excel interface. There are 8 sheets in the application file including: AquaticChemistry, Run_Control, Input, Output, PHREEQC.out, Calcit_PCM_Baker, Calcit_PCM_Juraperle, Water quality & Bed setup.

1. *AquaChemistry*

This sheet would be used as the main input page with simple return output as well.
Each cell color represents for the property and feature of that cell.

	Input cell
	auto-Excel computed cell
	Caption/Description cell
	PHREEC output/generated cell
	PHREEC output/generated cell
	PHREEC output/generated cell
	PHREEC output/generated cell

Only input the required data in the Input cell. If the required data is insignificant, the cell could be left blank (default = 0.0).
Remember to input the initial content of O_2 or CO_2 in water either in mg/L or atm (partial pressure unit) cell. If both cells are filled, the partial pressure would be taken as input value.
There are 13 calcite dissolution/precipitation kinetics models shown in this page with descriptions are provided in Table 34:

Table 34: Available calcite kinetics models in the developed application

Kinetics model	Description
Calcite	Default simplified PWP model in PHREEQC for aerated (open) system with constant pCO_2, however, NOT accurate enough to replace the full PWP model.
Calcit_PWP_k4	Full original PWP model, which could be used for both aerated and unaerated system
Calcit_PWP_SI	Simplified PWP model for unaerated (closed) system with varying pCO_2 over time, accurate enough to replace the full PWP model.
Calcit_Vosbeck_01_Dreybrodt	Dreybrodt model for simulate Baker calcite dissolution kinetics in Vosbeck experiment at pCO_2 = 0.01 atm
Calcit_Vosbeck_01_poly_JP	Polynomial function model to re-generate Juraperle dissolution kinetics in Vosbeck experiment at pCO_2 = 0.01 atm
Calcit_Vosbeck_005_poly_JP	Polynomial function model to re-generate Juraperle dissolution kinetics in Vosbeck experiment at pCO_2 = 0.005 atm
Calcit_Vosbeck_03_poly_JP	Polynomial function model to re-generate Juraperle dissolution kinetics in Vosbeck experiment at pCO_2 = 0.03 atm
Calcit_Vosbeck_01_poly_BK	Polynomial function model to re-generate Baker calcite dissolution kinetics in Vosbeck experiment at pCO_2 = 0.01 atm
Calcit_Vosbeck_005_poly_BK	Polynomial function model to re-generate Baker calcite dissolution kinetics in Vosbeck experiment at pCO_2 = 0.005 atm
Calcit_Vosbeck_03_poly_BK	Polynomial function model to re-generate Baker calcite dissolution kinetics in Vosbeck experiment at pCO_2 = 0.03 atm

Kinetics model	Description
Calcit_PWP_Chou	PWP-Chou kinetics model
Calcit_PCM_Baker	PCM model for pure (Baker) calcite dissolution kinetics simulation
Calcit_PCM_Juraperle	PCM model for natural limestone (Juraperle) dissolution kinetics simulation

Different kinetics models would be applied for different cases. However, most of the models only simulate the idealized dissolution kinetics in batch experiment conditions except the PCM model for Juraperle with the introduced (A/V) CRF parameter to simulate for real contactor condition. The "Run PHREEQC" button could be used for trigger simulation.

2. *Run Control*

This sheet provides the overall control of PHREEQC run in Excel.

3. *Input*

Details of commands and codes were built in this application for different models. Extra codes or editing work could be carried out in this sheet.

4. *Output*

Detail tabulated output from PHREEQC for each specified simulation.

5. *PHREEQC.out*

Original output file sheet from PHREEQC simulation

6. *Calcit_PCM_Baker*

This is a supporting sheet of appropriate parameters for simulating Baker/pure calcite kinetics dissolution. After filling in the initial CO_2 content either in mmol/L or atm, a set of input parameters (α_1, α_2, α_3, η, β) would be suggested and shown on the indication graphs (notice that β is not required for PCM for Baker calcite model hence there is no β graph, $\beta=0$). The user could base on that as reference to make a better choice of the input parameters which are lying more exactly on the curves in the graphs.

After the user choice cells have been filled. The vertical columns with all the chosen parameters are ready to be copied and pasted to the first sheet (AquaticChemistry) as input parameters.

7. *Calcit_PCM_Juraperle*

This sheet is similar to the previous Calcit_PCM_Baker sheet with the same user steps need to be done. However, the β graph is now available for PCM model of natural limestone. Be aware that η is different for different types of Juraperle (Vosbeck type and Hoenderloo type). Make sure only one of these two cells is filled.

8. *Water quality & Bed setup*

This sheet provides the default water quality and bed setup for three typical cases that had been investigated in this study: Vosbeck, Anderlohr and Hoenderloo.